GENETIC AND MOLECULAR CHARACTERIZATION

OF FUSARIUM WILT AND COTTON INTERACTIONS

A Dissertation

by

KEVIN BABILONIA

Submitted to the Office of Graduate and Professional Studies of
Texas A&M University
in partial fulfillment of the requirements for the degree of

DOCTOR OF PHILOSOPHY

Chair of Committee,	Ping He
Co-Chair of Committee,	Libo Shan
Committee Members,	Wayne Versaw
	Scott Finlayson
Interdepartmental Program Chair,	Dirk B. Hays

December 2019

Major Subject: Molecular and Environmental Plant Sciences

ABSTRACT

Cotton (*Gossypium* spp.) is an economically important crop that provides much of the world's supply of fiber, feed, foodstuff, oil, and biofuel products. However, several fungal diseases represent expanding threats to cotton production. Fusarium wilt of cotton, caused by *Fusarium oxysporum* f. sp. *vasinfectum* (*Fov*), is a major destructive disease of cotton. The conventional biological and chemical controls are not efficient against newly emerging *Fov* isolates. Thus, understanding the genetic basis of Fusarium wilt and cotton interactions could provide insights to control the disease. To respond to pathogen attacks, plants have evolved a sophisticated immune system. To date, a large number of plant immune receptors conferring resistance to fungal pathogens belong to the plasma membrane-localized receptor-like proteins (RLPs) with an extracellular domain that recognizes specific pathogen signatures. Upon perception of pathogen signatures, RLPs induce a series of defense responses, including massive transcriptional re-programming, in fending off pathogen attacks. In this study, I used an integrative genomic and molecular approach to identify and understand the functions of cotton RLPs in response to *Fov* infections at the whole genome level. Based on the in-silico prediction of RLP candidates in different cotton genomes, I systemically silenced 39 RLPs in upland cotton (*G. hirsutum*) with virus-induced gene silencing (VIGS). Seven of these showed reduced resistance to *Fov* infections, whereas silencing of one showed reduced susceptibility to *Fov* infections, suggesting that RLPs could play both positive and negative roles in cotton response to *Fov*. Silencing of two RLPs displayed reduced immune responses, including

mitogen-activated protein kinase (MAPK) phosphorylation, reactive oxygen species (ROS) burst and ethylene biosynthesis, to the conserved pathogen-associated molecular patterns (PAMPs), supporting a molecular mechanism of these RLPs in cotton resistance to *Fov*.

Plant immunity is triggered by recognition of pathogen signatures or PAMPs. I isolated the cell wall components of different *Fusarium oxysporum* isolates (FoCWEs) and tested their ability to trigger immune responses in both cotton and the model plant Arabidopsis. Significantly, FoCWE triggers MAPK activation, ROS burst, ethylene biosynthesis, growth inhibition, and stomatal closure in cotton and Arabidopsis. In addition, FoCWE protects cotton seeds against infections by virulent isolates of *Fov*, and Arabidopsis plants against *Pseudomonas syringae* pv tomato DC3000. The data indicate that FoCWE is a classical PAMP that is potentially recognized by a conserved pattern recognition receptor (PRR) in different plant species. Analysis of available PRR mutants in Arabidopsis indicates that FoCWE is perceived by a potential novel PRR. Further characterization of the eliciting component within FoCWE demonstrated that it is a heat-stable and water-soluble PAMP.

In summary, these findings shed light on the molecular basis of cotton-*Fov* interactions, and provide evidence that RLPs are key genes that can be used in breeding and genetic engineering of cotton resistance to fungal wilt pathogens. In addition, my data indicate that FoCWE can be used as a biocontrol agent to protect cotton against *Fov* infections. To conclude, my work provides new tools to develop different strategies to control Fusarium wilt of cotton.

ACKNOWLEDGEMENTS

First and foremost, I thank God for giving me the strength, knowledge, and everything I needed to undertake this research journey and to complete it satisfactorily. This achievement would not have been possible without his blessings. Second, I want to thank my advisors, Dr. Ping He and Dr. Libo Shan, for their support, patience, and guidance during this time. You both helped me grow as a scientist and as the person that I am today. I will eternally be grateful for the opportunity of having you both as advisors. I also want to thank my committee members, Dr. Wayne Versaw and Dr. Scott Finlayson, for their guidance and support. I am also very thankful to all of my current and former lab members. Doing research is a team effort and without you, this would have not been possible.

I also have to acknowledge the biggest source of my strength and motivation, my family. Thanks to my wife, Janeth Babilonia, for all the emotional support, for helping me with my experiments, for being patient when I was under stress writing this dissertation, and for making me feel loved every second that goes by. I love you and I am thankful our paths have crossed. I also want to thanks my parents who have always supported me in many ways, and my brother Brian Babilonia for also being my best friend. I love the three of you and I always count the days to see you again and have some good quality time. I am also grateful of my aunt, Marilyn Babilonia, who helped me establish in College Station and has always been there for me.

Last but not least, I want to thank my former advisor, Dr. Dimuth Siritunga, for his advice and encouragement to pursue my PhD. I am happy to say that you have also became a good friend. To conclude, I would like to thank all others who I failed to mention here who supported me in one way or another.

CONTRIBUTORS AND FUNDING SOURCES

Contributors

This work was supervised by a dissertation committee consisting of Professor Ping He (advisor) of the Department of Biochemistry & Biophysics, Professor Libo Shan of the Department of Plant Pathology & Microbiology, Professor Scott Finlayson of the Department of Soil & Crop Sciences, and Professor Wayne Versaw of the Department of Biology.

The bioinformatic data in Chapter 2 was analyzed by Pierce Jamieson of the Department of Plant Pathology & Microbiology. The RNA-seq data in Chapter 3 was analyzed by Lin Zhang of the Department of Biochemistry & Biophysics.

All the remaining work conducted for the dissertation was completed by the student independently.

Funding Sources

No outside funding was received for the research and writing of this document.

NOMENCLATURE

BAK1	BRI1-associated Receptor Kinase 1
BR	Brassinosteroid
CERK1	Chitin Elicitor Receptor Kinase 1
CLV2	Clavata2
DAMP	Damage-Associated Molecular Pattern
ECD	Extra-Cellular Domain
EF-Tu	Elongation Factor Tu
EGF	Epidermal Growth Factor
EIX	Ethylene-Inducing Xylanase
FLS2	Flagellin-Sensitive 2
FLS3	Flagellin-Sensing 3
Fol	Fusarium oxysporum f. sp. lycopersici
Fov	Fusarium oxysporum f.sp. vasinfectum
FovCWE	Fusarium oxysporum vasinfectum Cell Wall Extract
FRK1	Flg22-induced Receptor-like Kinase 1
JA	Jasmonic Acid
LPS	Lipopolysaccharide
LRR	Leucine-Rich Repeat
LUC	Luciferase
LYK4/5	LysM-containing Receptor Kinase 4/5

LYM1/3	LysM Domain-Containing GPI-Anchored Protein 1
LysM	Lysine Motifs
MAPK	Mitogen-Activated Protein Kinases
NB-LRR	Nucleotide-Binding Leucine-Rich Repeat
NEP1	Necrosis and Ethylene-Inducing Peptide 1
NLP	NEP1-Like Protein
PAMP/MAMP	Pathogen/Microbe-Associated Molecular Patterns
PEPR1/2	Pep Receptor 1/2
PGN	Peptidoglycan
PRR	Pattern-Recognition Receptor
PTI	PAMP-Triggered Immunity
QTLs	Quantitative Trait Loci
R gene	Resistance gene
RFO2	Resistance to Fusarium Oxysporum 2
RLCK	Receptor-Like Cytoplasmic Kinase
RLK	Receptor-Like Kinase
RLP	Receptor-Like Protein
ROS	Reactive Oxygen Species
SIX	Secreted In Xylem
SNC2	Suppressor of NPR1, Constitutive-2
SOBIR1	Suppressor Of BIR1-1
TMM	Too Many Mouths

Ve	Verticillium
VIGS	Virus-induced Gene Silencing

TABLE OF CONTENTS

Page

LIST OF FIGURES

Page

LIST OF TABLES

Page

1. INTRODUCTION AND LITERATURE REVIEW*

1.1. Mechanisms of Plant Pattern-Triggered Immunity

Over evolutionary time, plants have developed a series of sophisticated defense mechanisms to defend against their associated pathogens. One of the inducible defense responses is triggered upon recognition of pathogen/microbe-associated molecular patterns (PAMP/MAMP) by specific plant pattern-recognition receptors (PRRs) on the cell surface. This recognition induces a series of host immune responses and leads to PAMP-triggered immunity (PTI) (Bigeard et al., 2015). PRRs can be divided into two major groups: Receptor-like kinases (RLKs) and Receptor-like Proteins (RLPs). The extracellular domains (ECD) of PRRs are responsible for the perception of different MAMPs, including peptides, peptidoglycan (PGN), lipopolysaccharide (LPS), chitin, among others (Afzal et al., 2008; Gish and Clark, 2011; Newman et al., 2013). The downstream responses of PRRs include the activation of protein kinases, callose deposition, reactive oxygen species (ROS) bursts, ethylene biosynthesis, root inhibition, defense gene transcription, and others (Boller and Felix, 2009; Li et al., 2016a; Macho and Zipfel, 2014). RLP- and RLK-mediated PTI is important for plant basal defense to a broad spectrum of pathogens and some RLPs and RLKs have been classified as "Resistance" (R) genes, which are thought to have coevolved to defend against specific pathogen races as defined in the "gene-for-gene" hypothesis (van der Does and Rep, 2007).

*Part of this chapter is reprinted from "Return of old foes — recurrence of bacterial blight and Fusarium wilt of cotton" by Kevin L. Cox Jr., Kevin Babilonia, Terry Wheeler, Ping He, and Libo Shan, 2019. *Current Opinion in Plant Biology*, 50, 95-103, Copyright 2019 by Elsevier Ltd.

1.1.1. Structural domains of RLKs and RLPs

In plants, RLKs are transmembrane kinases similar to the tyrosine kinases (RTKs) in animals, structurally containing a ligand-binding extracellular domain, a single-transmembrane domain, and a cytoplasmic kinase domain (Shiu and Bleecker, 2001). The structure of an RLP is essentially that of an RLK without the cytoplasmic domain, which resembles the Toll-like receptors in animals (Medzhitov et al., 1997). The ECD of RLKs and RLPs are highly variable and can recognize a wide range of ligands to confer resistance to bacterial, viral, fungal, oomycete, nematode, or insect attack (Dangl and Jones, 2001; Tang et al., 2017). The majority of RLPs and RLKs possess extracellular leucine-rich repeat domains (LRR), but other ECDs include lysine motifs (LysM), lectin domain, and epidermal growth factor (EGF)-like domain (Couto and Zipfel, 2016). The genome of Arabidopsis contains more than 200 LRR-RLKs and 57 LRR-RLPs with a range of 3-34 LRR repeats per RLP/RLK (Belkhadir et al., 2014; Jamieson et al., 2018).

1.1.2. RLKs in plant immunity

Many RLKs have been shown to function in plant immunity, but the cognate ligands have been only identified for a few RLKs. Two well studied LRR-RLKs include the bacterial flagellin receptor FLAGELLIN-SENSITIVE 2 (FLS2) and the bacterial elongation factor Tu (EF-Tu) receptor EFR, which recognize a conserved 22-amino-acid peptide (flg22) of flagellin and an 18-amino-acid peptide (elf18) of EF-Tu, respectively (Li et al., 2016a). Following ligand perception, both FLS2 and EFR heterodimerize with

the LRR-RLK family co-receptor BRI1-ASSOCIATED RECEPTOR KINASE 1 (BAK1) (Ma et al., 2016). After the formation of these heteromeric PRR complexes, interaction with receptor-like cytoplasmic kinases (RLCKs) occurs to initiate intracellular signaling and defense responses. Other RLKs perceive damage-associated molecular patterns (DAMPs) released into the extracellular space upon pathogen infection with the goal of triggering immune responses on nearby cells (Yamada et al., 2016). For example, the Arabidopsis PEP RECEPTOR1 (PEPR1) and PEPR2 perceive proteinaceous DAMPs from a small family of pro-peptides called PROPEPs (Yamaguchi et al., 2010). Furthermore, other non-LRR RLK are known for their importance in plant immune signaling. For instance, the Arabidopsis LysM-RLKs CHITIN ELICITOR RECEPTOR KINASE1 (CERK1), LysM-CONTAINING RECEPTOR KINASE4 (LYK4), and LYK5, are required for the perception of chitin, a component of the fungal cell wall (Petutschnig et al., 2014). Other examples of RLKs in plant defense include the tomato FLAGELLIN-SENSING 3 (FLS3), which recognizes a second epitope of flagellin termed flgII-28 (Clarke et al., 2013; Hind et al., 2016), the rice XA21, which recognize a tyrosine-sulfated protein from a Gram-negative bacterium (Pruitt et al., 2015; Shimizu et al., 2010), and the Arabidopsis LIPOOLIGOSACCHARIDE-SPECIFIC REDUCED ELICITATION (LORE), which recognizes LPS (Ranf et al., 2015).

1.1.3. RLPs in plant immunity

Many RLPs are also important in immunity. Interestingly, several RLPs play a major role in plant defense against fungal pathogens, including *Fusarium*, in different

plant species. The Arabidopsis RLP23 binds and recognizes the conserved peptide nlp20 from NECROSIS AND ETHYLENE-INDUCING PEPTIDE1 (NEP1)-LIKE PROTEINS (NLPs), which are widespread proteins among diverse groups of microbes, including *Fusarium oxysporum* f. sp *erythroxyli*, that can induce cell death and ethylene accumulation in plants (Albert et al., 2015). Importantly, RLPs I-1 and I-7 in tomato confer resistance to *F. oxysporum* f.sp. *lycopersici* (De Wit, 2016), and the Arabidopsis RESISTANCE TO FUSARIUM OXYSPORUM 2 (RLP3/RFO2) confers resistance to multiple species of *Fusarium* (Diener and Ausubel, 2005; Shen and Diener, 2013). Other Arabidopsis RLPs include ReMAX, which recognizes a proteinaceous MAMP from Xanthomonas (Jehle et al., 2013), RLP30, which confers resistance against the bacterial pathogen *Pseudomonas syringae* pv *phaseolicola* (Wang et al., 2008), RLP42/RBPG1, which is essential for the recognition of fungal endopolygalacturonases (Zhang et al., 2014), RLP51/SNC2, which is required for basal resistance against the bacterial pathogen *P. syringae* pv tomato DC3000 (Zhang et al., 2010), and RLP52, which provides resistance against the powdery mildew pathogen *Erysiphe cichoracearum* (Ramonell et al., 2005). Furthermore, the Arabidopsis LysM-RLPs LysM DOMAIN-CONTAINING GPI-ANCHORED PROTEIN 1 (LYM1) and LYM3 are required for response to bacterial PGN (Willmann et al., 2011). In rice, chitin is perceived by the LysM-RLPs OsCERK1 and CHITIN OLIGOSACCHARIDE ELICITOR BINDING PROTEIN (CEBiP) (Shimizu et al., 2010). In tomato, several RLPs provide resistance against fungal pathogens, including Cf-4 and Cf-9, which recognize avirulence effector proteins from *Cladosporium fulvum* (Postma et al., 2016; Rivas and Thomas, 2005; Stergiopoulos and de Wit, 2009), Ve1 and

Ve2, which confer race-specific resistance against *Verticillium* (Kawchuk et al., 2001), and Eix1 and Eix2, which recognize the fungal protein ethylene-inducing xylanase (EIX) (Ron and Avni, 2004). Other examples include the apple Vfa1 and Vfa2, which are important against the apple fungal pathogen *Venturia inaequalis*, the causal agent of apple-scab disease (Malnoy et al., 2008), the rapeseed LepR3, Lm1 and RLM2, which confer resistance to the fungal pathogen *Leptosphaeria maculans*, the causal agent of blackleg disease (Larkan et al., 2013; Larkan et al., 2015), and the potato ELICITIN RESPONSE (ELR), which mediates extracellular recognition of the PAMP elicitin from Phytophthora species (Du et al., 2015).

1.1.4. RLPs in plant growth and development

Several RLPs in Arabidopsis have been shown to regulate growth and development by recognizing endogenous hormones or peptides (He et al., 2018). For instance, the Arabidopsis LRR-RLP TOO MANY MOUTHS (TMM) is involved in the regulation of stomata patterning as seen in the disrupted patterning and asymmetric cell division in the leaves, and no stomata in the stem in the *tmm* mutant (Nadeau and Sack, 2002; Shpak et al., 2005). Moreover, AtCLAVATA2 (CLV2) controls shoot apical meristem development and recent evidence suggest its involvement in other physiological roles involving root meristem maintenance, regulation of protoxylem formation, root development, and plant-microbe interactions (Ogawa et al., 2008; Pan et al., 2016). The AtCLV2 maize ortholog FASCIATED EAR2 (FEA2) also regulates shoot meristem proliferation (Taguchi-Shiobara et al., 2001). In addition, the Arabidopsis RLP44 is

involved in the brassinosteroid hormone signaling pathway and is required for normal growth and stress responses (Wolf et al., 2014).

1.1.5. RLPs need adapter kinases for functionality

Because RLPs lack a cytoplasmic kinase domain, they interact with RLKs or adapter kinases to activate downstream signaling in a similar manner to their RLK counterparts (Gust and Felix, 2014). For instance, the Arabidopsis LRR-RLK SUPPRESSOR OF BIR1-1 (SOBIR1) was found in complex with multiple LRR-RLPs involved in plant immunity or growth and development such as Cf-4, Ve1, LepR3, Rlm2, AtRLP1, AtRLP23, AtRLP30, and AtRLP42 (Liebrand et al., 2013; Lv et al., 2016). Also, AtTMM forms complexes with the LRR-RLKs ERECTA and ERECTA-LIKE 1 (ERL1) to recognize the peptides EPIDERMAL PATTERNING FACTOR 1 (EPF1) and EPF2 to regulate stomatal development and patterning (Lee et al., 2012; Lin et al., 2017). Similarly, AtCLV2 interacts with the membrane-associated receptor kinase CORYNE (CRN) to perceive CLV3 signal (Bleckmann et al., 2010; Zhu et al., 2010).

1.2. Mechanisms of Cotton Resistance and Susceptibility to Fusarium Wilt

1.2.1. Cotton genomics

As an economically important crop, cotton (Gossypium spp.) supplies the world a significant source of fiber, feed, foodstuff, oil, and biofuel products. In particular, upland cotton (*Gossypium hirsutum*) provides nearly 95% of those cotton resources. The United States currently ranks as the second largest exporter of upland cotton in the world with

approximately $7.5 billion dollars in its export value in 2017, which is equivalent to 20 million bales of cotton (Workman, 2018). The business revenue stimulated by cotton per year is approximately $120 billion.

In addition to upland cotton (2n = 4x = 52; AADD genome), other cultivated species are *G. barbadense*, *G. arboretum* and *G. herbaceum*. Phylogenetic analysis indicates that upland cotton is the progeny of the diploid species *G. arboreum* (2n = 2x = 26; AA genome) and *G. raimondii* (DD genome), which can be used as references to study the tetraploid genome (Flagel et al., 2012; Yoo and Wendel, 2014). It is believed that the five tetraploid species that we have today diversified from upland cotton. The remaining 45 species are diploids that can be classified into 8 sub-genomes (AA, BB, CC, DD, EE, FF, GG, KK) (Zhai et al., 2015).

1.2.2. Fusarium wilt of cotton

Fusarium wilt of cotton, caused by *Fusarium oxysporum* f. sp. *vasinfectum* (*Fov*), was first identified in the U.S. in 1892 (Atkinson, 1892). The typical symptoms of fusarium wilt in infected plants include brown discoloration of the vascular system, plant stunting and wilting, and eventually necrosis and death (Figures 1A, B, C & D). This pathogen is particularly difficult to control in cotton as the hyphae reside in the woody vascular tissues and produce chlamydospores, which may allow for long-term survival in soil (Cianchetta and Davis, 2015; Sanogo and Zhang, 2016). This fungus is also associated with organic matter and plant residues (Cianchetta and Davis, 2015; Sanogo and Zhang,

2016). The spores spread through soil, plant debris, and seeds, and cannot be eradicated from infested fields.

1.2.3. Different *Fov* races

Fov has been classified into at least eight races initially based on their pathogenicity in cotton and other plant species, but later by sequence differences in genes encoding putative translational elongation factor (EF-1α), phosphate permease-like protein (PHO), mitochondrial small subunit rDNA (mtSSU), nitrate reductase (NIR), β-tubulin (BT), and intergenic spacer (IGS) regions (Appel and Gordon, 1996; O'Donnell et al., 2009). Among them, race 1 (*Fov1*) is often detected with root-knot nematode infections in the field and appears to be predominant in the U.S. (Kim et al., 2005; Wang et al., 2018). Race 4 (*Fov4*), a highly virulent isolate that does not require root-knot nematode to cause significant diseases in the field, was initially identified in California and was reported in a pima cotton field east of El Paso in Texas in 2017 (Halpern et al., 2017; Kim et al., 2005).

1.2.4. Occurrences of Fusarium wilt in the U.S.

The occurrences of Fusarium wilt were managed at relatively low levels until 2014. One possible factor contributing to this may be the planting of specific Deltapine cotton varieties that carry resistance to root-knot nematodes. These varieties (DP 1454NRB2RF, DP 1558NRB2RF, and DP 1747NRB2XF) were introduced from 2014 to 2017. However, these Deltapine cotton varieties were highly susceptible to *Fov1*,

increasing the frequency of this disease (T. Wheeler, personal observations). In regard to *Fov4*, in 2017 it was identified outside of California for the first time since 2001. Since *Fov*4 is highly virulent on most upland cotton, there is concern that it could spread to other cotton growing states if proper disease management practices are not implemented. While it is still unclear how *Fov4* spread to Texas, one potential contributing factor is the transfer of infected seeds. Since it can take several years after *Fov* is introduced in field to observe disease symptoms on cotton plants, it is possible that *Fov*-contaminated seeds were harvested from plants grown in *Fov*-infected fields and transferred to the cotton field in El Paso, Texas. Therefore, it is likely that Fusarium wilt has resurged in the U.S. due to the planting of different cultivars and transferring contaminated seeds. In addition, it remains elusive whether the composition and identity of the *Fov* isolates detected in California and Texas are the same at the whole genome level. There remain open questions whether a genetic virulence shift of these *Fov* isolates contributed to the recurrence.

1.2.5. Genetic basis of Fusarium wilt of cotton

Most of the upland cotton germplasms are susceptible to *Fov4*, though with variable symptoms, indicating a complex and quantitative genetic response (Wang et al., 2018). In addition, the postulated pathogenicity mechanisms and the inheritance of *Fov* resistance significantly differ among *Fov* races for cotton genotypes (Wang et al., 2018). Phenotypic analyses indicated that resistance to *Fov* was determined by one or two major genes with complete to incomplete dominance, and additional minor genes (Ulloa et al., 2013b; Ulloa et al., 2011; Wang and Roberts, 2006). Some strategies used to decrease

fusarium wilt of cotton include controlling the nematode population and the use of cultivars tolerant to *Fov*, although the latest has been achieved more efficiently in Egyptian Pima cotton (*G. barbadense*) than upland cotton (Ogallo et al., 1997).

1.2.6. Molecular mechanisms of *Fov* infection and plant resistance

The molecular mechanism of *Fov* infection in cotton remains largely elusive (Figures 1E & F). *F. oxysporum* f. sp. *lycopersici* (*Fol*), the causal agent of tomato wilt, can secrete a number of virulence effectors, known as Secreted In Xylem (SIX), in the xylem sap of tomato plants to facilitate disease progression (Gawehns et al., 2015; Houterman et al., 2007; Lievens et al., 2009; Ma et al., 2015; Rep et al., 2005). In addition, resistance genes against *Fol* have been identified in tomato (Table 1). Resistance proteins convey plant resistance by direct or indirect interaction with avirulence proteins secreted by pathogens. Although the typical resistance genes encode cytoplasmic Nucleotide-Binding Leucine-Rich Repeat (NB-LRR) proteins, cell surface-resident receptors such as RLPs and RLKs also play an important role in plant disease resistance (Jones and Dangl, 2006). So far, both NB-LRR and RLK/RLP proteins have been identified to confer resistance against *Fol* in tomato (Table 1). Notably, putative SIX orthologs have been identified in *Fov* (Chakrabarti et al., 2011) and the orthologs of some of the resistance genes exist in cotton. It is possible that a similar mechanism partly contributes to the *Fov*-cotton interaction (Figure 1F). Systematical examination of the repertoire and functions of resistance genes in cotton by targeted capture sequencing and expression profiling in diverse cotton species/cultivars with differential *Fov* responses provides a promising

approach to develop markers and identify resistance genes associated with fusarium wilt diseases. Furthermore, *F. oxysporum* was reported to hijack the plant defense hormone jasmonic acid (JA)-signaling pathway in Arabidopsis to cause wilting, however, the role of JA in tomato response to fusarium wilt was not observed (Di et al., 2017; Thatcher et al., 2009).

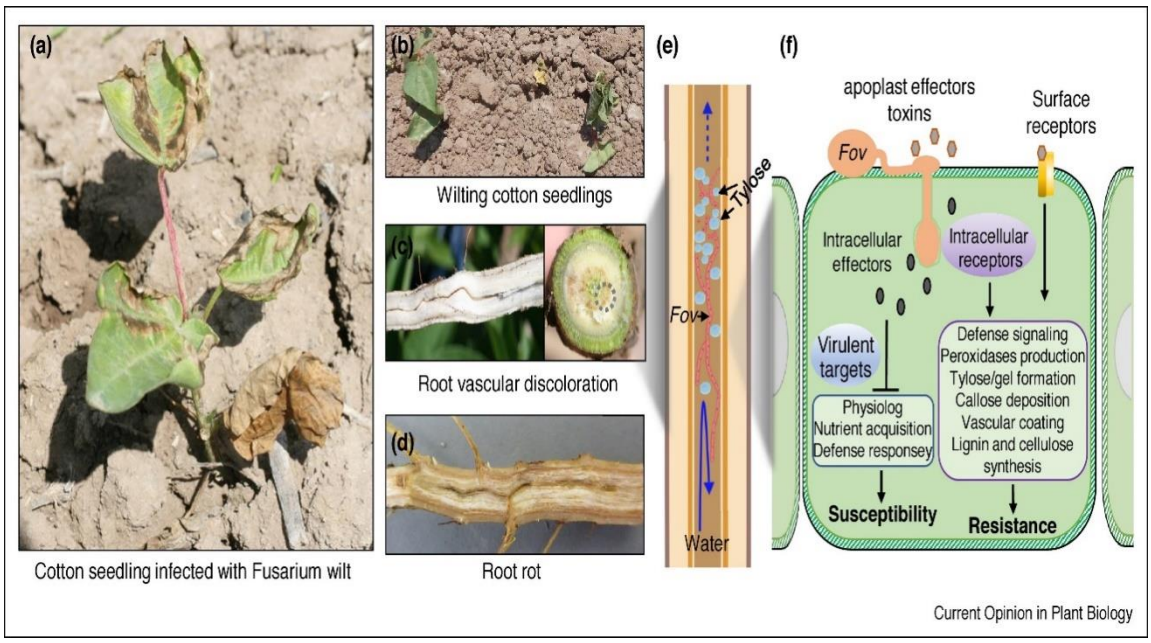

Figure 1. The battleground between Fusarium and cotton plants. (Cox et al., 2019; reprinted)
The typical symptoms of Fusarium wilt in infected cotton include plant stunting, leaf chlorosis and necrosis (a), seedling wilting (b), brown discoloration of the vascular system (c) and root rot (d). The wilting symptom may occur due to *Fov* occupying the xylem vessels or plant tylose, callose or gels produced as a defense mechanism to prevent the pathogen from spreading, thereby obstructing the water and nutrient flow of the host (e). At the cellular level, pathogens secrete apoplastic or intracellular effectors or toxins to cause disease, whereas plants use cell surface or intracellular immune receptors to recognize these effectors or other elicitors to induce defense responses (f).

Table 1. Resistance genes against Fusarium species (Cox et al., 2019; reprinted)

Resistance gene	Gene identity	Host	Cognate avirulence gene	*Fusarium* species	Reference
I-1	Unknown	Tomato	*SIX4*	*F. oxysporum* f. sp. *lycopercisi*	*(Bohn and Tucker, 1939; Houterman et al., 2008)*
I-2	CC-NBS-LRR	Tomato	*SIX3, SIX5*	*F. oxysporum* f. sp. *lycopercisi*	*(Ma et al., 2015)*
I-3	Receptor-like kinase	Tomato	*SIX1*	*F. oxysporum* f. sp. *lycopercisi*	*(Catanzariti et al., 2015)*
I-7	Receptor-like protein	Tomato	Unknown	*F. oxysporum* f. sp. *lycopercisi*	*(Gonzalez-Cendales et al., 2016)*
RFO1	Receptor-like kinase	*Arabidopsis*	Unknown	*F. oxysporum* f. sp. *matthioli*	*(Diener and Ausubel, 2005)*
RFO2	Receptor-like protein	*Arabidopsis*	Unknown	*F. oxysporum* f. sp. *matthioli*	*(Shen and Diener, 2013)*
RFO3	Receptor-like kinase	*Arabidopsis*	Unknown	*F. oxysporum* f. sp. *matthioli*	*(Cole and Diener, 2013)*
FOV1	Unknown	*Gossypium barbadense* Pima S-7	Unknown	*F. oxysporum* f. sp. *vasinfectum* race 1	*(Ulloa et al., 2011; Wang and Roberts, 2006)*
FOV4	Unknown	*Gossypium barbadense* Pima S-6	Unknown	*F. oxysporum* f. sp. *vasinfectum* race 4	*(Ulloa et al., 2013b)*

1.2.7. *Fov* infection process

Fusarium wilt in cotton results in blackened vascular tissue at the later stages of infections (Davis et al., 2006). However, the cause of the blackening remains unknown and it appears that the infected plants suffer from alteration of water transports in vascular tissues via either dehydration or excessive water (Yadeta and Thomma, 2013). For *Fov4* infection, the severity of blackening (brown vs. black) of the root necrosis depends on different cotton cultivars and possibly different inoculum densities. *Fov* tends to rapidly

establish and accumulate in the xylem once entering the plant root, and microconidia can disseminate with xylem sap movements (Yadeta and Thomma, 2013). At the later stages of infection, a fungal mat can develop within the xylem, causing parts of the vascular tissue to blacken in the stem. It is speculated that the fungus remains in the xylem to feed on secondary nitrogen sources and sugars released by degradation of cell wall components (Divon et al., 2006). The "wilting" symptom likely occurs due to *Fov* occupying the xylem vessels, thereby obstructing the water and nutrient flow of the host (Yadeta and Thomma, 2013). Alternatively, the "wilting" symptom could be a lethal side effect of the plant activating a defense response to *Fov*. In an attempted effort to prevent the pathogen from spreading to adjacent xylem vessels, plants produce tyloses, callose, gums, and gels to seal off the pathogen (Beattie, 2011; Yadeta and Thomma, 2013). However, this can also cause the host to be more susceptible to drought stress, which results in wilting (Beattie, 2011).

1.2.8. Elevated humidity and temperature accelerate disease progression.

The disease triangle model remains a core principal of plant pathology as it describes the complex interactions among the environment, the pathogen, and the plant, and explains the seasonal dynamics of disease variabilities in the field. An optimal environment is essential for a virulent pathogen to cause disease in a susceptible plant. Global climate changes with a trend of warming and unstable weather conditions, such as flooding, are playing an increasing role in disease epidemics. Notably, fusarium wilt has historically been more destructive to cotton fields in climates with an elevated temperature and humidity (Scott et al., 2010). Additionally, high humidity is an important factor for

spore germination in *Fusarium spp.* and increased conidia counts are present under constant humid conditions (Gracia-Garza and Fravel, 1998). Increased soil moistures with heavy rainfalls, particularly in the early planting season, foster an optimal environment for fusarium wilt to develop and spread rapidly. Studying the effects of environmental factors on the virulence of this pathogen will help further describe its molecular mechanisms of infection, progression, and direct effective disease management in the field.

1.2.9. Strategies to manage Fusarium wilt and improve resistance in cotton

Fusarium wilt in much of the U.S. was managed primarily by applying the nematicide aldicarb at planting, and later by utilizing partial resistance to root-knot nematode (primarily with certain Stoneville varieties) since some *Fov* races require root-knot nematode to enhance disease. Management of Fusarium wilt races that do not require root-knot nematode has been more difficult historically because of the few cultivars that were truly effective (Cianchetta and Davis, 2015). In 2017, Fusarium wilt of cotton caused a yield loss of about $25 million U.S. dollars. The increasing yield loss in each subsequent year has generated a pressing need to understand the pathological and molecular mechanisms of the disease in order to develop new strategies for biological control.

Disease control of fusarium wilt in cotton is challenging because this pathogen resides in the woody vascular tissues as well as seeds. Crop rotation and use of fungicides are generally not successful for control of fusarium wilt. For *Fov* races that require root-knot nematodes to cause significant disease in the field, control of the nematode can be

effective. However, the link between nematode resistant cultivars and *Fov* management was broken with several root-knot nematode resistant cultivars that were introduced starting in 2014 (DP 1454NRB2RF, DP 1558NRB2RF, and DP 1747NRB2XF). These cultivars had heightened sensitivity to *Fov* and were more susceptible than "normal" susceptible cultivars. There are no effective resistant cultivars available for upland cottons against *Fov4* which does not require nematodes to cause disease in the field. A strong source of resistance was initially found against *Fov4* in Pima cotton PHY 800, which originated from Pima S-6 (Ulloa et al., 2013a). The mechanisms mediating this resistance have not been determined, although it does reduce the fungal biomass in the stem and the plants are not significantly affected by high soil inoculum density of the fungus (Hao et al., 2009).

Resistance (*R)* genes provide a robust counter attack against pathogens (Kourelis and van der Hoorn, 2018). However, *R* genes have not been well-characterized in cotton, especially against *Fov*. This may be partly due to the complexity of the tetraploid genome of upland cotton. Resistance to *Fov* is mainly controlled by quantitative trait loci (QTLs). Two cotton lines of *G. barbadense*, Pima S-6 and S-7, carry QTLs against *Fov4* and *Fov1*, respectively (Ulloa et al., 2013b; Ulloa et al., 2011). In addition, there appears to be additional QTLs in *G. hirsutum* and *G. barbadense* mediating resistance to *Fov* (Wang et al., 2018). In the *Fov* pathosystem, there are cotton cultivars that are resistant against a specific race but are still susceptible to other races. For example, Pima S-7 is resistant to *Fov1* but susceptible to *Fov4* (Wang et al., 2018). Similarly, the *G. hirsutum* cultivar Acala NemX, a nematode resistant cultivar, is more tolerant to *Fov4* but susceptible to *Fov1*

(Hao et al., 2009; Ulloa et al., 2013b; Ulloa et al., 2011; Wang and Roberts, 2006). However, none of the genes or QTLs has been identified or functionally characterized, and the mechanisms of resistance in these tolerant cotton lines remain unknown.

1.3. Fusarium Elicitors

To date, many elicitors have been isolated and identified from various organisms including bacteria, fungi, oomycete and viruses. These elicitors include proteins, peptides, lipids and oligosaccharides (Chen et al., 2012). It has been reported that a cell wall preparation from *Fusarium oxysporum* f.sp. *matthioli* race 1 functions as an elicitor that can induce ROS production in Arabidopsis, although the identity of the elicitor is unknown (Davies et al., 2006). Similarly, the protein elicitor PeFOC1 from *Fusarium oxysporum* f. sp. *cubense* (FOC), which infects banana, can trigger defense responses in tobacco (Li et al., 2019). Furthermore, an oligochitosan elicitor from *Fusarium sambucinum*, one of the causal agents of potato dry rot, induces defense responses in *Zanthoxylum simulans* (Rutaceae) (Li et al., 2016b).

1.4. Objective and Importance for the Study

Cotton losses due to fungal infections have an enormous impact on the economy and societal stability. To date, the use of cultivars with tolerance to *Fov* has been one of the most successful strategies to control the disease, however, the mechanism and genetic identity of cotton resistance to this devastating disease remain elusive. In plants, RLPs play a major role in resistance to different fungal pathogens, including Fusarium, as

discussed earlier. These findings point toward the significance of RLPs not only in cotton resistance to *Fov*, but also broad-spectrum resistance against different fungal pathogens.

In this work, I aim to elucidate the genetic and molecular basis of cotton response to *Fov* infections, and to utilize genetic resources to control the disease. In particular, I focus on the role of RLPs due to their contributions in plant defense against fungal pathogens in different plant species. By combining bioinformatic analysis, molecular and biochemical characterization, and high-throughput virus-induced gene silencing (VIGS)-based functional genomics, I aim to understand RLP-mediated cotton resistance to *Fov*. Furthermore, I aim to identify and characterize components in Fusarium that can trigger immune response in cotton and Arabidopsis. These findings can provide effective tools to control Fusarium wilt of cotton through breeding and genetic engineering of *Fov* resistant cotton varieties.

2. COMPUTATIONAL, FUNCTIONAL AND BIOCHEMICAL GENOMICS OF RECEPTOR-LIKE PROTEIN (RLP)-MEDIATED DEFENSE IN FUSARIUM WILT OF COTTON

2.1. Summary

Fusarium wilt of cotton, caused by *Fusarium oxysporum* f. sp. *vasinfectum* (*Fov*), is a major destructive disease which represents a major threat to cotton industry. Because the conventional biological and chemical controls are not efficient against newly emerging *Fov* isolates, understanding the genetic basis of Fusarium wilt and cotton interactions could provide insights to control the disease. To respond to pathogen attacks, plants have evolved a sophisticated immune system. To date, a large number of plant immune receptors conferring resistance to fungal pathogens belong to the plasma membrane-localized receptor-like proteins (RLPs) with an extracellular domain that recognizes specific pathogen signatures. Upon perception of pathogen signatures, RLPs induce a series of defense responses, including massive transcriptional re-programming, in fending off pathogen attacks. In this study, I used an integrative genomic and molecular approach to identify and understand the functions of cotton RLPs in response to *Fov* infections at the whole genome level. Based on the in-silico prediction of potential RLP candidates in different cotton genomes, I systemically silenced 39 RLPs in upland cotton (*Gossypium hirsutum* L.) with virus-induced gene silencing (VIGS). Among them, silencing of seven in cotton showed reduced resistance to *Fov* infections, whereas silencing of one showed reduced susceptibility to *Fov* infections, suggesting that RLPs could play both positive

and negative roles in cotton response to *Fov*. Silencing of two RLPs showed reduced immune responses, including mitogen-activated protein kinase (MAPK) phosphorylation, reactive oxygen species (ROS) burst and ethylene biosynthesis, to the conserved pathogen-associated molecular patterns (PAMPs), supporting a molecular mechanism of these several RLPs in cotton resistance to *Fov*.

2.2. Introduction

Cotton is an economically important crop that supplies the world a significant source of fiber, feed, foodstuff, oil, and biofuel products. The majority of cotton lint is produced by the tetraploid species *Gossypium hirsutum* (Upland) and *Gossypium barbadense* (Pima), although *G. hirsutum* provides nearly 95% of all cotton resources (Cox et al., 2019). Unfortunately, several fungal diseases represent expanding threats to cotton production. In particular, *Fusarium oxysporum* f. sp. *vasinfectum (Fov)*, the causal agent of Fusarium wilt, is of concern to growers due to the severe economic losses attributed to it (Cianchetta and Davis, 2015; Sanogo and Zhang, 2016). The typical symptoms of fusarium wilt in infected plants include brown discoloration of the vascular system, plant stunting and wilting, and eventually necrosis and death. This pathogen is particularly difficult to control in cotton due to the hyphae residing in the woody vascular tissues, its long-term survival in soil, and its association with organic matter (Cianchetta and Davis, 2015; Sanogo and Zhang, 2016).

Plants defend against their associated pathogens by sensing the presence of pathogen/microbe-associated molecular patterns (PAMP/MAMP) through the cell

surface-localized pattern recognition receptors (PRRs). Well-studied PAMPs include the 22-amino-acid peptide flg22 which corresponds to a region near the amino-terminus of flagellin, the bacterial elongation factor EF-Tu, and the fungal cell wall component chitin (Afzal et al., 2008; Boller and Felix, 2009; Gish and Clark, 2011; Newman et al., 2013). Plant PRRs can be divided in receptor-like kinases (RLKs) and receptor-like proteins (RLPs). RLKs are transmembrane kinases similar to the tyrosine kinases (RTKs) in animals, structurally containing a ligand-binding extracellular domain (ECB), a single-transmembrane domain, and a cytoplasmic kinase domain (Shiu and Bleecker, 2001). The structure of an RLP is essentially that of an RLK without the cytoplasmic domain, and resembles the Toll-like receptors in animals (Medzhitov et al., 1997). The majority of RLPs and RLKs possess extracellular leucine-rich repeat (LRR) domains in the ECD region which can recognize a wide range of ligands (Dangl and Jones, 2001; Tang et al., 2017). The downstream responses of PRRs lead to pattern-triggered immunity (PTI), including the activation of protein kinases, callose deposition, reactive oxygen species (ROS) bursts, ethylene biosynthesis, root inhibition, callus deposition, defense gene transcription, and others (Boller and Felix, 2009; Li et al., 2016a; Macho and Zipfel, 2014; Zeidler et al., 2004; Zipfel et al., 2004).

RLP- and RLK-mediated PTI is important for plant basal defense to a broad spectrum of pathogens and some RLPs and RLKs have been classified as “Resistance” (R) genes, which are thought to have coevolved to defend against specific pathogen races as defined in the “gene-for-gene” hypothesis (van der Does and Rep, 2007). Interestingly, several LRR-RLPs play a major role in plant defense against fungal pathogens, including

Fusarium, in different plant species. For instance, the Arabidopsis RLP23 binds and recognizes the conserved amino acid peptide nlp20 from NECROSIS AND ETHYLENE-INDUCING PEPTIDE1 (NEP1)-LIKE PROTEINS (NLPs) which is conserved among *Fusarium oxysporum* isolates and other microbes (Albert et al., 2015). Furthermore, RLPs I-1 and I-7 in tomato confer resistance to *F. oxysporum* f.sp. *lycopersici* (De Wit, 2016), and the Arabidopsis RESISTANCE TO FUSARIUM OXYSPORUM 2 (RLP3/RFO2) confers resistance to multiple species of *Fusarium* (Diener and Ausubel, 2005; Shen and Diener, 2013). Other LRR-RLPs important in fungal resistance include the Arabidopsis ReMAX, RLP30, RLP42/RBPG1, RLP51/SNC2, and RLP52 (Jehle et al., 2013; Ramonell et al., 2005; Wang et al., 2008; Zhang et al., 2014; Zhang et al., 2010), the tomato Cf-4/9, Ve1/2, and Eix1/2 (Kawchuk et al., 2001; Postma et al., 2016; Rivas and Thomas, 2005; Ron and Avni, 2004; Stergiopoulos and de Wit, 2009), the apple Vfa1/2 (Malnoy et al., 2008), the rapeseed LepR3, Lm1 and RLM2 (Larkan et al., 2013; Larkan et al., 2015), and the potato ELR (Du et al., 2015).

In addition to their role in immunity, RLPs also regulate growth and development. The Arabidopsis LRR-RLP TOO MANY MOUTHS (TMM) is involved in the regulation of stomal patterning as shown in the disrupted patterning and asymmetric cell division in the leaves of the *tmm* mutant (Nadeau and Sack, 2002; Shpak et al., 2005). Moreover, the Arabidopsis RLP44 is involved in the brassinosteroid (BR) hormone signaling pathway and is required for normal growth and stress responses (Wolf et al., 2014). In addition, the Arabidopsis CLAVATA2 (CLV2) and its maize counterpart regulate the shoot apical

meristem proliferation and other physiological responses (Ogawa et al., 2008; Pan et al., 2016; Taguchi-Shiobara et al., 2001).

The increasing yield loss of cotton due to Fusarium wilt has generated a pressing need to understand the pathological and molecular mechanisms of the disease to develop new strategies for biological control. It is known that *R* genes provide a robust counter attack against pathogens (Kourelis and van der Hoorn, 2018). However, *R* genes have not been well-characterized in cotton, especially against *Fov*. In this work, we aimed to elucidate the genetic and molecular basis of cotton response to *Fov* infections by combining bioinformatic analysis, high-throughput virus-induced gene silencing (VIGS), and functional analysis to study RLPs. We identified 55 and 31 LRR-RLPs in the D-subgenome and A-subgenome of *G. hirsutum*, respectively. Our reverse genetics screens identified seven positive regulators of defense against *Fov* infections, two of which play an important role in PAMP-induced PTI responses. We also report *GhRLP2* as an *AtRLP44* ortholog and demonstrate that these genes may have similar functions in immunity. These findings can provide effective tools to control Fusarium wilt of cotton through breeding and genetic engineering efforts to produce *Fov* resistant cotton varieties.

2.3. Material and Methods

2.3.1. Plant materials and growth conditions

Arabidopsis accession Col-0 (WT) and the *rlp44* mutant used in this study were grown in soil (Metro Mix 366) in a growth room at 23°C, 60% relative humidity, 70 μmoles $m^{-2}s^{-1}$ light with a 12-hr light/12-hr dark photoperiod for four weeks. The *rlp44*

mutant (CS825413) was obtained from the Arabidopsis Biological Resource Center (ABRC) and confirmed by PCR. Seedlings were grown on agar plates containing half-strength Murashige and Skoog medium (½MS) with 0.5% sucrose, 0.8% agar and 2.5 mM MES at pH 5.7, in a growth chamber at 23°C, 70 μE $m^{-2}s^{-1}$ light with a 12-hr light/12-hr dark photoperiod. *Gossypium hirsutum* cv CA 4002 (PI 665226) was grown in 3.5-inch square pots containing soil (Jolly Gardener PRO-LINE C/25) in a controlled growth chamber at 23°C, 30% relative humidity and 100 μmol m^{-2} s^{-1} light with a 12-h light/12-hr dark photoperiod. One-week-old cotton plants were used for *Agrobacterium*-mediated VIGS assay or protoplast isolation.

2.3.2. *Agrobacterium tumefaciens*-mediated VIGS

The VIGS system is an RNAi-based gene silencing process. A fragment of the gene to be silenced is inserted into a vector which also encodes a coat protein (pTRV-RNA2). The Agrobacterium carrying the pTRV-RNA2 constructs is co-inoculated into the plants together with an Agrobacterium carrying the pTRV-RNA1 construct, which encodes replicase and movement proteins. Fragments (300-500bp) of *GhRLPs* were amplified by PCR from cDNA with primers described in Table 5 and inserted into the *pYL156* (pTRV-RNA2) vector with restriction sites *Eco*RI and *Kpn*I. The agrobacterial cultures carrying pTRV-RNA1 and the above pTRV-RNA2 constructs were resuspended in infiltration buffer (10 mM MES, pH 5.7, 10 mM MgCl2, 200 μM acetosyringone). *A. tumefaciens* pTRV-RNA1 was mixed with pTRV-RNA2 at a 1:1 ratio to a final OD_{600} of 0.75 each and hand infiltrated into two fully expanded cotyledons of one-week-old soil-

grown plants (Gao et al., 2011; Gao et al., 2013). At least 12 plants were inoculated for each construct. The pYL156-*GhCla1* construct was included as a visual marker for VIGS efficiency. The silencing of the gene of interest was confirmed by RT-PCR.

2.3.3. MAPK assay

Three leaf discs from individual 3-week-old cotton plants were ground in 100 μl 1× SDS buffer (62.5 mM Tris-HCl, pH 6.8, 1% SDS, 0.025% bromophenol blue, 10% glycerol, 1× protease inhibitor, 2 μl 1 M NaF and 2 μl 1 M Na_3VO_4 for 1 ml of buffer), heated at 95°C for 5 min, and centrifuged to collect the supernatant. For Arabidopsis, 10-day-old seedlings germinated on ½MS plate were transferred to 2 ml H_2O in a 12-well plate overnight for recovery, and treated with 1 mg/ml FovCWE, 1×10^7/ml *Fo47* spores, 100nM flg22, or 100 mg/ml chitin. The seedlings were ground in IP buffer (10 mM HEPES (pH 7.5), 100 mM NaCl, 1 mM EDTA, 10% glycerol, 1% protease inhibitor cocktail), centrifuged, and the cleared lysate was mixed with SDS buffer. For protoplasts, 100 μl of the 1× SDS buffer were added to lysed cells, boiled at 95°C for 5 min, and centrifuged to collect the supernatant. Proteins were separated in a 10% sodium dodecyl sulfate–polyacrylamide gel electrophoresis (SDS-PAGE) gel and activated MAPKs were detected by immunoblotting with phosphorylated Extracellular Regulated protein Kinases (α-pERK1/2) antibodies (Cell Signaling, USA).

2.3.4. ROS analyses

ROS burst was determined by a luminol-based assay. 24 leaves of three-week-old cotton plants were excised into leaf discs of 0.25 cm^2, cut into five strips with a razor blade, and incubated in a 96-well plate with 100 µl of H_2O for recovery. H_2O was then replaced by 100 µl of a reaction solution containing 50 µM luminol, 10 µg/ml horseradish peroxidase (Sigma, USA), and 0.1 mg/ml chitin. The measurements were conducted immediately in a luminometer (Perkin Elmer, 2030 Multilabel Reader, Victor X3) after adding the solution. Each sample was measured 30 times with a 1 min interval between reads. The measurement values for ROS production from 24 leaf discs were indicated as means of Relative Light Units (RLU).

2.3.5. Ethylene biosynthesis

Twelve leaves of four-week-old Arabidopsis plants or 3-week-old cotton plants were excised into leaf discs of 0.25 or 0.50 cm^2, respectively, followed by overnight incubation in a 25 ml glass vial with 1ml of H_2O for recovery. The H_2O was then replaced by 1ml of FovCWE (1 mg/ml) or chitin (0.1 mg/ml) and the vials were capped immediately with a rubber stopper and incubated at room temperature with gentle agitation. One ml of the vial headspace was injected into a PhotoVac 10sPlus Gas Chromatography with photoionization detector (PID) at the indicated time points.

2.3.6. Measurements of Stomatal Aperture

Stomatal aperture was measured on epidermal peels excised from the abaxial side of leaves of three-week-old cotton plants as described in (Rodrigues et al., 2017). Epidermal peels from three independent plants were first incubated for 30 min in darkness in a bathing solution containing 30 mM KCl and 10 mM MES/Tris pH 6.0, followed by exposure to white light in a growth chamber (120μmoles m^{-2} s^{-1}) for 180 min to induce maximal stomatal opening. FovCWE (1 mg/ml) was added to the bathing solution and stomatal aperture was monitored during the next 180 min in >60 stomata for each independent repetition. Average inner stomatal aperture was measured using Image J (http://rsb.info.nih.gov/ij/).

2.3.7. Pathogen assays

Fusarium oxysporum f. sp. *vasinfectum* race 1 (CA10/*Fov1*) was cultured for four days in Potato Dextrose Broth (Difco) and the spores were collected by culture filtration using two layers of cheese cloth. Spores were centrifuged and resuspended in H_2O at a concentration of 1×10^7/ml. Four-week-old cotton plants were inoculated with *Fov* (1×10^7 conidia/ml) using the root dipping technique by submerging the roots in the spore solution for five min. Plants were transferred back to the 3.5-inch square pots with soil and left at room temperature overnight before moving them to a growth chamber at 28°C, 50% humidity and 100 μE $m^{-2}s^{-1}$ light with a 12h photoperiod. At least 12 plants were inoculated per treatment. The disease ratio was calculated as the percentage of wilting plants to the total infected plants. The disease levels among all the plants per treatment

were calculated at the last time point. For *Arabidopsis* infections, four-weeks-old plants were root dipped with *Fusarium oxysporum* 5178 (1×10^7 conidia/ml) for five min. Plants were transferred back to soil in a growth room at 23 °C, 60% relative humidity, and 75 $\mu Em^{-2}s^{-1}$ light with a 12 hr photoperiod. *Pseudomonas syringae* pv. *tomato* (*Pst*) DC3000 *hrcC* was cultured overnight at 28°C in King's B medium with 50 µg/ml rifampicin. Bacteria were harvested by centrifugation, washed, and adjusted to $OD_{600}=1\times10^{-5}$ with 10 mM $MgCl_2$. Leaves of four-week-old plants were inoculated with *Pst* DC3000 *hrcC* using a 1-ml needleless syringe. To measure bacterial growth, two leaf discs were ground in 100 µl dH_2O and serial dilutions were plated on TSA medium (1% Bacto tryptone, 1% sucrose, 0.1% glutamic acid, 1.5% agar) with appropriate antibiotics. Bacterial colony forming units (CFU) were counted two days after incubation at 28°C. Each data point is the average of three replicates.

2.3.8. RNA isolation and RT-PCR

RNA was extracted from leaves of four-week-old plants using TRIzol reagent (Life Technologies, USA) and quantified with a NanoDrop spectrophotometer. The RNA was treated with RQ1 RNase-free DNase I (Promega, USA) for 30 min at 37°C, and then reverse transcribed with M-MuLV Reverse Transcriptase (NEB, USA). Real-time RT-PCR was carried out using iTaq Universal SYBR Green Supermix (Bio-Rad, USA) on a 7900HT Fast Real-Time PCR System (Applied Biosystems, USA). The primers used to detect specific transcript by real-time RT-PCR are listed in Table 5.

2.3.9. Protoplast isolation

Cotton protoplasts were isolated from cotyledons of one-week-old seedlings. Detached cotyledons were cut with a razor blade and digested in an enzyme solution (1.5% cellulose R10, 0.4% macerozyme R10, 0.4 M mannitol, 20 mM KCl, 20 mM MES pH 5.7) supplemented with 2% sucrose for 0.5 hr under vacuum. Arabidopsis protoplasts were isolated from leaves of four-week-old plants. Detached leaves were cut with a razor blade and digested in the above enzyme solution without sucrose for 0.5 hr under vacuum. Subsequently, the enzyme solutions were incubated without vacuum at room temperature for 3-6 hr. Protoplasts were released by filtering through a 30 μm-nylon mesh, then washed with W5 solution (154 mM NaCl, 125 mM CaCl2, 5 mM KCl, 2 mM MES pH 5.7), and diluted in MMG solution (0.4 M mannitol, 15 mM MgCl2, 4 mM MES pH 5.7) to a density of 2×10^5 cells/ml (Gao et al. 2011). An aliquot of 200 μl of protoplasts for each sample was used for MAPK treatment.

2.3.10. Protoplast transfection and reporter assay

The *GhRLP2* gene was amplified from *G. hirsutum* (CA 4002) with primers containing *Bam*HI at N-terminus and *Stu*I at C-terminus (Table 5), and ligated into a plant protoplast expression vector *pHBT* with a CaMV 35S promoter at N-terminus and Flag epitope-tag at C-terminus. Protoplast transient expression were carried out as reported previously (He et al., 2006). Arabidopsis protoplasts were transfected with Flag-tagged *GhRLP2* and *pFRK1::LUC*, followed by PAMP treatment for another four hours. *UBQ10-GUS* was always co-transfected with *FRK1::LUC* as an internal control, and the promoter

activity was presented as LUC/GUS ratio. Protoplasts transfected with plasmid DNA without *GhRLP2* were used as controls. For MAPK, Arabidopsis and cotton protoplasts were transfected with Flag-tagged *GhRLP2* and incubated for 7 hr. 200ul of protoplasts were treated with PAMPs for 15 and 30 min, and proteins were isolated with 2 x SDS loading buffer and subjected to immunoblot analysis.

2.3.11. Bioinformatic analysis

RLP amino acid sequences were aligned using MUSCLE and the resulting alignment was used to produce the evolutionary history using the Maximum Likelihood method and JTT matrix-based model. Initial tree(s) for the heuristic search were obtained automatically by applying Neighbor-Join and BioNJ algorithms to a matrix of pairwise distances estimated using a JTT model, and then selecting the topology with superior log likelihood value. These analyses were conducted using MEGA X.

2.4. Results

2.4.1. Bioinformatic prediction of cotton LRR-RLPs

To date, several RLPs have been identified as key players in plant fungal defense (Albert et al., 2015; Diener and Ausubel, 2005; Gijzen and Nurnberger, 2006; Kawchuk et al., 2001; Oome and Van den Ackerveken, 2014; Postma et al., 2016; Shen and Diener, 2013). In order to understand the importance of cotton RLPs in Fusarium wilt of cotton, we conducted a genome-wide bioinformatic search of LRR-RLPs in *G. hirsutum*. The set of 57 known LRR-RLPs in Arabidopsis were used as a query dataset for a BLASTp search

(NBI dataset; https://www.cottongen.org/). From the resulting hits, genes which contained a kinase domain of any kind as predicted by InterProScan HMM-based domain prediction software were removed. Next, genes without an extracellular LRR domain were also removed, and "Transmembrane Helices; Hidden Markov Model" (TMHMM) was used to confirm the correct protein topology in the resulting dataset. This analysis was repeated in the genome sequences of *G. arboreum* and *G. raimondii* (NBI dataset; https://www.cottongen.org/). We identified 55 and 31 RLPs in the D-subgenome and A-subgenome of *G. hirsutum*, respectively, 40 RLPs in *G. arboreum*, and 55 in *G. raimondii*. The tetraploid *G. hirsutum* originated from interspecific hybridization between the diploid species *G. arboreum* (A-genome) and *G. raimondii* (D-genome) (Xiang et al., 2017). Because *G. raimondii* is more resistant to fungal pathogens than *G. arboretum* (Xiang et al., 2017; Yingfan et al., 2009), and because there are more LRR-RLPs in the *G. hirsutum* D-subgenome than the A-subgenome, we decided to focus on the D-subgenome of *G. hirsutum* for further analysis. When constructing a phylogenetic tree using GhRLPs from the D-subgenome of *G. hirsutum* (black) and Arabidopsis (green), we can observe that AtRLPs with a known function interleave with their corresponding cotton orthologs on the northside part of the tree (Figure 2). However, the majority of the cotton and Arabidopsis RLPs have radiated and expanded their own gene families in directions which are not convergent for the most part.

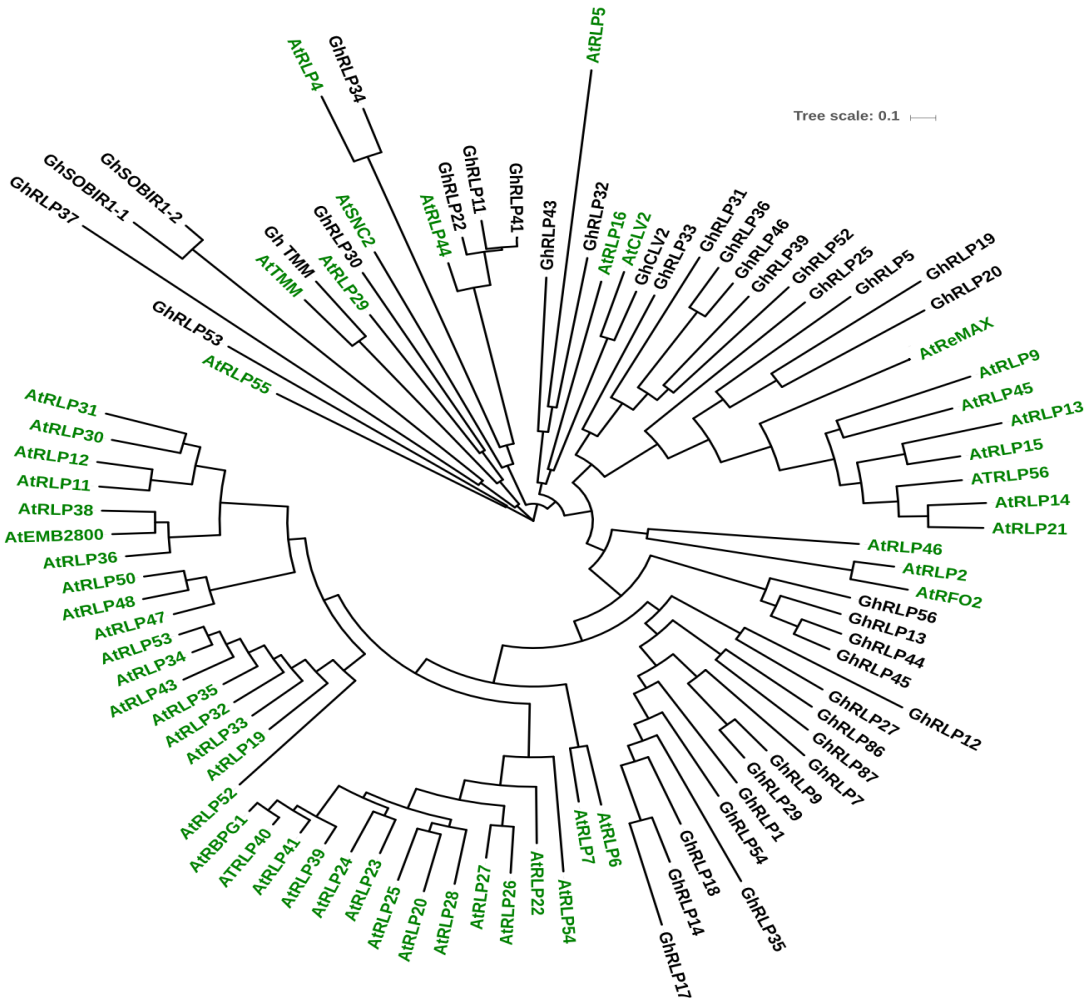

Figure 2. Phylogenetic tree depicting relatedness of Arabidopsis and *G. hirsutum* LRR-RLPs.
GhRLPs (black) can be seen to interleave with their probable Arabidopsis orthologs (green).

2.4.2. LRR-RLP gene family evolution is asymmetrical between *G. hirsutum* subgenomes

We detected the numbers of LRR in the RLPs by using LRRsearch (Bej et al., 2014), LRRfinder (Offord et al., 2010), and CDD: NCBI's conserved domain database (Marchler-Bauer et al., 2015). Arabidopsis and cotton LRR-RLPs show a similar distribution in ectodomain repeat content (Figure 3). However, cotton has more LRR-RLPs in the 4-10 repeat length range than Arabidopsis (Figure 3B,C).

2.4.3. Homeologous connections between *G. raimondii* and *G. hirsutum* D-subgenome

A circos plot was constructed (Yu et al., 2018) by finding the RLPs in both *G. raimondii* and *G. hirsutum* D-subgenomes that shared the most identity with each other with a minimum of 75% identity (Figure 4). The chromosome names are from the numbering used in NCBI and cottongen (https://www.cottongen.org/). We can observe that RLPs often cluster to sub-telomeric regions of the chromosomes they are in, and that the RLPs that are close to the centromere often contain a homeolog that is also close to the centromere. Also, sub-telomeric RLPs often come in clusters, suggesting that their position facilitates the generation of paralogs.

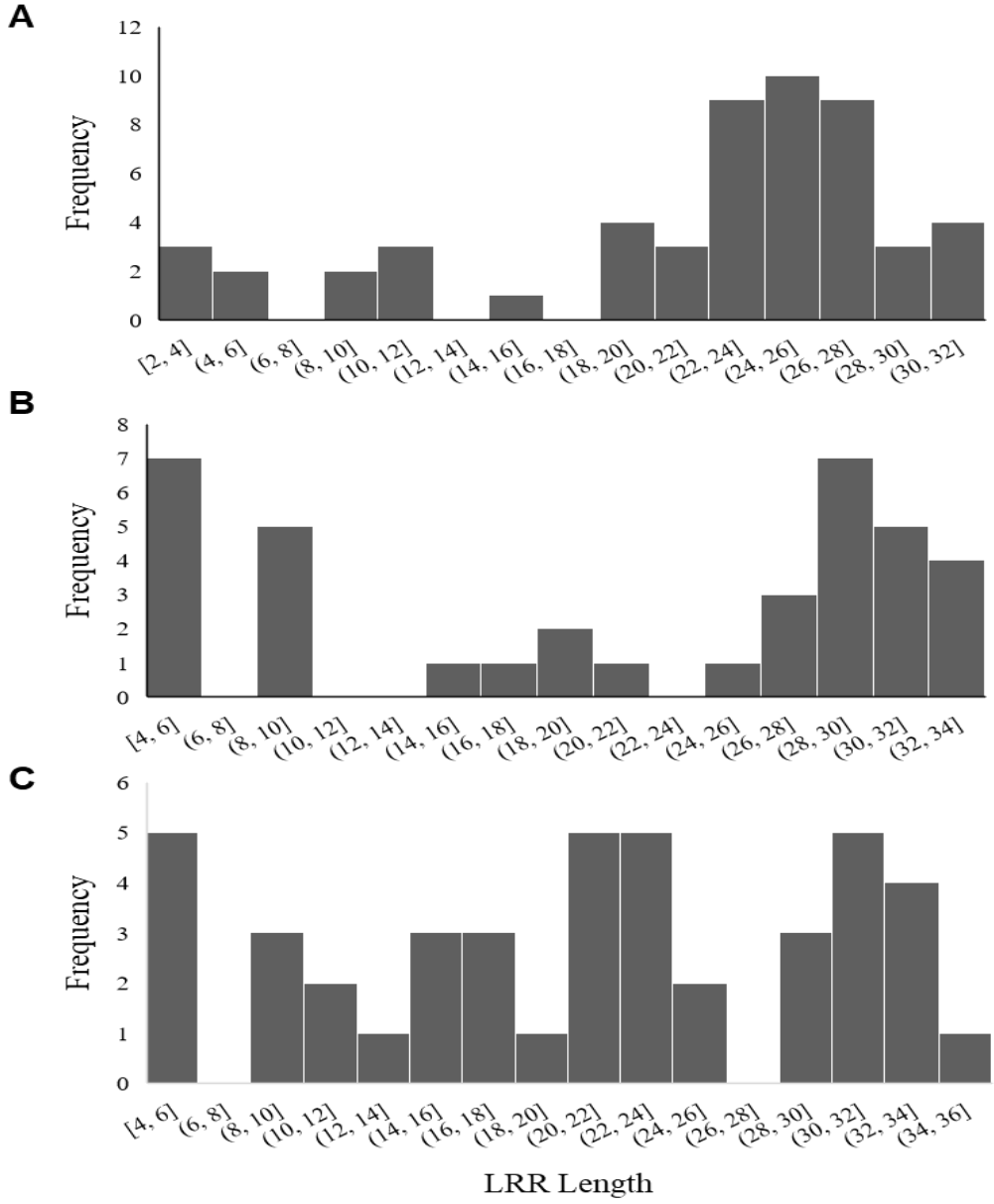

Figure 3. Histograms depicting frequency of repeats in LRR-RLP ectodomains for Arabidopsis, *G. hirsutum* A-subgenome, and *G. hirsutum* D-subgenome.
(A) LRR distribution in Arabidopsis RLPs. (B) LRR distribution in *Gh* D-subgenome RLPs. (C) LRR distribution in *Gh* A-subgenome RLPs.

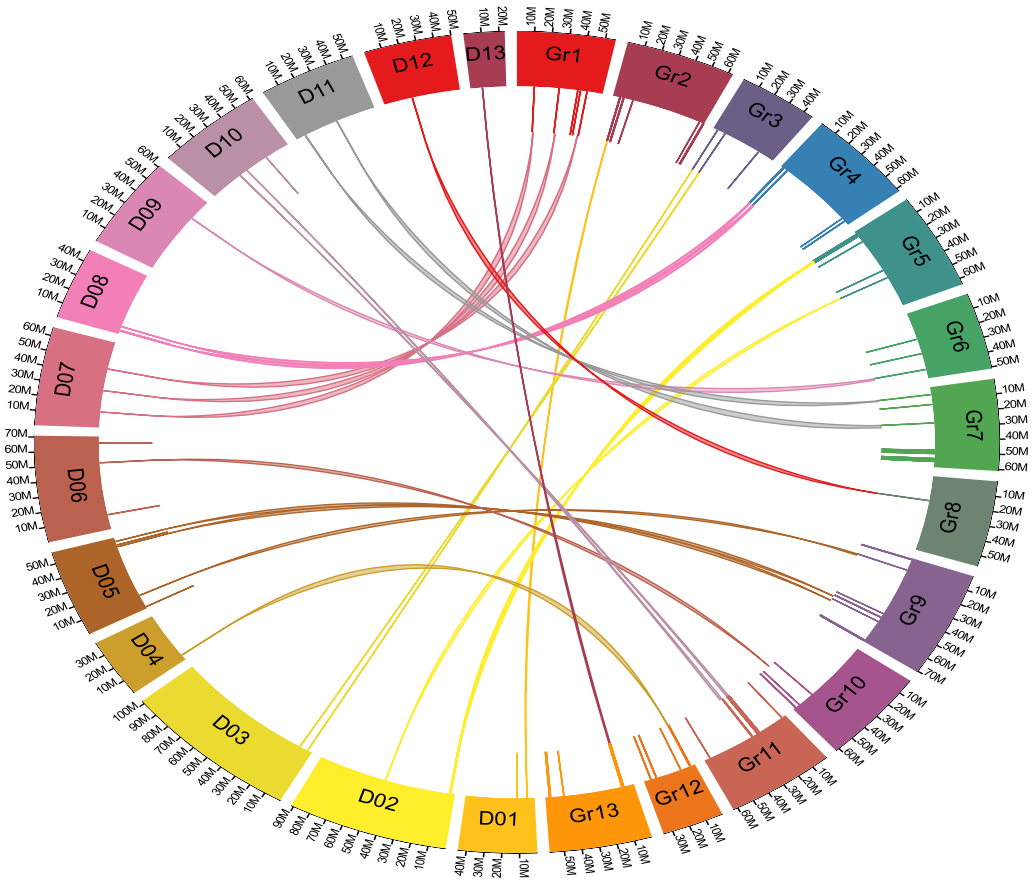

Figure 4. **Circos plot depicting position and homeology of LRR-RLPs in *G. hirsutum* D-subgenome and *G. raimondii*.**
LRR-RLPs are represented as lines on the inner face of the circular fragments that depict chromosomes from each species. Each chromosome is annotated with 10MB tick marks along its outer edge to represent length. For the LRR-RLPs in the *G. hirsutum* D-subgenome for which a homeolog could be inferred, a curved line was drawn between this LRR-RLP and its corresponding *G. raimondii* homeolog. Inferences of homology were based on inferred evolutionary distances visualized using a phylogenetic tree constructed in the same manner as Figure 1 using *G. raimondii* LRR-RLPs and *G. hirsutum* LRR-RLPs.

2.4.4. GhRLP19, RLP20, RLP22, RLP25, and RLP31 are positive regulators in cotton defense against Fusarium infections

A functional genomics approach in cotton (*G. hirsutum* CA 4002) was used by silencing 39 of the putative *RLPs* in the D-subgenome using virus-induced gene silencing (VIGS), and subjecting the silenced cotton plants to *Fusarium oxysporum* f. sp. *vasinfectum* race1 (*Fov1*; CA10) infection to test if any *RLP* plays an important role in this interaction. When using this approach, A-subgenome copies of the RLPs are also silenced due to the high sequence homology between the two subgenomes. We used *Fov1* because it showed high pathogenicity levels in CA 4002 compared to other isolates (not shown). The summary of the *Fov* infections in the VIGSed population can be found in Table 2. The disease index of *Fov*-infected plants was calculated at several time points (Table 3) and the percentages of disease levels were calculated on the last time point (Table 4).

Table 2. Summary of *Fov* infections in cotton plants with silenced RLPs.

RLP #	Gene ID	# repeats	More susceptible	Slightly more susceptible	No disease phenotype	Less susceptible
RLP1	Gh_D01G0393	1			1	
RLP2	Gh_D12G0745	2			1	1
RLP3	Gh_D04G1293	3		1	2	
RLP4	Gh_D07G1774	1			1	
RLP5	Gh_D06G2016	2	1		1	
RLP6	Gh_D07G1953	1			1	
RLP7	Gh_D01G0772	2		1	1	
RLP9	Gh_D05G3670	2			1	1
RLP11	Gh_D11G2056	2	1		1	
RLP12	Gh_D10G1381	2	1		1	
RLP13	Gh_D09G1576	2			2	
RLP14	Gh_D08G0203	2		1	1	
RLP17	Gh_D08G0250	3		1	2	
RLP18	Gh_D13G1586	3		1	2	
RLP19	Gh_D10G1222	4	3		1	
RLP20	Gh_D10G1221	5	5			
RLP21	Gh_D09G0711	2		1	1	
RLP22	Gh_D03G0283	6	1	2	3	
RLP25	Gh_D04G1454	6	3	1	2	
RLP27	Gh_D02G0259	2			2	
RLP29	Gh_D05G3622	2			1	1

Table 2. Continued

RLP #	Gene ID	# repeats	More susceptible	Slightly more susceptible	No disease phenotype	Less susceptible
RLP31	Gh_D07G0874	3	2		1	
RLP32	Gh_D13G0548	4	1	1	2	
RLP33	Gh_D03G0505	3	2		1	
RLP35	Gh_D01G2320	2			2	
RLP36	Gh_D11G3383	3		1	1	1
RLP37	Gh_D05G3892	2			2	
RLP38	Gh_D04G0212	2			2	
RLP39	Gh_D10G1575	3	1	1	1	
RLP41	Gh_D12G0745	2			2	
RLP43	Gh_D02G1328	2			1	1
RLP44	Gh_D01G2187	2			2	
RLP45	Gh_D01G2188	2	1		1	
RLP46	Gh_D11G3000	2		1	1	
RLP52	Gh_D11G0740	3	2	1		
RLP53	Gh_D07G0286	2			1	1
RLP54	Gh_D05G3192	1			1	
TMM	Gh_D05G1174	2	2			
SOBIR1	Gh_D03G0968/ Gh_D12G1850	2	2			

Table 3. Disease index at different time points.

RLP #	Repeats	7	8	9	10	11	12	13	14	16	17	18	19	21	22	23	Batch#
Ctrl	1					9			26			50					1
	2								19			47			60		2
	3				5				50			75					3
	4	2			20				54		71						4
	5				9				9			30		34			5
	6		16				34			50			66		68		6
	7											25			31		7
	8				20				32			44		60			8
	9				11				46			71		77			9
	10		18				34		42			56			62		10
	11	10			16				28		44			54			11
	12	13			25				47		55			70			12
	13				22			27		44							13
	14				27			28			53						14
	15			13			28			55			72			74	15
	16			16			38			58			64			64	16
	17	24				58			73			73					17
	18		9				47			60			64				18
	19		35				52					70					19
	20		12				38			58			75				20
	21		18				49			55			73				21
RLP 1	1				23			25			40						14
RLP2	1				11				11			31		31			5
	2		13				28			23				43	40		6
	3				13				20			60		60			8
	4				11				40			54		66			9

Table 3. Continued

RLP #	Repeats	7	8	9	10	11	12	13	14	16	17	18	19	21	22	23	Batch#
RLP3	1				26			26		51							13
	2				31			44			62						14
RLP4	1			28			46			66			70			74	16
RLP5	1		18				39			52			61		68		6
	2	25			38				62		77			80			12
RLP6	1			17			46			60			68			71	16
RLP7	1		14				38			61			75		77		6
	2				25			25		30							13
RLP9	1				8			10		31							13
	2				21			30			39						14
RLP11	1	7			12				20		31			50			11
	2	18			33				80		80			86			12
RLP12	1	8			16				34		42			68			11
	2	9			16				29		55			67			12
RLP13	1					12			30			58					1
	2		8				48			53			68		75		6
RLP14	1					13			26			57					1
	2		15				35			46			52		55		6
RLP17	1								22						55		2
	2	0			12				50								4
	3		25				39			59			80		84		6
RLP18	1					7			36			62					1
	2	9			41				70		88						4
	3		23				41			61			65		68		6
RLP19	1					23			42			60					1
	2	8			35				66		83						4
	3				8				13			25		25			5

Table 3. Continued

RLP #	Repeats	7	8	9	10	11	12	13	14	16	17	18	19	21	22	23	Batch#
RLP19	4		16				34			45			75		82		6
RLP20	1					16			20			55					1
	2	21			50				92		100						4
	3				0				11			39		75			5
	4		23				50			68			82		84		6
	5		30				50		62			76			76		10
RLP21	1	16			26				32		37			48			11
	2	22			38				53		73			77			12
RLP22	1								33			48			54		2
	2				20				55			85					3
	3				14				18			21		46			5
	4		28				44			64			69		73		6
	5		18				47		53			56			65		10
RLP25	1								22			34			53		2
	2				50				92			100					3
	3				16				19			41		66			5
	4		22				41			53			69		69		6
	5		13				23		25			60			60		10
	6		9				44			62			69				18
RLP27	1				15			20		40							13
	2				24			31			50						14
RLP29	1				17				67			92					3
	2		16				33			33			39		44		6
RLP30	1	26				52			52			70					17
RLP31	1				6				6			55		61			5
	2											78			88		7
	3		18				42		52			64			64		10

Table 3. Continued

RLP #	Repeats	7	8	9	10	11	12	13	14	16	17	18	19	21	22	23	Batch#
RLP32	1				21				38			50		54			5
	2											28			41		7
	3		24				27		40			44			51		10
	4				52			57			58						14
RLP33	1	15			20				32		58			66			11
	2				22			22		38							13
	3	48				86			86			86					17
RLP35	1	12			20				28		58			62			11
	2				20			23		32							13
RLP36	1				6				22			31		44			5
	2											44			50		7
	3	16			16				12		22			22			11
RLP37	1				9				25			44		53			5
	2											25			41		7
RLP38	1				3				11			33		39			5
	2											34			47		7
RLP39	1				0				13			38		61			5
	2											50			63		7
	3	48				66			68			78					17
RLP41	1			17			38			58			67			77	15
	2			11			35			49			55			55	16
RLP43	1			13			35			57			67			63	15
	2			14			29			45			51			52	16
RLP44	1			16			29			43			64			74	15
	2			18			42			56			64			60	16
RLP45	1			19			39			56			66			66	15
	2			18			55			75			77			78	16

Table 3. Continued

RLP #	Repeats	7	8	9	10	11	12	13	14	16	17	18	19	21	22	23	Batch#
RLP46	1			18			55			71			75			77	15
	2			14			37			59			64			64	16
RLP52	1				35			43		53							13
	2				60			61			71						14
	3	50				76			76			78					17
RLP53	1				6				50			69					3
	2	8			22				28		35			62			12
RLP54	1				27			28			52						14
TMM	1			22			58			75			83			83	15
	2		37				63			70			83				21
SOBR1	1		27				46			60			71				20
	2		47				67			73			87				21

Table 4. Levels of disease on the last time point

RLP #	Repeats	level 1	level 2	level 3	level 4	Batch #
Ctrl	1	19	13	6	63	1
	2	0	17	83	0	2
	3	20	20	0	60	3
	4	21	21	7	50	4
	5	27	45	18	9	5
	6	27	18	0	55	6
	7	43	29	14	14	7
	8	0	40	20	40	8
	9	14	0	0	86	9
	10	9	27	27	36	10
	11	0	20	10	70	11
	12	0	17	17	67	12
	13	14	36	43	7	13
	14	0	33	50	17	14
	15	15	0	0	85	15
	16	27	0	18	55	16
	17	9	9	0	82	17
	18	11	22	0	67	18
	19	0	15	25	60	19
	20	8	0	17	75	20
	21	0	13	25	63	21

Table 4. Continued

RLP #	Repeats	level 1	level 2	level 3	level 4	Batch #
RLP 1	1	15	46	31	8	14
RLP2	1	0	33	44	22	5
	2	40	20	0	30	6
	3	17	17	33	33	8
	4	0	29	14	57	9
RLP3	1	23	15	46	15	13
	2	0	23	38	38	14
RLP4	1	0	10	20	70	16
RLP5	1	0	36	9	55	6
	2	0	8	8	83	12
RLP6	1	15	0	15	69	16
RLP7	1	18	9	0	73	6
	2	33	50	17	0	13
RLP9	1	36	45	18	0	13
	2	7	57	29	7	14
RLP11	1	0	25	25	50	11
	2	0	0	0	100	12
RLP12	1	0	10	20	70	11
	2	0	18	27	55	12

Table 4. Continued

RLP #	Repeats	level 1	level 2	level 3	level 4	Batch #
RLP13	1	0	23	0	77	1
	2	20	10	0	70	6
RLP14	1	0	9	0	91	1
	2	25	25	0	50	6
RLP17	1	13	13	75	0	2
	2	15	31	8	46	4
	3	9	9	0	82	6
RLP18	1	21	7	0	71	1
	2	10	10	0	80	4
	3	18	18	0	64	6
RLP19	1	9	0	9	82	1
	2	17	0	17	67	4
	3	17	33	33	17	5
	4	9	18	0	73	6
RLP20	1	0	0	0	100	1
	2	0	0	0	100	4
	3	25	13	0	63	5
	4	9	9	9	73	6
	5	0	10	10	80	10

Table 4. Continued

RLP #	Repeats	level 1	level 2	level 3	level 4	Batch #
RLP21	1	0	40	20	40	11
	2	0	8	8	83	12
RLP22	1	14	14	71	0	2
	2	20	0	0	80	3
	3	29	0	0	71	5
	4	13	13	25	50	6
	5	9	36	0	55	10
RLP25	1	17	17	67	0	2
	2	0	0	0	100	3
	3	13	0	25	63	5
	4	13	13	13	63	6
	5	0	43	0	57	10
	6	0	22	11	67	18
RLP27	1	27	36	27	9	13
	2	14	29	36	21	14
RLP29	1	0	0	33	67	3
	2	56	0	22	22	6
RLP30	1	10	10	10	70	17
RLP31	1	11	11	11	67	5
	2	0	0	13	88	7
	3	13	25	13	50	10

Table 4. Continued

RLP #	Repeats	level 1	level 2	level 3	level 4	Batch #
RLP32	1	0	17	17	67	5
	2	40	0	20	40	7
	3	33	33	0	33	10
	4	0	33	25	42	14
RLP33	1	0	8	33	58	11
	2	9	55	36	0	13
	3	0	0	0	100	17
RLP35	1	0	11	22	67	11
	2	30	50	20	0	13
RLP36	1	13	38	13	38	5
	2	43	0	0	57	7
	3	20	70	10	0	11
RLP37	1	13	25	13	50	5
	2	20	20	0	60	7
RLP38	1	20	30	0	50	5
	2	33	0	17	50	7
RLP39	1	17	17	0	67	5
	2	17	0	0	83	7
	3	8	0	0	92	17
RLP41	1	8	0	8	83	15
	2	8	38	0	54	16

Table 4. Continued

RLP #	Repeats	level 1	level 2	level 3	level 4	Batch #
RLP43	1	17	17	0	67	15
	2	17	33	8	42	16
RLP44	1	7	0	21	71	15
	2	18	18	9	55	16
RLP45	1	14	14	0	71	15
	2	0	8	0	92	16
RLP46	1	0	8	8	85	15
	2	21	7	7	64	16
RLP52	1	8	33	25	33	13
	2	0	7	36	57	14
	3	10	0	0	90	17
RLP53	1	25	25	0	50	3
	2	0	25	33	42	12
RLP54	1	17	17	58	8	14
TMM	1	0	0	0	100	15
	2	0	0	17	83	21
SOBR1	1	0	14	29	57	20
	2	0	0	33	67	21

Silencing of five *GhRLPs*, *RLP19* (*Gh_D10G1222*), *RLP20* (*Gh_D10G1221*), *RLP22* (*Gh_D03G0283*), *RLP25* (*Gh_D04G1454*), and *RLP31* (*Gh_D07G0874*), resulted in enhanced susceptibility to *Fov* (Figure 5A). Silencing of *GhRLP20* and *GhRLP31* also resulted in enhanced susceptibility to the soilborne pathogen *Verticillium dahliae* (*Ve*) King isolate (Figure 5B). However, we did not observe an enhanced susceptibility to *Ve* when silencing *RLP19*, *RLP22*, and *RLP25* (not shown). The disease level scores were given based on visual observations as follows: 0- non-infected plants, 1- lightly infected, 2- moderately infected, 3- severely infected, 4- dead plants (Figure 5C). These results suggest that RLP20 and RLP31 are involved in the broad-spectrum resistance to pathogens, while RLP19, RLP22, and RLP25 may be specific to *Fov*.

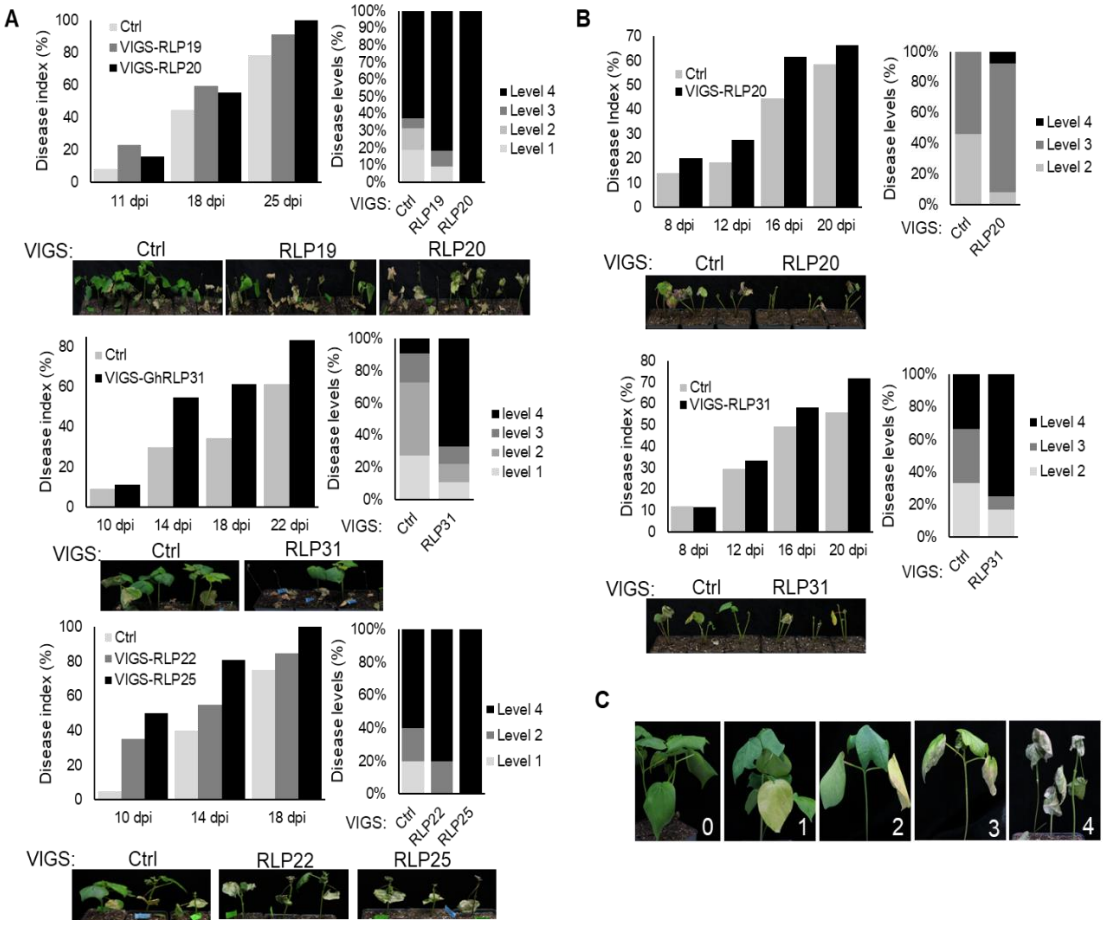

Figure 5. GhRLP19, RLP20, RLP22, RLP25, and RLP31 are positive regulators in defense against Fusarium infections.

(A) *Fusarium oxysporum* f. sp. *vasinfectum* (*Fov*) infection in cotton plants with silenced *RLP19*, *20*, *22*, *25*, and *31*. Four-week-old cotton plants were inoculated with *Fov* (1×10^7 conidia/ml) using the root dipping technique. At least 12 plants were inoculated per treatment. The disease ratio was calculated as the percentage of wilting plants to the total infected plants. The disease levels among all the plants per treatment were calculated on the last time point. (B) Cotton plants with silenced *RLP20* and *RLP31* are more susceptible to *Verticillium dalhiae* (*Ve*). Four-week-old cotton plants were inoculated with *Ve* (1×10^8 conidia/ml) using the root dipping technique. At least 12 plants were inoculated per treatment. Photos were taken on the last time point and are a representative of all the plants per treatment.

2.4.5. GhRLP20 and GhRLP31 are required for PTI responses

The downstream responses of PRRs include the activation of protein kinases, reactive oxygen species (ROS) bursts, ethylene biosynthesis, defense gene transcription, stomatal closing, and others (Boller and Felix, 2009; Li et al., 2016a; Macho and Zipfel, 2014). To determine if the *RLPs* identified in our VIGS screen are involved in the perception of *Fov* patterns or other PAMPs, we also measured some of the downstream PTI responses in these plants treated with FovCWE, an elicitor from *Fov* cell wall extracts that induces PTI responses in cotton and Arabidopsis (chapter III), and chitin, a well-known PAMP found in fungal cell walls (Petutschnig et al., 2014). Silencing of *GhRLP31* compromised the chitin-induced ROS burst (Figure 6A), ethylene biosynthesis induced by chitin and FovCWE (Figure 6B,C), and MAPK activation induced by chitin, but not FovCWE (Figure 6D,E). We also observed reduced basal levels of ethylene when silencing *GhRLP31* (Figure 6B). Silencing of *GhRLP20* compromised the chitin-induced ROS burst (Figure 6A) and ethylene biosynthesis induced by chitin and FovCWE (Figure 6B,C), but the plants showed normal MAPK activation (Figure 6D,E). In addition, silencing of *GhRLP19* did not affect PTI responses, while silencing of *GhRLP22* and *GhRLP25* only compromised the chitin-induced ROS burst (Figure 6A). Silencing of another *GhRLP*, *RLP2*, resulted in higher MAPK activation (Figure 6E, top). Taken together, *GhRLP19*, *GhRLP20*, *GhRLP22*, *GhRLP25*, and *GhRLP31* are positive regulators in defense against *Fov* infections, and *GhRLP20* and *GhRLP31* may also function as PRRs or regulate chitin receptor complex to trigger PTI responses upon recognition of conserved PAMPs.

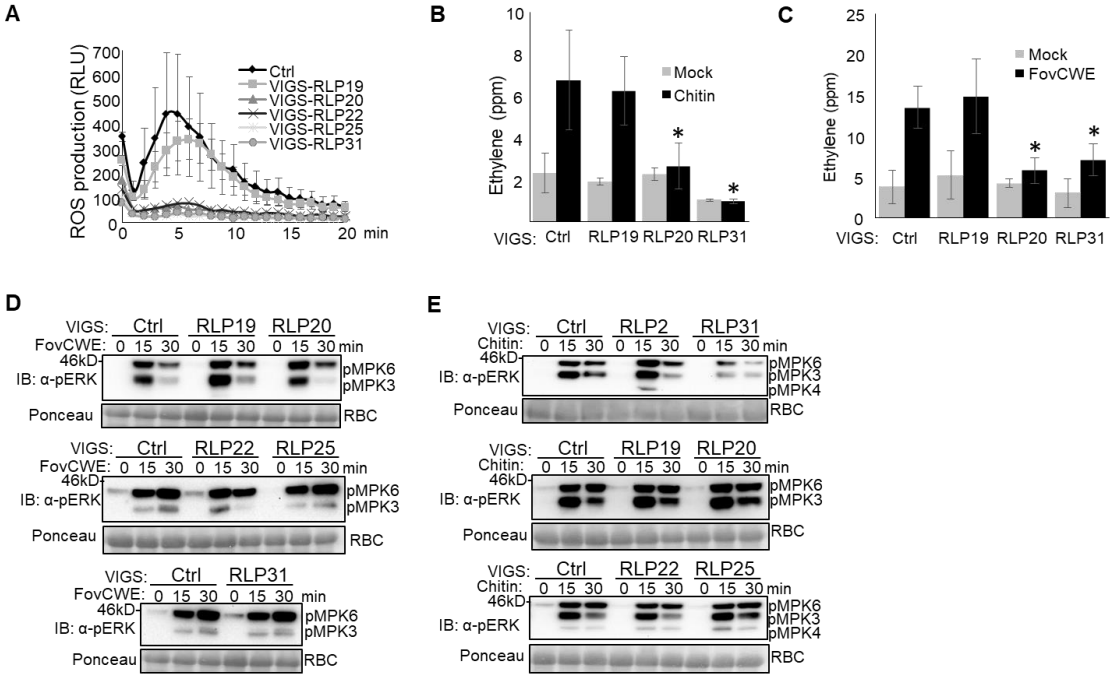

Figure 6. GhRLP20 and RLP31 are required for basal PTI responses.
(A) Chitin-induced ROS burst. Leaf disks from four-week-old cotton leaves were assayed for ROS production by measuring the relative light units (RLU) in a luminometer upon chitin (0.1 mg/ml) treatment. The data are shown as means ± SE (n = 12). (B) GhRLP20 and GhRLP31 are required for chitin-induced ethylene biosynthesis. Leaf disks from four-week-old cotton plants were assayed for ethylene production during a course of four hours upon chitin (0.1 mg/ml) treatment. Data shown as mean ± SE from three independent repeats. * indicates a significant difference with a Student's t-test ($p<0.05$) when compared to Ctrl. (C) GhRLP20 and GhRLP31 are required for FovCWE-induced ethylene biosynthesis. Data shown as means ± SE from three independent repeats. * indicates a significant difference with a Student's t-test ($p<0.05$) when compared to Ctrl. (D) FovCWE-induced MAPK activation. Leaf disks from four-week-old cotton true leaves were treated with FovCWE (1 mg/ml) for 15 and 30 min. The MAPK activation was analyzed by immunoblot with α-pERK antibodies (top panel). The protein loading is shown using Ponceau S staining for RuBisCo (RBC) (bottom panel). (E) Chitin-induced MAPK activation. Leaf disks from four-week-old cotton true leaves were treated with chitin (0.1 mg/ml) for 15 and 30 min.

2.4.6. GhTMM mediates Fov resistance through regulation of stomatal closure.

The Arabidopsis LRR-RLP TOO MANY MOUTHS (TMM) is important for normal stomata patterning (Nadeau and Sack, 2002; Shpak et al., 2005). We used AtTMM as the query for a BLASTp search and found cotton ortholog (Gh_D05G1174). As shown in Figure 7A, cotton plants with silenced *TMM* were highly susceptible to Fusarium wilt from an early infection time point when compared to control. However, PTI responses such as ethylene biosynthesis and MAPK activation induced by chitin and FovCWE were not affected in plants with silenced *GhTMM* (Figure 7B,C). PAMP treatment induces stomatal closure as a defense strategy to prevent subsequent infections (Melotto et al., 2006). Interestingly, we did not observe stomatal closure induced by FovCWE in plants with silenced *GhTMM* when compared to WT (Figure 7D). These results indicate that GhTMM may regulate stomatal movements.

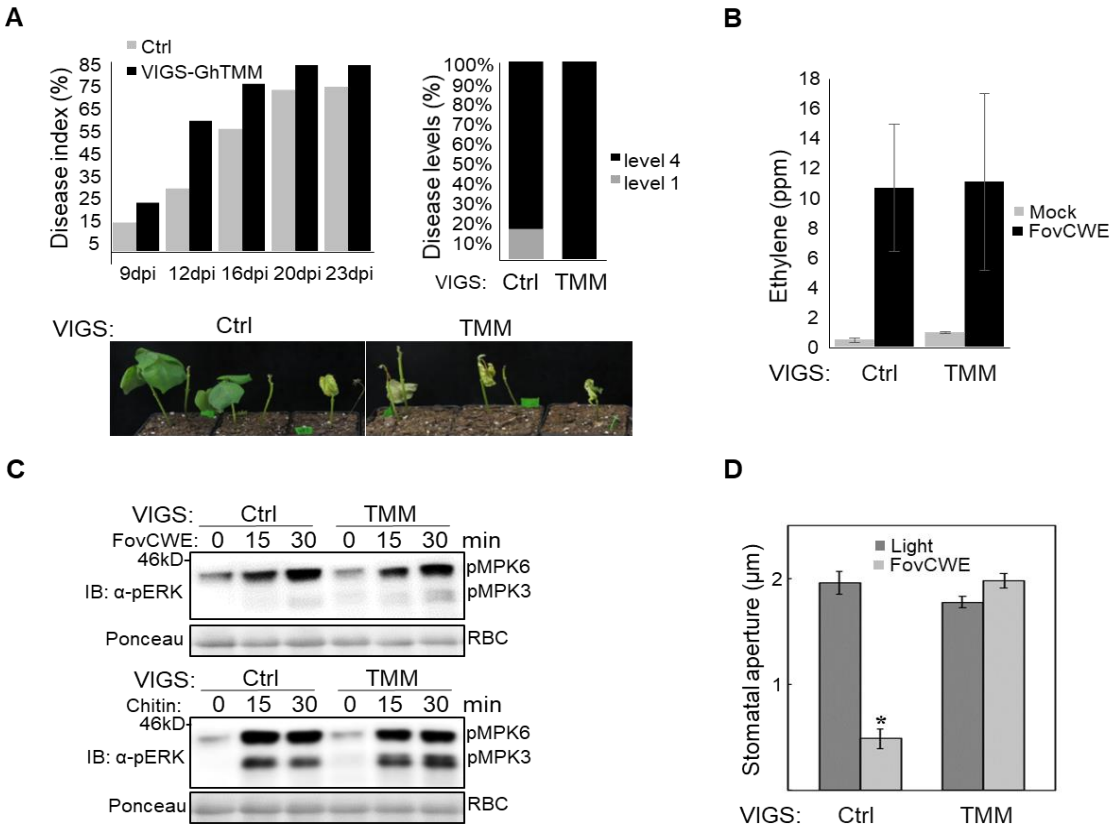

Figure 7. GhTMM may have different stomata regulation functions compared to its *Arabidopsis* ortholog.

(A) Enhanced susceptibility to *Fov* in cotton plants with silenced *GhTMM*. Four-week-old cotton plants were inoculated with *Fov* (1×10^7 conidia/ml) using the root dipping technique. At least 12 plants were inoculated per treatment. The disease ratio was calculated as the percentage of wilting plants to the total infected plants. The disease levels among all the plants per treatment was calculated on the last time point. Picture was taken on the last time point. (B) FovCWE-induced ethylene biosynthesis in cotton plants with silenced *GhTMM*. Leaf disks from four-week-old cotton plants were assayed for ethylene production during a course of four hours upon FovCWE (1 mg/ml) treatment. Data shown as mean ± SE from three independent repeats. (C) GhTMM is not required for chitin- and FovCWE-induced MAPK activation. Leaf disks from four-week-old cotton true leaves were treated with FovCWE (1 mg/ml) or chitin (0.1 mg/ml) for 15 and 30 min. The MAPK activation was analyzed by immunoblot with α-pERK antibodies (top panel). The protein loading is shown using Ponceau S staining for RuBisCo (RBC) (bottom panel). (D) FovCWE-induced stomatal closure in cotton plants with silenced *GhTMM*. Epidermal cells were incubated in a bathing solution under light and treated with FovCWE (1mg/ml). Data shown as mean ± SE from three independent plant cultures, each with 60 stomata per genotype.

2.4.7. GhSOBIR1 is a positive regulator in defense against Fusarium wilt infections

The Arabidopsis LRR-RLK SUPPRESSOR OF BIR1-1 (SOBIR1) has been found in complex with multiple LRR-RLPs involved in defense against fungal pathogens and is therefore a key player in immunity (Liebrand et al., 2013; Lv et al., 2016). The cotton genome has two AtSOBIR1 orthologs (GhSOBIR1-1: Gh_A03G0563/Gh_D03G0968; GhSOBIR1-2: Gh_A12G1689/ Gh_D12G1850). We therefore designed a VIGS construct to silence both *GhSOBIR1* orthologs and tested the silenced plants against *Fov* infections (Figure 8A). Cotton plants with silenced GhSOBIR1 were more susceptible to *Fov* (Figure 8A). However, its silencing did not affect MAPK activation and ethylene biosynthesis (Figure 8B,C).

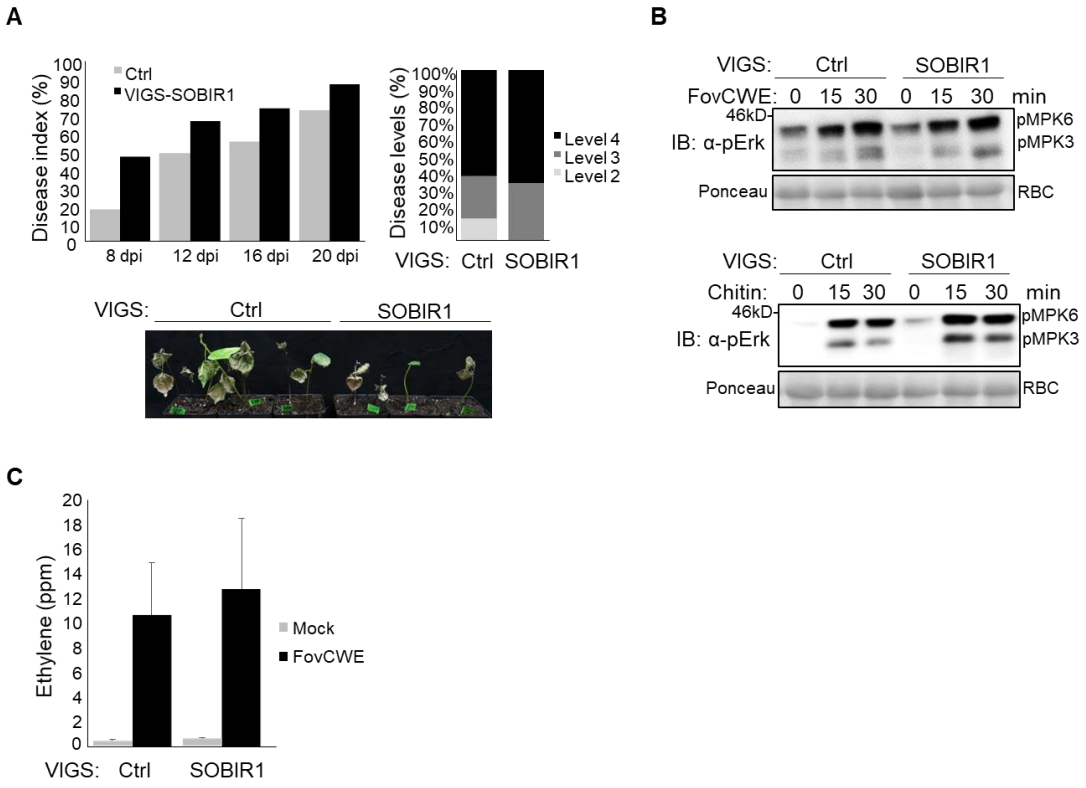

Figure 8. **GhSOBIR1 is a positive regulator in defense against Fusarium wilt infections.**

(A) Fusarium oxysporum f. sp. vasinfectum (*Fov*) infection in cotton plants with silenced GhSOBIR1. Four-weeks-old cotton plants were inoculated with Fov (1×10^7 conidia/ml) using the root dipping technique. At least 12 plants were inoculated per treatment. The disease ratio was calculated as the percentage of wilting plants to the total infected plants. The disease levels among all the plants per treatment were calculated on the last time point. (B) Chitin- and FovCWE-induced MAPK activation in cotton plants with silenced GhSOBIR1. Leaf disks from four-week-old cotton true leaves were treated with FovCWE (1 mg/ml) or chitin (0.1 mg/ml) for 15 and 30 min. The MAPK activation was analyzed by immunoblot with α-pERK antibodies (top panel). The protein loading is shown using Ponceau S staining for RuBisCo (RBC) (bottom panel). (C) FovCWE-induced ethylene biosynthesis in cotton plants with silenced GhSOBIR1. Leaf disks from four-week-old cotton plants were assayed for ethylene production during a course of four hours upon FovCWE (1 mg/ml) treatment. Data shown as mean ± SE from three independent repeats.

2.4.8. GhRLP2 is a negative regulator of MAPK

Silencing of *GhRLP2* decreased plant susceptibility to *Fov* infections in the first two experiments, but we did not observe the phenotype in subsequent infections (not shown). However, we consistently observed enhanced MAPK activation induced by several PAMPs in plants with silenced *GhRLP2* (Figure 9A). The ethylene biosynthesis and ROS burst in these plants were not altered (not shown). We hypothesized that GhRLP2 negatively regulates at least MAPK activation, and that its over-expression can suppress it. When over-expressed in cotton protoplasts, GhRLP2 with a FLAG epitope tag could suppress the MAPK activation induced by chitin and FovCWE (Figure 9B). PAMP perception also triggers profound gene transcriptional reprograming in Arabidopsis and induces the expression of a large group of immune-related genes, including *Flg22-induced Receptor-like Kinase 1* (*FRK1*) (Li et al., 2016a). We expressed *GhRLP2* in Arabidopsis protoplasts together with a firefly *LUCIFERASE* (*LUC*) gene under the control of the *FRK1* promoter (*pFRK1::LUC*) to test if GhRLP2 can suppress the expression of *FRK1*. Notably, GhRLP2 could suppress the *pFRK1::LUC* activity induced by flg22, chitin and FovCWE after 4 hours post-treatment, and the level of suppression was similar to the *P. syringae* avirulence effector AvrPto which is known to inhibit PTI in plants (Figure 9C)(Aime et al., 2013). Similarly, we observed less MAPK activation after chitin, FovCWE and flg22 treatment in Arabidopsis protoplasts over-expressing GhRLP2 (Figure 9D). The expression of GhRLP2 in cotton and Arabidopsis protoplasts was detected by immuno-blots using the α-Flag antibodies (Figure 9B,C).

Further, we generated transgenic Arabidopsis plants expressing GhRLP2 without an epitope tag and performed RT-PCR to confirm GhRLP2 expression (Figure 9E). We chose a line with low GhRLP2 expression levels (GhRLP2-2) and a line with high expression levels (GhRLP2-4) for subsequent experiments. Both lines showed reduced flg22- and FovCWE-induced MAPK activation, although GhRLP2-4 showed a higher reduction than GhRLP2-2 (Figure 9F). Moreover, GhRLP2-4 showed less chitin-induced MAPK activation but we did not observe a reduction in GhRLP2-2 possibly due to the low GhRLP2 expression in this line (Figure 9F). Taken together, these results show that GhRLP2 is a negative regulator of MAPK, and that it may function in other PTI responses.

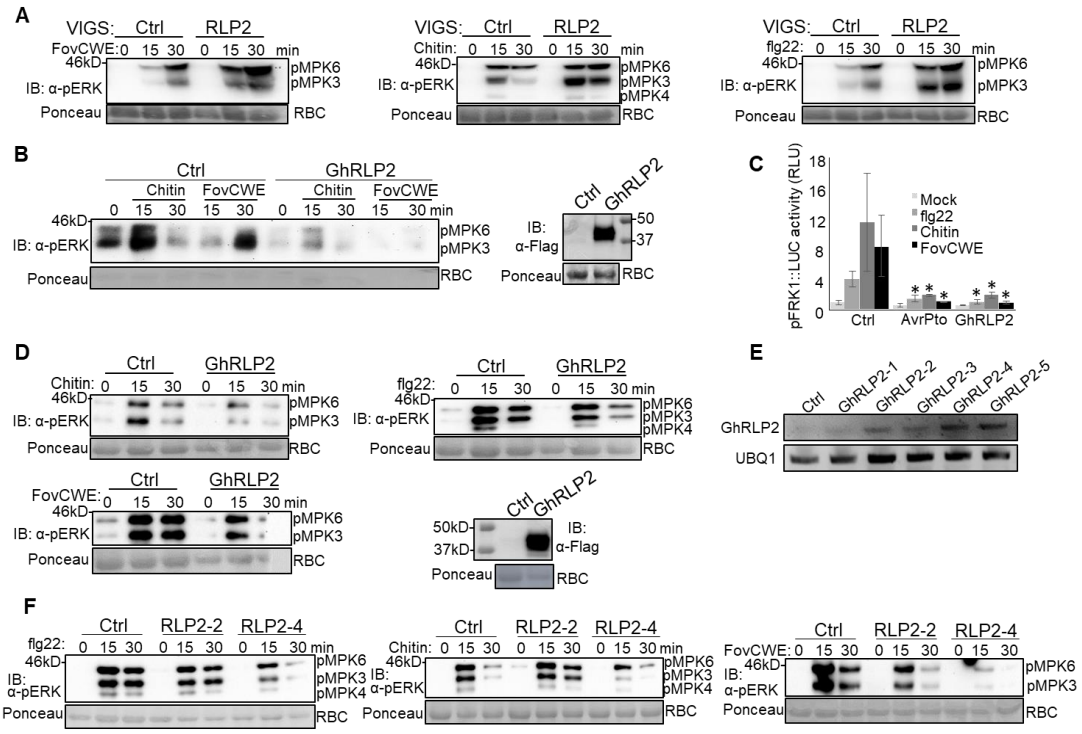

Figure 9. **GhRLP2 is a negative regulator of MAPK.**
(A) PAMP-induced MAPK activation in cotton plants with silenced *GhRLP2*. Leaf disks from four-week-old cotton true leaves were treated with FovCWE (1 mg/ml), chitin (0.1 mg/ml), and flg22 (100 mM) for 15 and 30 min. The MAPK activation was analyzed by immunoblot with α-pERK antibodies (top panel). The protein loading is shown using Ponceau S staining for RuBisCo (RBC) (bottom panel). (B) Reduced chitin- and FovCWE-induced MAPK activation in cotton protoplasts over-expressing GhRLP2. Cotton protoplasts isolated from four-week-old cotton true leaves were transfected with *GhRLP2* and treated with FovCWE (1 mg/ml) and chitin (0.1 mg/ml) for 15 and 30 min. The GhRLP2 expression was analyzed by immunoblot with α-Flag antibodies (right panel). (C) Reduced PAMP-induced *pFRK1::LUC* activity in Arabidopsis protoplasts over-expressing GhRLP2. Arabidopsis protoplasts isolated from four-week old plants were transfected with *GhRLP2* and *pFRK1::LUC*, incubated for six hours, and treated with H_2O, flg22 (100nM), chitin (0.1 mg/ml), and FovCWE (1 mg/ml). The *pFRK1::LUC* activity was measured with a luminometer at the indicated time points. * indicates a significant difference with a Student's t-test ($p<0.05$) when compared to Ctrl. (D) Reduced PAMP-induced MAPK activation in Arabidopsis protoplasts over-expressing GhRLP2. *Arabidopsis* protoplasts isolated from four-week old plants were transfected with *GhRLP2* and treated with FovCWE (1 mg/ml), chitin (0.1 mg/ml), and flg22 (100 mM) for 15 and 30 min. (E) RT-PCR of Arabidopsis GhRLP2 transgenic lines. (F) Reduced PAMP-induced MAPK activation in Arabidopsis GhRLP2 transgenic lines. Ten-day-old seedlings grown on ½MS plates were treated with FovCWE (1 mg/ml), chitin (0.1 mg/ml), and flg22 (100 mM) for 15 and 30 min.

2.4.9. The Arabidopsis GhRLP2 ortholog, AtRLP44, has similar functions in immunity

AtRLP44 (AT3G49750) is a GhRLP2 ortholog according to a pBLAST search (TAIR; Identities = 67%, Positives 75%). Both AtRLP44 and GhRLP2 proteins have six LRRs, and their protein lengths differ by only seven amino acids (Figure 10A). AtRLP44 is required for normal growth and abiotic stresses responses, and it is believed to interact with BRI1-ASSOCIATED RECEPTOR KINASE 1 (BAK1) to regulate brassinosteroid signaling (Wolf et al., 2014). As reported (Wolf et al., 2014), the Arabidopsis *rlp44* mutant showed a reduced size (Figure 10B). However, cotton plants silenced with *GhRLP2* showed a normal growth phenotype (not shown). We then examined whether AtRLP44 has a similar function to GhRLP2 in immunity. Interestingly, the *rlp44* mutant displayed enhanced resistance to the non-pathogenic bacterium *Pseudomonas syringae pv*. *tomato* (*Pst*) DC3000 hrcC defective in type III secretion of effectors (Figure 10C). We did not observe enhanced resistance when infecting the plants with the pathogenic *pst* DC3000 (not shown). Furthermore, *rlp44* showed higher MAPK activation triggered by FovCWE, chitin, and flg22 (Figure 9D), similar to cotton plants with silenced *GhRLP2* (Figure 9A). When infected with *Fusarium oxysporum* isolate 5176 (*Fo5176*), which is virulent in Arabidopsis (Thatcher et al., 2012), *rlp44* showed slightly less susceptibility (Figure 10E). However, *Fo5176* did not show high virulence in our experiments. Taken together, these results indicate that in addition to its role in BR signaling, AtRLP44 may be a negative regulator of defense responses.

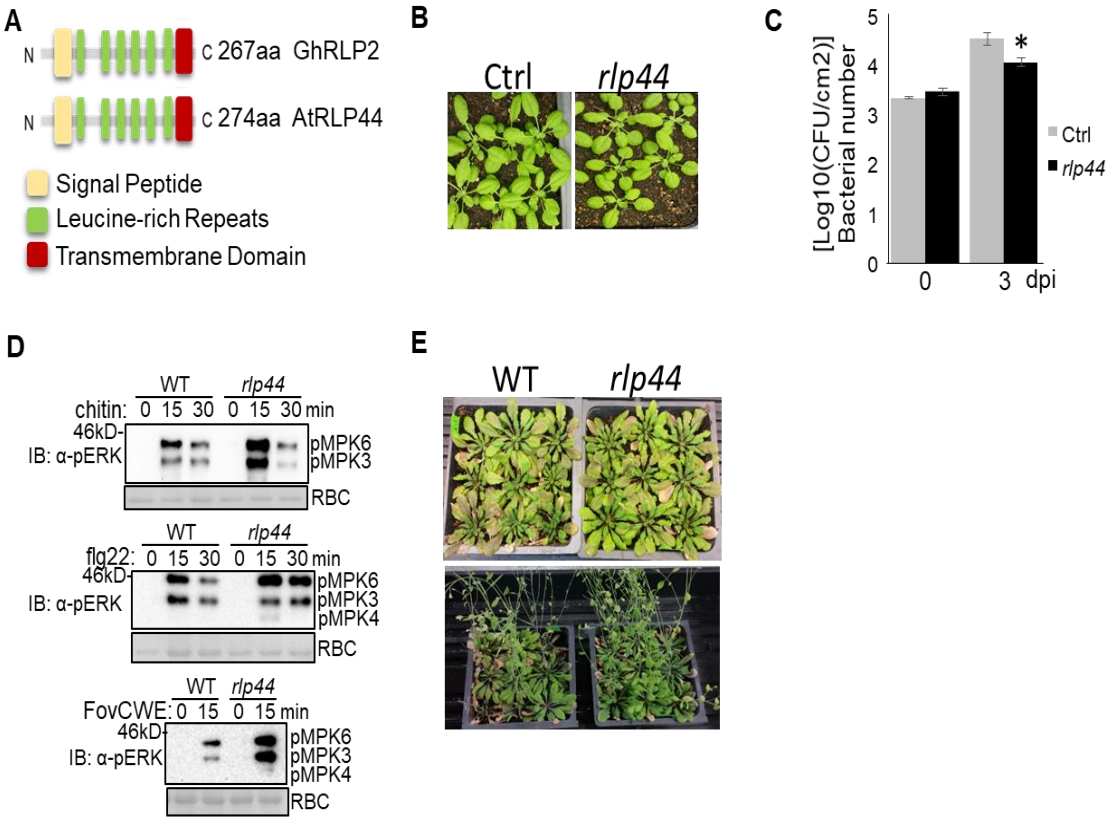

Figure 10. AtRLP44 is a negative regulator in plant immunity.
(A) Domain structure of GhRLP2 and AtRLP44. (B) Growth phenotype of *rlp44* mutant. (C) Enhanced resistance to *pst* DC3000 hrcC in *rlp44*. Leaves of four-week-old Arabidopsis plants were inoculated with *Pst* DC3000 hrcC (OD=0.00001). Bacterial colony forming units (CFU) were counted 0 and 3 days after pathogen inoculation. Data shown as mean ± SE from three independent repeats. * indicates a significant difference with a Student's t-test ($p<0.05$) when compared to Ctrl. (D) Reduced PAMP-induced MAPK activation in *rlp44*. Ten-day-old seedlings grown on ½MS plates were treated with FovCWE (1mg/ml), chitin (0.1mg/ml), and flg22 (100mM) for 15 and 30 min. (E) Reduced susceptibility to *Fusarium oxysporum* in *rlp44*. Four-week old plants were inoculated with *Fo5176* (1×10^7 conidia/ml) using the root dipping technique. Pictures taken at three (top) and six (bottom) weeks post inoculation.

Table 5. Primers used in this study.

Cloning primers for VIGS.

Gene	Forward primer (5' to 3')	Reverse primer (5' to 3')
RLP1	CGGAATTCCAGCATCTCTCGGAAACCTC	CCGCTCGAGATTGGAATTGCTTGCACTGG
RLP2	CGGAATTCCCTTTCCAACTGCTCCTCTG	GGGGTACCTCAACATGGGTCAGGTTCAG
RLP3	CGGAATTCGTTCCCAATAGGCCATTTCC	GGGGTACC CCACTTTGGAAATGAAAGG
RLP4	CGGAATTCGGCTGGTTCCATGAAAGTTG	GGGGTACCCCAAGGAACTCGGGAATTTG
RLP5	CGGAATTCTTGTTTCAATGGCAGCATTC	GGGGTACCGTTCCTGCTCACATCCAATG
RLP6	CGGAATTCACCTTTGGTTCCAAGATTCC	GGGGTACCGGTAGCCCACCAGACAATTG
RLP7	CGGAATTCTGGGATACCATTCGCCTACC	GGGGTACCGCTTGAAAGCCAATGAGATC
RLP9	CGGAATTCCATACATGGGTGTGCAAGATG	GGGGTACCTTGTTTTCCTTGAGGGATGC
RLP11	CGGAATTCTTTACTCACTGGCCAGATTCC	GGGGTACCTCAGGCATAGGGTGACTCATC

Table 5. Continued

Gene	Forward primer (5’ to 3’)	Reverse primer (5’ to 3’)
RLP13	CGGAATTCACGCGATATTGGTGACTTCC	GGGGTACCGGCTCCTCTCTGAACAATGC
RLP14	CGGAATTCTTGGCAAGATCCCTGACTC	GGGGTACCAAATGGCCACAGTCTTCGTC
RLP17	CGGAATTCTTTTCCGGTTGGTTAGCTTC	GGGGTACCGAAATTGAGCATTTGCAAGG
RLP18	CGGAATTCGGATCACTGCCTCGATCATTG	GGGGTACCTGGCTGTTAAGATAGCCAAGG
RLP19	CGGAATTCTTGAGAGCATAAGGAGTTTCC	GGGGTACCGAGCAGGTAAAGCGTCATTTAG
RLP20	CGGAATTCACTGGAATTGTTGCCGACAC	GGGGTACCAAGTGGACCGACGATTGAAG
RLP21	CGGAATTCTAATGCAACGGCACCAAGTC	GGGGTACCTCAGGATTACACCTCTACCC
RLP22	CGGAATTCTCGCCTTGAAGGAGAGATCC	GGGGTACCCAGGCATGAACTGACCAATC
RLP25	CGGAATTCAGGGAACATTCCTCCTTGCC	GGGGTACCCCCGAGCATTTCCTTTGTAG
RLP27	CGGAATTCGCAAATCTTAGTCACCTGGTG	GGGGTACCTTTACGTTCGACAGCGTCAG

Table 5. Continued

Gene	Forward primer (5' to 3')	Reverse primer (5' to 3')
RLP29	CGGAATTCTTGAAGGGGGTATTCCAGAG	GGGGTACCATCAACACCACTTTCCAACC
RLP30	CGGAATTCGATCCCAGAGAGCTTGAGC	GGGGTACCCAACGCACAGTTCTGGATTG
RLP31	CGGAATTCGTCATTGGGGAATCTCTGCC	GGGGTACCATCCAAGAGCACCAGTTGAG
RLP32	CGGAATTCGAGCGGCTCATCTCTGTTTG	GGGGTACCTTTTCTGAGGTTGCCCAGAG
RLP33	CGGAATTCGTTCCCAATAGGCCATTTCC	GGGGTACCGAAATGAAGGGCCTAAATAGC
RLP35	CGGAATTCACCACCTGACATGGGAAATC	GGGGTACCGCTGTGGGATTACACCTTGG
RLP36	CGGAATTCTGGATTGGGGACAAACTCTC	GGGGTACCCAATTTCGTCCGGTATATTTCC
RLP37	CGGAATTCGGCTGGTAATGATTTGAGTGG	GGGGTACCGTCGTTGTAACCAGGCTCTG
RLP38	CGGAATTCGATTTATCAGGCCCTCTTCC	GGGGTACCAACCCTGCCAAGGTTAGTGG
RLP39	CGGAATTCGTGAGAGGCAAGCCCTTTTC	GGGGTACCCCAAGTTGATTAGGGACCAAG

Table 5. Continued

Gene	Forward primer (5' to 3')	Reverse primer (5' to 3')
RLP41	CGGAATTCACTTCCATGGGCTTCATCAG	GGGGTACCACCGGAGATGGAGTTTGAAG
RLP43	CGGAATTCCTGTTTTAGTGTGTTGTCTGG	GGGGTACCGAAAAGGTGGTGGGAATTTG
RLP44	CGGAATTCTCCTCAATTTCTTTCCCCAC	GGGGTACCATATCGACCGAGGGATACTC
RLP45	CGGAATTCTCTTTCCCTAACATCAGCAC	GGGGTACCCTCCCATTGAAGTTATTGCC
RLP46	CGGAATTCGTCGAACTATCGAATTGGGTC	GGGGTACCCCAGCAATCTGGAATTTCTCC
RLP52	CGGAATTCCCAAGGCAACATTCCTGATC	GGGGTACCAACCAATTCACCGCAATGTC
RLP53	CGGAATTCACAAGCACGGACGAACAATG	GGGGTACCCTTTTCCTGCCCAGAAGAAG
RLP54	CGGAATTCCCTGGGAAGCATCTATCAGC	GGGGTACCCAAGTTGGTTGTCATTGAGGTT
SOBIR1-1	CGGAATTCCGTACAACAAGTATCAGAAGGC	GGGGATTTGATCAGCTGATGATATTCAGGTGCG
SOBIR1-2	ACCTGAATATCATCAGCTGATCAAATCCCCGCC	GGGGTACCCCAATTGATTGTTTGCAAGGG

Table 5. Continued

Gene	Forward primer (5’ to 3’)	Reverse primer (5’ to 3’)
TMM	CGGAATTCTTTTCCGGTTG GTTAGCTTC	GGGGTACCGAAATTGAGCATTT GCAAGG

Note: The restriction enzyme sites are underlined.

RT-PCR primers

Gene	Forward primer (5’ to 3’)	Reverse primer (5’ to 3’)
GhRLP2	ACTTCCATGGGCTTCATCAG	ATAATCAGGCATATATTGAC
UBQ1	ACCGGCAAGACCATCACTCT	AGGCCTCAACTGGTTGCTGT

Full length cloning primers

Gene	Forward primer (5’ to 3’)	Reverse primer (5’ to 3’)
RLP2	CGGGATCCATGGGTCTGCTAA TTGTG	TCCCCCGGGATAATCAGGCATAT ATTGAC

2.5. Discussion

Fusarium wilt disease of cotton, caused by *Fusarium oxysporum* f.sp. *vasinfectum* (*Fov*), has been an emergent problem causing worldwide losses since 1993 (Kochman, 1995). The vulnerability of cotton production to this pathogen highlights the need for research to protect cotton production areas from current or new virulent populations of *Fov* (Ulloa et al., 2006). In order to elucidate the genetic and molecular basis of cotton response to *Fov* infections, we focused on the role of RLPs due to their importance in plant

defense against fungal pathogens, including *Fusarium* (Albert et al., 2015; Diener and Ausubel, 2005; Gijzen and Nurnberger, 2006; Kawchuk et al., 2001; Oome and Van den Ackerveken, 2014; Postma et al., 2016; Shen and Diener, 2013). We used an integrative genomics approach to predict potential RLP candidates in cotton (*G. hirsutum*) by homology-based search to the 57 known *Arabidopsis* RLPs. In this work, we report seven positive regulators of defense against *Fov*, and one negative regulator of PAMP-induced MAPK activation, which is AtRLP44 ortholog. Furthermore, silencing of two *RLPs* compromised PTI responses in cotton. These findings can provide effective genetic tools to control Fusarium wilt of cotton by interspecies transfer of these *RLPs*.

It is possible that the capability of *G. raimondii* to tolerate more diseases compared to *G. arboretum* comes from the larger RLP number in its genome. These differences are still present in *G. hirsutum*, which is expected as we know it originated from interspecific hybridization between *G. arboreum* and *G. raimondii*. A close examination of the relatedness of the LRR-RLPs in *G. hirsutum* subgenomes reveals a greater frequency with which D-subgenome LRR-RLPs exist as members of highly similar and often proximally located gene clusters which likely arose due to paralogous duplication. This suggests that a functional redundancy in D-subgenome LRR-RLPs may exist. It would be interesting to silence groups of RLPs that cluster in the same chromosome location and test those plants against Fusarium infections.

GhRLP20 and GhRLP31 seems to be important not only against *Fov* infections, but in basal defense responses as indicated in the enhanced susceptibility against *Fov* and *Ve* infections, and reduced PTI responses in plants with silenced *GhRLP20* and *GhRLP31*

(Figure 6). It is interesting that we only observed a reduction in MAPK activation upon FovCWE treatment, but not chitin, in plants with silenced *GhRLP31*, which is consistent with a decreased but yet noticeable FovCWE-induced ethylene biosynthesis and no chitin-induced ethylene (Figure 6B,C). Perhaps GhRLP31 is mainly involved in the mechanism of chitin perception and therefore plants with silenced *GhRLP31* are deficient in basal defense responses upon fungal attack, which enables the pathogen to infect them at an earlier stage. On the other hand, GhRLP20 may be involved in basal defense responses in a non-specific manner. The enhanced *Fov* susceptibility in plants with silenced *GhRLP19*, *GhRLP22*, and *GhRLP25*, but normal PTI responses, may indicate that they have specificity to *Fov* infections possibly by recognizing a specific protein or component from the pathogen. Future work should focus on the biochemical characterization of these RLPs and their role against different *Fov* races.

After colonization of the root meristematic tissues, *Fov* invades the vascular cylinder and spread through the xylem by producing microconidia which are carried up towards the sap stream (Rodriguez-Galvez and Mendgen, 1995). At the same time, plants undergo a series of defense responses in the xylem such as production of tylose, gels, and gums to prevent vascular pathogen from spreading to adjacent xylem vessels (Fradin and Thomma, 2006). However, the combination of mycelial growth and gels production can result in clogged vessels which can block the water uptake thus resulting in drought stress (Fradin and Thomma, 2006). It is believed that the cotton "wilting" symptom after *Fov* infection can be a result of *Fov* occupying the xylem vessels, thereby obstructing the water and nutrient flow of the host (Yadeta and Thomma, 2013). Since stomatal control of water

losses has been identified as an early event in plant response to water, plants with abnormal stomata regulation could be more susceptible to *Fov*-induced drought stress and may show a wilting phenotype at earlier time points (Chaves et al., 2002; Flexas and Medrano, 2002; Zhao et al., 2017). This may explain the enhanced susceptibility of cotton plants with silenced *TMM* (Figure 7). Although we observed normal PTI responses and stomata patterning in these plants (not shown), the FovCWE-induced stomata closure was impaired. It is then possible that plants with silenced *TMM* loose more water under *Fov* invasion and will therefore die at earlier stages. FovCWE perception in WT plants, on the other hand, can induce stomata closure as a mechanism to prevent invasion. Although *Fov* penetrates through the roots and not the stomates, the stomatal closure can be beneficial to preserve water and survive for a longer time. It would be interesting to test VIGS-*GhTMM* plants against pathogen with different lifestyles, and to measure the stomata closure induced by other PAMPs.

Because RLPs lack a cytoplasmic kinase domain, they interact with RLKs or adapter kinases to activate downstream signaling in a similar manner to their RLK counterparts (Gust and Felix, 2014). The Arabidopsis LRR-RLK SUPPRESSOR OF BIR1-1 (SOBIR1) and its tomato counterpart have been found in complex with multiple LRR-RLPs involved in fungal immunity, including Cf-2/4, Ve1, LepR3, Rlm2, AtRLP23, AtRLP30 and AtRLP42 (Liebrand et al., 2013; Lv et al., 2016). Due to its importance in immunity in other plant species, we also tested GhSOBIR1 against *Fov* infections. Plants with silenced *GhSOBIR1* display normal PTI responses but enhanced susceptibility to *Fov*, similar to *GhTMM* silencing (Figure 8). It is possible that GhSOBIR1 interact with

multiple GhRLPs and it would be interesting to test its silencing against *Ve* and other pathogens, and to determine if GhSOBIR1 can interact with GhRLP19, 20, 22, 25, 31, or others.

AtRLP44 was shown to be in a complex with BRASSINOSTEROID INSENSITIVE 1 (BRI1) and BAK1, and is required for the BR-mediated response to cell-wall modification (Holzwart et al., 2018; Wolf et al., 2014). It is also important for the maintenance of cell fate in the root vasculature and xylem differentiation, and it has been shown that its over-expression elevates BR signaling. However, we did not observe the growth phenotype reported in the *rlp44 Arabidopsis* mutant when we silenced *GhRLP2*. Instead, cotton plants with silenced *GhRLP2* show elevated PAMP-induced MAPK activation and its over expression in cotton and Arabidopsis can reduce it (Figure 9). We did not observe an alteration in other PTI responses in cotton although its overexpression in Arabidopsis can suppress the *pFRK1::LUC* activity induced by several PAMPs. It is possible that GhRLP2 is involved in the activation of other unknown cascades or components which result in different outcomes than when silencing RLPs that play a specific role in immunity. We also know that GhRLP11 is the closest GhRLP2 paralog, which may play a redundant role. The altered MAPK activation in the *rlp44* mutant and the enhanced resistance to pathogens may be a consequence of altered BR signaling, as we know that hormones regulate diverse biochemical pathways. Future work should focus on testing if GhRLP2 can complement the Arabidopsis *rlp44* mutant, to study the BR signaling in cotton plants with silenced *GhRLP2*, and to silence *GhRLP2 t*ogether with its paralogs, including *GhRLP11*.

In this chapter, I have demonstrated that RLPs indeed serve as molecular links between extracellular stimulus and intracellular signaling by activating immune defense responses upon recognition of conserve patterns. Furthermore, RLPs play both positive and negative roles in defense against Fusarium wilt infections.

3. AN ELICITOR FROM FUSARIUM CELL WALL EXTRACTS TRIGGERS IMMUNE RESPONSES IN ARABIDOPSIS AND COTTON

3.1. Summary

Plants can recognize a wide range of microbe/pathogen-associated molecular patterns (MAMPs/PAMPs), also termed elicitors, through cell surface-resident pattern-recognition receptors (PRRs) to activate host defense responses known as "PAMP-triggered immunity" (PTI). Numerous elicitors from different plant pathogens have been identified to date. We have isolated the cell wall components of different *Fusarium oxysporum* isolates (FoCWEs) and tested their ability to trigger immune responses in both cotton and the model plant Arabidopsis. Significantly, FoCWE triggers MAPK activation, ROS burst, ethylene biosynthesis, growth inhibition, and stomatal closure in cotton and Arabidopsis. In addition, FoCWE protects cotton seeds against infections by virulent isolates of *Fov*, and Arabidopsis plants against *Pseudomonas syringae* pv tomato DC3000. These data indicate that FoCWE is a classical PAMP that is potentially recognized by a conserved pattern recognition receptor (PRR) in different plant species. Analysis of available PRR mutants in Arabidopsis indicate that FoCWE is perceived by a novel PRR. Further characterization of the eliciting component within FoCWE demonstrated that it is a heat-stable and water soluble PAMP.

3.2. Introduction

Over evolutionary time, plants have developed a series of sophisticated defense mechanisms to defend against their associated pathogens. At the cellular level, plant immunity is an exquisitely regulated and poorly understood process. One facet of this immunity, termed "pattern-triggered immunity" (PTI), is triggered when pathogen/microbe-associated molecular patterns (PAMPs/MAMPs), or elicitors, are recognized by plant cell surface-resident "pattern-recognition receptors" (PRRs) (Bigeard et al., 2015). This recognition often triggers the formation of a receptor complex enabling the transduction of the PAMP signal which contributes towards changes in cellular physiology associated with improved basal defense (Liebrand et al., 2013; Lv et al., 2016; Ma et al., 2016).

One of the downstream responses of PRRs is the initiation of a mitogen-activated protein kinase (MAPK) cascade which consist of three sequentially activated kinases of a MAPK kinase kinase (MAP3K or MEKK), a MAPK kinase (MAP2K or MKK), and a MAPK (MPK) (Asai et al., 2002; Yu et al., 2017). In this cascade, MAP3Ks, once directly or indirectly activated by PRRs, lead the phosphorylation of the downstream MAPKs which eventually result in defense responses and gene reprogramming (Rasmussen et al., 2012). Therefore, MAPKs are a direct link between plant surface receptors and intracellular signaling. Among the 90 MAPKs in Arabidopsis, MPK3, MPK4 and MPK6 are implicated in defense responses and have been studied intensively (Asai et al., 2002; Ichimura et al., 2002; Petersen et al., 2000). These three MAPKs are also activated by PAMPs. Other PRR-dependent downstream responses include callus deposition, reactive

oxygen species (ROS) bursts, ethylene biosynthesis, root inhibition, stomatal closure, defense gene transcription, and others (Boller and Felix, 2009; Li et al., 2016a; Macho and Zipfel, 2014).

Two well studied PRRs include the bacterial flagellin receptor FLAGELLIN-SENSITIVE 2 (FLS2) and elongation factor Tu (EF-Tu) receptor EFR, which recognize a conserved 22-amino-acid peptide (flg22) of flagellin and an 18-amino-acid peptide (elf18) of EF-Tu, respectively (Li et al., 2016a). Following ligand perception, both FLS2 and EFR heterodimerize with the co-receptor BRI1-ASSOCIATED RECEPTOR KINASE 1 (BAK1) to initiate intracellular signaling and defense responses (Ma et al., 2016). Other well-studied PRRs include the Arabidopsis CHITIN ELICITOR RECEPTOR KINASE1 (CERK1), LysM-CONTAINING RECEPTOR KINASE4 (LYK4), and LYK5, required for the perception of the fungal cell wall component chitin (Petutschnig et al., 2014). PRR-mediated PTI is important for plant defense to a broad spectrum of pathogens.

The taxon *Fusarium oxysporum* (*Fo*) represents a diverse fungal morphospecies with several members specialized to infect economically important plant hosts. Although *Fo* has no known sexual cycle, it has been demonstrated to horizontally share or dispense with a set of supernumerary chromosomes that often contain a high concentration of genes related to pathogenicity (van Dam et al., 2017). This fact represents a challenge to pathologists and breeders attempting to classify different isolates of the pathogen. Different *formae speciales* (f. sp.) of *Fo* exist, which were defined by their host specificity (Edel-Hermann and Lecomte, 2019). *Fusarium oxysporum* f. sp. *vasinfectum* (*Fov*) is the

causal agent of Fusarium wilt of cotton, a devastating disease affecting cotton production around the world, including the US. *Fov* has been classified into at least eight races based on their pathogenicity in cotton and other plant species, and by sequence differences in genes (Appel and Gordon, 1996; O'Donnell et al., 2009). Race 1 (*Fov1*) has often been detected with root-knot nematode infections in the field, and race 4 (*Fov4*) is a highly virulent isolate that does not require root-knot nematode to cause significant diseases (Halpern et al., 2017; Kim et al., 2005; Wang et al., 2018). Most of the upland cotton germplasms show variable symptoms to different *Fov* races, indicating a complex and quantitative genetic response (Wang et al., 2018). Although the molecular mechanism of *Fov* infection in cotton remains largely elusive, Fusarium wilt in other plant species have been studied extensively and may provide some insights about the molecular mechanisms of *Fov* infection. For instance, *F. oxysporum* f. sp. *lycopersici* (*Fol*), the causal agent of tomato wilt, is known to secrete a number of virulence effectors, known as Secreted In Xylem (SIX), in the xylem sap of tomato plants to facilitate disease progression, very likely by suppressing basal defense responses in the plant (Gawehns et al., 2015; Houterman et al., 2007; Lievens et al., 2009; Ma et al., 2015; Rep et al., 2005). Thus, the pathogenicity of a *Fov* isolate may be determined by its ability to escape host defense responses, something that can be accomplished by manipulating the signaling pathways.

To date, many elicitors have been isolated and identified from various organisms including bacteria, fungi, oomycete and viruses. These elicitors include proteins, peptides, lipids, glycoproteins, and oligosaccharides, which are either components of the pathogen cell wall or secreted to kill or degrade plant cells (Chen et al., 2012; Wang et al., 2012).

Some studies have reported eliciting-capabilities in the cell wall of different Fusarium species (Davies et al., 2006; Li et al., 2016b). In this article, we show that cell wall preparations from the non-virulent strain *Fo47*, the Arabidopsis-infecting isolate *Fo5176*, and three *Fov* isolates (*Fov1*, Fov3, and *Fov4*) can trigger MAPK activation and PTI responses in cotton and Arabidopsis. The cell wall preparation can also protect cotton seeds against *Fov* infection. Interestingly, the elicitor perception is independent of some of the major PRRs involved in plant immunity. Because pathogenic and non-pathogenic isolates of *Fo* can trigger PTI responses plants, we can infer that virulent isolates have evolved with a way to suppress plant immunity, possibly by secreting virulence factors.

3.3. Materials and Methods

3.3.1. Plant materials and growth conditions

Arabidopsis accession Col-0 (WT) and the mutants used in this study were grown in soil (Metro Mix 366) in a growth room at 23°C, 60% relative humidity, 70 μmoles $m^{-2}s^{-1}$ light with a 12-hr light/12-hr dark photoperiod for four weeks. The *sobir1-12* (CS69917) mutant was obtained from the Arabidopsis Biological Resource Center (ABRC) and confirmed by PCR. The *bak1-5/serk4* mutant was obtained by crossing *bak1-5* (Schwessinger et al., 2011) and *serk4* (SALK_057955) single mutants. *Atcerk1* (GABI-KAT 096F09) and *Atlyk4/Atlyk5-2* (*Atlyk4/5*) were obtained from Dr. Gary Stacey (Cao et al., 2014). Seedlings were grown on agar plates containing half-strength Murashige and Skoog medium (½MS) with 0.5% sucrose, 0.8% agar and 2.5 mM MES at pH 5.7, in a growth chamber at 23°C, 70 μE $m^{-2}s^{-1}$ light with a 12-hr light/12-hr dark photoperiod.

Gossypium hirsutum cv CA 4002 (PI 665226) was grown in 3.5-inch square pots containing soil (Jolly Gardener PRO-LINE C/25) in a controlled growth chamber at 23°C, 30% relative humidity and 100 μmol m^{-2} s^{-1} light with a 12-h light/12-hr dark photoperiod. One-week-old cotton plants were used for *Agrobacterium*-mediated VIGS assay or protoplast isolation.

3.3.2. Fusarium cell wall preparation

The cell wall of different *Fo* isolates was prepared according to (Davies et al., 2006). Different isolates were cultured for four days in Potato Dextrose Broth (Difco), centrifuged, and washed twice with 200 ml of 500 mM KH_2PO_4. The pellet was then sequentially washed and centrifuged in chloroform/methanol (1:1 v/v) and acetone (100%). Lastly, the pellet was dried, resuspended in dd$H_2$0 (10g/l), and autoclaved for 30 min at 121°C. The resuspended pellet was stored at -20°C.

3.3.3. *Agrobacterium tumefaciens*-mediated VIGS

Fragments (300-500bp) of *GhMPK3*, *GhMPK6*, *GhBAK1* and *GhSOBIR1* were amplified by PCR from cDNA with primers described in Table 7 and inserted into the *pYL156* (pTRV-RNA2) vector with restriction sites *Eco*RI and *Kpn*I. The agrobacterial cultures carrying pTRV-RNA1 and the above pTRV-RNA2 constructs were resuspended in infiltration buffer (10 mM MES, pH 5.7, 10 mM $MgCl_2$, 200 μM acetosyringone). *A. tumefaciens* pTRV-RNA1 was mixed with pTRV-RNA2 at a 1:1 ratio to a final OD_{600} of 0.75 each and hand infiltrated into two fully expanded cotyledons of one-week-old soil-

grown plants (Gao et al., 2011; Gao et al., 2013). At least 12 plants were inoculated for each construct. Because plants with silenced *GhCla1* develop a typical albino phenotype indicative of silencing this gene, we included *pYL156-GhCla1* as a visual marker for VIGS efficiency. The silencing of the gene of interest was confirmed by RT-PCR.

3.3.4. MAPK assay

Three leaf discs from individual 3-week-old cotton plants were ground in 100 µl 1× SDS buffer (62.5 mM Tris-HCl, pH 6.8, 1% SDS, 0.025% bromophenol blue, 10% glycerol, 1× protease inhibitor, 2 µl 1 M NaF and 2 µl 1 M Na_3VO_4 for 1 ml of buffer), boiled at 95°C for 5 min, and centrifuged to collect the supernatant. For protoplasts, 100 µl of the 1× SDS buffer was added to lysed cells, boiled at 95°C for 5 min, and centrifuged to collect the supernatant. For Arabidopsis, ten-day-old seedlings germinated on ½ MS plates were transferred to 2 ml H_2O in a 12-well plate overnight for recovery, and treated with 1 mg/ml FovCWE, 1×10^7/ml *Fo47* spores, 100 nM flg22, or 100 mg/l chitin. The seedlings were ground in IP buffer, centrifuged, and the cleared lysate was mixed with SDS buffer. Proteins were separated in a 10% sodium dodecyl sulfate–polyacrylamide gel electrophoresis (SDS-PAGE) gel and activated MAPKs were detected by immunoblotting with phosphorylated Extracellular Regulated protein Kinases (α-pERK1/2) antibody (Cell Signaling, USA).

3.3.5. ROS analyses

ROS burst was determined by a luminol-based assay. 24 leaves of four-week-old Arabidopsis plants or three-weeks old cotton plants were excised into leaf discs of 0.25 cm^2, followed by an overnight incubation in a 96-well plate with 100 µl of H_2O for recovery. Cotton leaf discs were further cut into 5 strips with a razor blade. H_2O was then replaced by 100 µl of a reaction solution containing 50 µM luminol and 10 µg/ml horseradish peroxidase (Sigma, USA), with or without 1 mg/ml FovCWE. The measurements were conducted immediately in a luminometer (Perkin Elmer, 2030 Multilabel Reader, Victor X3) after adding the solution, with a 1 min interval reading time for a period of 30 min. The measurement values for ROS production from 24 leaf discs were indicated as means of Relative Light Units (RLU).

3.3.6. Measurements of Stomatal Aperture

Stomatal aperture was measured on epidermal peels excised from the abaxial side of leaves of three- to four-week-old plants as described in Rodrigues et al. (2017). Two epidermal peels from two independent plants of Col-0 and the mutants were first incubated for 30 min in darkness in a bathing solution containing 30 mM KCl and 10 mM MES/Tris pH6.0, prior to exposure to the indicated treatment. Epidermal peels were first exposed to white light in a growth chamber (120 µmoles m^{-2} s^{-1}) for 180 min to induce maximal stomatal opening. flg22 (1 µM) or FovCWE (0.001, 0.01, or 0.1 mg/ml) was then added to the bathing solution and stomatal aperture was monitored during the next 180 min in

>60 stomata for each independent repetition. Average inner stomatal aperture was measured using Image J (http://rsb.info.nih.gov/ij/).

3.3.7. Root inhibition assay

Three-days-old seedlings of Col-0 (WT), *sobir1* and *bak1-5/serk4* grown on ½ MS were transferred to liquid ½ MS with or without 1 mg/ml FovCWE and incubated for another seven days. The fresh weight was calculated after seven days post-treatment.

3.3.8. Protoplast isolation

Cotton protoplasts were isolated from cotyledons of one-week-old seedlings. Detached cotyledons were cut with a razor blade and digested in an enzyme solution (1.5% cellulose R10, 0.4% macerozyme R10, 0.4 M mannitol, 20 mM KCl, 20 mM MES pH 5.7) supplemented with 2% sucrose for 0.5 h under vacuum. Subsequently, the enzyme solution was incubated without vacuum at room temperature for 6 h. Protoplasts were released by filtering through a 30 µm-nylon mesh, washed with W5 solution (154 mM NaCl, 125 mM $CaCl_2$, 5 mM KCl, 2 mM MES pH 5.7) and diluted in MMG solution (0.4 M mannitol, 15 mM $MgCl_2$, 4 mM MES pH 5.7) to a density of 2×10^5 cells/ml (Gao et al. 2011). A measure of 200 µl of protoplasts for each sample was used for MAPK treatment.

3.3.9. Reporter assay

The *pFRK1::LUC* construct in a binary vector was transformed into Arabidopsis Col-0 plants, and 10 days-old ½MS grown homozygous transgenic *pFRK1-LUC* seedlings were transferred to water for overnight and treated with H_2O, 1×10^7 /ml *Fo47* spores, or 100nM flg22 at the indicated time points. Seedlings were transferred to a 96-well plate, sprayed with 0.2 mM luciferin, and the bioluminescence from induced *pFRK1::LUC* expression was measured by a luminometer (Perkin Elmer, 2030 Multilabel Reader, Victor X3).

3.3.10. Ethylene production

Twelve leaves of four-week-old Arabidopsis plants or three-week-old cotton plants were excised into leaf discs of 0.25 or 0.50 cm^2, respectively, followed by overnight incubation in a 25 ml glass vial with 1 mL of H_2O for recovery. The H_2O was then replaced by 1 ml of FovCWE (1 mg/ml) and the vials were capped immediately with a rubber stopper and incubated at room temperature with gentile agitation. One ml of the vial headspace was injected into a PhotoVac 10sPlus GC with photoionization detector (PID) at the indicated time points.

3.3.11. Pathogen assays

Pseudomonas syringae pv. *tomato* (*Pst*) DC3000 was cultured overnight at 28°C in King's B medium with 50 µg/ml rifampicin. Bacteria were harvested by centrifugation, washed, and adjusted to $OD_{600}=1\times10^{-5}$ with 10 mM $MgCl_2$. Leaves of four-week-old

plants were pre-inoculated with H_2O or 1 mg/ml FovCWE one day before inoculation with *Pst* DC3000 using a 1-ml needleless syringe. To measure bacterial growth, two leaf discs were ground in 100 µl dH_2O and serial dilutions were plated on TSA medium (1% Bacto tryptone, 1% sucrose, 0.1% glutamic acid, 1.5% agar) with appropriate antibiotics. Bacterial colony forming units (CFU) were counted two days after incubation at 28°C. Each data point is shown as triplicates. *Botrytis cinerea* strain BO5-10 was cultured on Potato Dextrose Agar (Difco) and incubated at room temperature. Conidia were re-suspended in 1/4X Potato Dextrose Broth (Difco) with 0.5% Knox Gelatin. The suspension was filtered through a Miracloth and the conidia concentration was adjusted to 2.5×10^5 spores/ml. Leaves of four-week-old plants hand pre-inoculated with H_2O or 1 mg/ml FovCWE were drop-inoculated with 8 µl *B. cinerea* spore suspension at the above concentration and the lesion size was measured at two days post-inoculation. *Fusarium oxysporum* f. sp. *vasinfectum* race 1 (CA10/*Fov1*) was cultured for four days in Potato Dextrose Broth (Difco) and the spores were collected by culture filtration using two layers of cheese cloth. Spores were centrifuged and resuspended in H_2O at a concentration of 1×10^8/ml. Cotton seeds (CA 4002) were surface sterilized with 40% bleach for 2 min, washed several times with H_2O and soaked in 1 mg/ml FovCWE or H_2O for 12 hours. The seeds were then soaked in H_2O or *Fov1* spores for another 12 hours, transferred to a petri dish with wet paper towel and kept in a growth chamber at 28 °C, 50% humidity and 100 µE $m^{-2}s^{-1}$ light with a 12-h light/12-h dark photoperiod for four days.

3.4. Results

3.4.1. Race-nonspecific elicitor from *Fusarium* activates defense responses in Arabidopsis

We hypothesized that PAMPs derived from *Fo* can be recognized by plant PRRs to activate defense responses. One of the hallmarks of immune responses triggered upon perception of PAMPs by PRRs is the rapid and transient activation of mitogen-activated protein kinase (MAPK) cascades (Rasmussen et al., 2012). In *Arabidopsis thaliana*, a wide range of PAMPs, including flg22, activate MAPKs, which can be readily detected by immuno-blots using the α-pERK antibodies (Felix et al., 1999; Rasmussen et al., 2012). We first applied a spore solution from *Fo* isolate 47 (*Fo47*) to wild-type Arabidopsis Col-0 seedlings and examined whether *Fo47* spores could activate MAPKs (Figure 11A). *Fo47* is a non-pathogenic strain isolated from soils suppressive to Fusarium wilts and has been shown to protect plants against different diseases, including Fusarium wilt induced by pathogenic *Fo* isolates (Aime et al., 2013; Fuchs et al., 1997; Veloso et al., 2016). We found that *Fo47* spores could trigger MAPK activation at 15 and 30 min after treatment as detected by the α-pERK antibodies, similar to flg22 but to a lesser extent (Figure 11A). PAMP perception triggers profound gene transcriptional reprograming and induces the expression of a large number of immune-related genes, including *FLG22-INDUCED RECEPTOR-LIKE KINASE 1* (*FRK1*) (Li et al., 2016a). The Arabidopsis transgenic plants carrying a firefly *luciferase* (*LUC*) gene under the control of the *FRK1* promoter (*pFRK1::LUC*) have been developed as a reporter line to monitor elicitation of PTI responses (Li et al., 2014). We found that *Fo47* spores could potently trigger *pFRK1::LUC*

activities at different time points with higher activation levels than flg22 treatment at 24 or 36 hr post-inoculation (Figure 11B). Thus, the data suggest that spores from *Fo47*, a non-pathogenic *Fusarium* isolate, trigger defense responses.

To determine whether any conserved cell wall components from *Fo47* spores contribute to the defense elicitation activity, we isolated the cell wall crude extracts from an expanded collection of *Fusarium* isolates. We have included *Fo* isolate 5176 (*Fo5176*), which is virulent in Arabidopsis (Thatcher et al., 2012). In addition, three isolates *of Fusarium oxysporum f. sp.* vasinfectum (*Fov*), which are specialized to infect *Gossypium*, including *Fov1*-CA10, *Fov3*-CA11, and *Fov4*-CA14, have been included. Notably, they have been classified as different races with different levels of pathogenicity towards a panel of cotton cultivars, and isolated from distinct geographic locations with *Fov1*-CA10 as race1, *Fov3*-CA11 as race 3 and *Fov4*-CA14 as race 4. Based on a reported protocol (Davies et al., 2006), we isolated the cell wall extracts from these *Fusarium* isolates (FoCWE) (Figure 11C) and examined their capacities to elicit PTI responses in Arabidopsis. Although only *Fo5176*, but none the others, is pathogenic in Arabidopsis, FoCWEs from all these isolates, including *Fov1*, *Fov3* and *Fov4*, could activate MAPKs to a similar extent in terms of timing and strength (Figure 11D), suggesting that conserved component(s) from FoCWEs across *Fo* contribute to the MAPK activation in Arabidopsis. Since FoCWEs from all different *Fo* isolates could activate MAPKs similarly, we used the cell wall extracts of *Fov1* (FovCWE) for the remaining experiments.

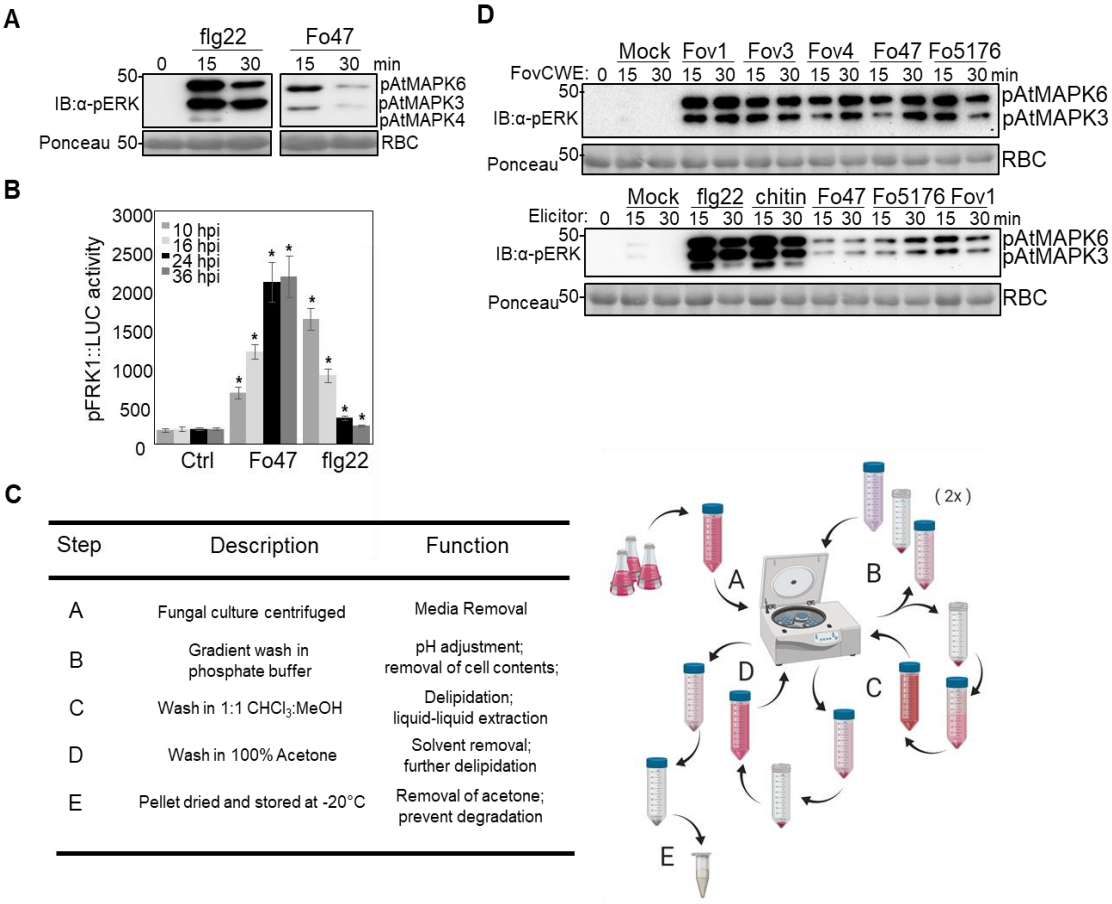

Figure 11. **Race-nonspecific elicitor from Fusarium activates defense responses in Arabidopsis.**

(A) Spores of the nonpathogenic *F. oxysporum* strain *Fo47* activate MAPKs in Arabidopsis. Ten-day-old seedlings were treated with *Fo47* spores (1×10^7/ml) for 15 and 30 min. The MAPK activation was analyzed by immunoblot with α-pERK1/2 antibody (top panel). The protein loading is shown by Ponceau S staining for RuBisCo (RBC) (bottom panel). (B) *Fo47* spores induce *pFRK1::LUC* activity. Ten-day-old *pFRK1::LUC* seedlings grown on ½MS plates were treated with H_2O, flg22 (200nM) and *Fo47* spores (1×10^7/ml), and the *pFRK1::LUC* activity was measured with a luminometer at the indicated time points. * indicates a significant difference with a Student's t-test ($p<0.05$) when compared to H_2O (Ctrl). (C) Scheme of FoCWE isolation. The method for extraction of FoCWE is illustrated with letters describing each step that correspond to the associated table. (D) Different FoCWEs activate MAPKs in Arabidopsis. Ten-day-old seedlings grown on ½MS plates were treated with different FoCWEs (1 mg/l) for 15 and 30 min. Double sterilized H_2O treatment (Mock) was used as negative control. Treatments with 100nM flg22 and 100 mg/l chitin were included for comparison. Fov1: *Fusarium oxysporum* f. sp. *vasinfectum* (*Fov*) CA10 race 1; Fov3: *Fov* CA11 race 3; Fov4: *Fov* CA14 race 4.

3.4.2. FovCWE induces different PTI responses in Arabidopsis

To confirm the identity of the MAPK bands detected with the α-pERK antibody, we have included the Arabidopsis *mpk3* and *mpk6* mutants and observed no MAPK band corresponding to the mutated MPK (Figure 12A). Therefore, FovCWE activates at least MPK3 and MPK6 in Arabidopsis, which is consistent with the activation of other PAMPs. Next, we tested FovCWE for its capacity to activate other known PTI responses in Arabidopsis. ROS production is another early PTI signaling event (Yu et al., 2017). As shown in Figure 12B, FovCWE could induce a ROS burst in four-week-old Arabidopsis leaves. Perception of some PAMPs also induces the production of ethylene, a plant defense hormone (Yu et al., 2017). We observed that FovCWE could also induce ethylene production three-fold higher at six hours post inoculation and five-fold higher at 24 hours post inoculation compared to the mock treatment (Figure 12C). Further, PAMP treatment induces stomatal closure to prevent pathogen entry (Melotto et al., 2006). As shown in Figure 12D, similar to flg22, FoCWE induced stomatal closure of Arabidopsis epidermal cells compared to non-treatment (under light) in a dosage dependent manner. Prolonged treatment of PAMPs also inhibits seedling growth likely due to the cost of PTI responses activation (Huot et al., 2014; Lozano-Duran et al., 2013). When treated with FovCWE, we observed a clear root growth inhibition of Arabidopsis seedlings at seven days post treatment (Figure 12E). Taken together, these data indicate that FovCWE can induce typical PTI responses in Arabidopsis.

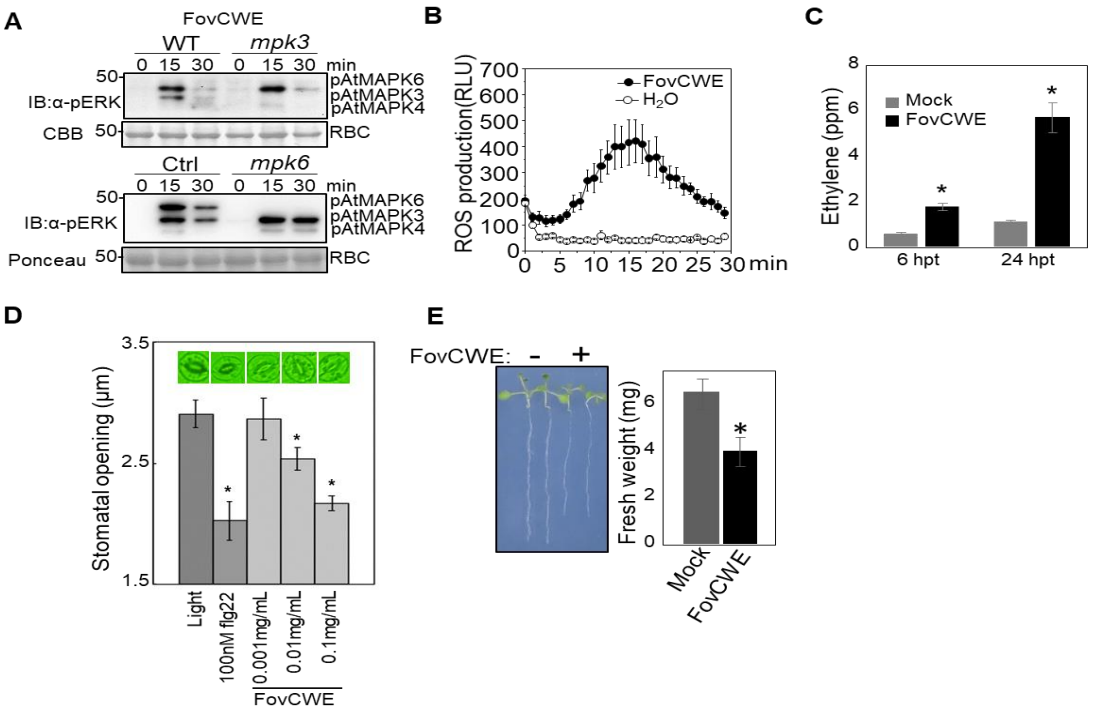

Figure 12. FovCWE induces different PTI responses in Arabidopsis.
(A) FovCWE-induced MAPK activation in *mpk3* and *mpk6* mutants. Ten-day-old WT (Col-0), *mpk3* and *mpk6* mutant seedlings grown on ½ MS plates were treated with FovCWE (1 mg/l) for 15 and 30 min. The MAPK activation was analyzed by immunoblot with α-pERK1/2 antibody (top panel). The protein loading is shown using Ponceau S staining for RuBisCo (RBC) (bottom panel). (B) FovCWE induces ROS burst. Leaf disks from four-week-old plants were assayed for ROS production by measuring the relative light units (RLU) in a luminometer upon FovCWE (1 mg/l) treatment. The data are shown as mean ± SE (n = 24). (C) FovCWE induces ethylene production. Leaf disks from four-week-old plants were assayed for ethylene production during a course of 4 hr upon mock (H_20) and FovCWE (1 mg/l) treatment. Data is shown as mean ± SE from three independent repeats. * indicates a significant difference with a Student's t-test ($p<0.05$) when comparing to mock treatment. (D) FovCWE can induce stomatal closure. Epidermal cells were incubated in a bathing solution under light and treated with flg22 (100nM) and different FovCWE concentrations. Data shown as mean ± SE from three independent plant cultures, each with 60 stomata per genotype. * indicates a significant difference ($p<0.05$) with ANOVA, Newman-Keuls when compared to non-treatment (light). (E) FovCWE inhibits root growth. Three-day-old seedlings were grown in solid ½MS plates and transferred into liquid ½MS with or without FovCWE (1 mg/ml) for another seven days. Fresh weight data is shown as mean ± SE from three independent repeats. * indicates a significant difference with a Student's t-test ($p<0.05$) when comparing to mock (H_2O) treatment.

3.4.3. FovCWE induces different PTI responses in cotton

Because *Fov* is a devastating pathogen affecting cotton production worldwide, we tested if FovCWE could also induce PTI responses in cotton by its capacity to trigger MAPK phosphorylation in three-week-old upland cotton (*Gossypium hirsutum;* CA 4002) (Figure 13A). We observed phosphorylation of MAPK in the leaves of these cotton plants (Figure 13A, top). While the peak of MAPK activation was observed at 15 minutes post-treatment in Arabidopsis, we observed the MAPK activation peak in cotton at 30 minutes post-treatment. We also observed MAPK activation in protoplasts isolated from one-week-old cotyledons (Figure 13A, bottom). To confirm the identity of the MAPK bands detected with the α-pERK antibody, we silenced *GhMPK3* and *GhMPK6* by virus-induced gene silencing (VIGS) (Figure 3B). Silencing of *GhCLA1*, which leads to plant albino phenotype two weeks after Agrobacterium infiltration, was included as a visual marker for VIGS efficiency (not shown). We did not observe a GhMAPK3 band when silencing *GhMPK3* by VIGS, and although we observed the GhMPK6 band in the immunoblot after silencing *GhMPK6*, its intensity was reduced (Figure 13B). These results confirmed that the bands seen in the immunoblot correspond to GhMPK3 and GhMPK6. Next, we measured ethylene biosynthesis and observed a two-fold increase in three-week-old leaves treated with FovCWE when compared to mock (Figure 13C). Furthermore, FovCWE could also trigger ROS burst in cotton leaves over the course of 30 min (Figure 13D). These results indicate that FovCWE functions as a PAMP that can induce defense responses in cotton and Arabidopsis.

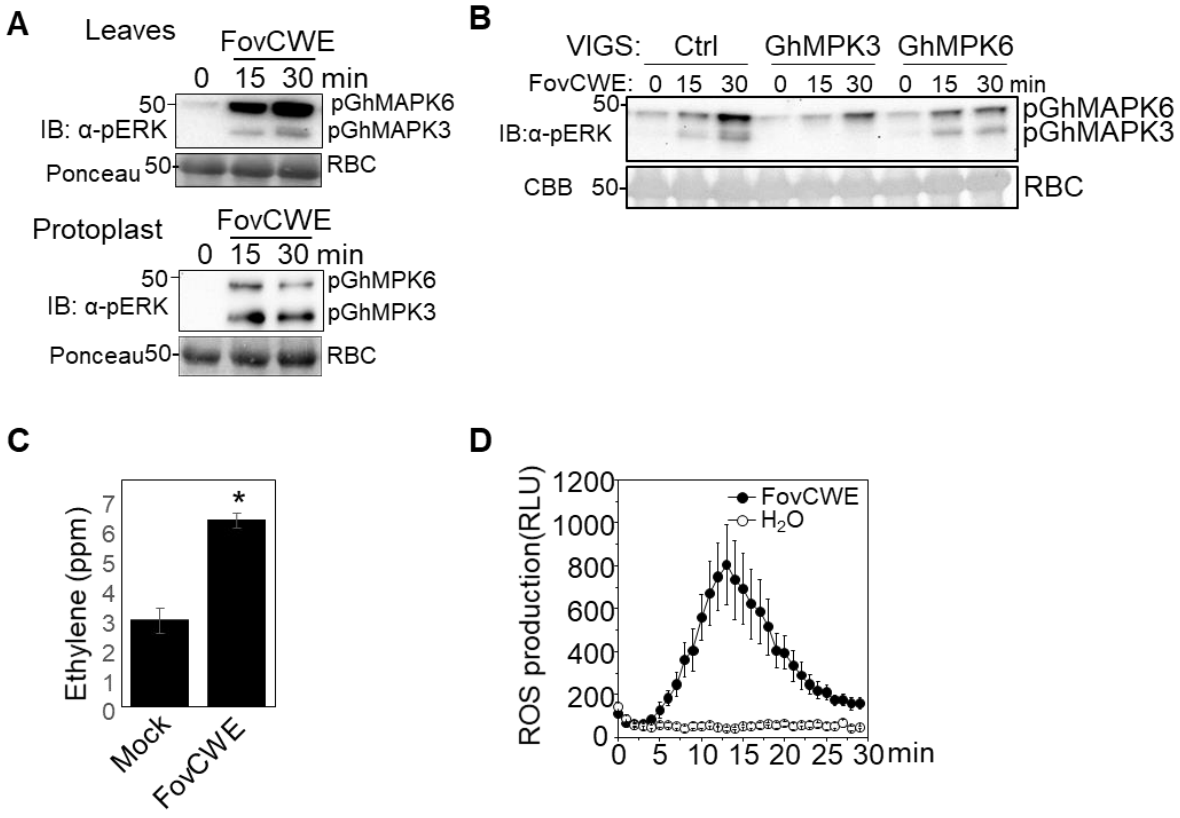

Figure 13. FovCWE induces different PTI responses in cotton.
(A) FoCWE activates MAPKs in cotton. Leaf disks from four-week-old cotton true leaves and protoplasts isolated from cotyledons were treated with FovCWE (1 mg/ml) for 15 and 30 min, respectively. The MAPK activation was analyzed by immunoblot with α-pERK antibodies (top panel). The protein loading is shown using Ponceau S staining for RuBisCo (RBC) (bottom panel). (B) FovCWE-induced MAPK activation in VIGS-*GhMAPK3* and VIGS-*GhMAPK6* plants. Leaf disks from cotton plants with silenced *GhMPK3* or *GhMPK6* by VIGS were treated with FovCWE (1 mg/l) for 15 and 30 min. (C) FovCWE induces ethylene production. Leaf disks from four-week-old cotton plants were assayed for ethylene production during a course of four hours upon FovCWE (1 mg/ml) treatment. Data shown as mean ± SE from three independent repeats. * indicates a significant difference with a Student's t-test ($p<0.05$) when compared to mock. (D) FovCWE induces ROS burst in cotton leaves. Leaf disks from four-week-old cotton leaves were assayed for ROS production by measuring the relative light units (RLU) in a luminometer upon FovCWE (1 mg/l) treatment. The data are shown as mean ± SE (n = 24).

3.4.4. FovCWE promotes plant resistance to pathogen infections

Because PAMPs can activate basal defense responses, pre-inoculation with a PAMP can often protect the hosts against pathogen infections (El Hadrami et al., 2010). We therefore tested whether FovCWE could protect Arabidopsis against the hemi-biotrophic *Pst* DC3000 infection by hand-inoculating the elicitor one day before *Pst* DC3000 hand-inoculation (Figure 14A). We observed a significant reduction in bacterial colony forming units (CFU) at two days post inoculation when pre-treating the leaves with FovCWE, compared to H_2O (ctrl) pre-treatment (Figure 14A). By contrast, FovCWE could not protect Arabidopsis against colonization by the necrotrophic fungus *Botrytis cinerea*, as demonstrated by symptom development and lesion progression after infection (Figure 14B). We also performed a FovCWE protection assay in cotton (CA 4002) seedlings against *Fov1* (CA10), a *Fusarium* isolate known to infect CA 4002, by soaking the seeds with the elicitor or a water solution control for 12 hr followed by another 12 hr treatment with *Fov1* spores ($1x10^7$) or H_2O. In this assay, severely infected seeds do not typically germinate, while germination is observed in lightly infected or non-infected seeds. Consistent with the *Pst* DC3000 results in Arabidopsis, FovCWE could protect cotton seeds from *Fov1* infections as shown in the images taken four days post-infection (Figure 14C). Seeds pre-treated with the elicitor but not infected with *Fov1* showed similar germination rates to the H_2O control, suggesting that FovCWE treatment did not affect seed germination. Because *Fov* is often considered a hemi-biotrophic pathogen, these results indicate that FovCWE may protect plants against hemi-biotrophic pathogens but not necrotrophic pathogens.

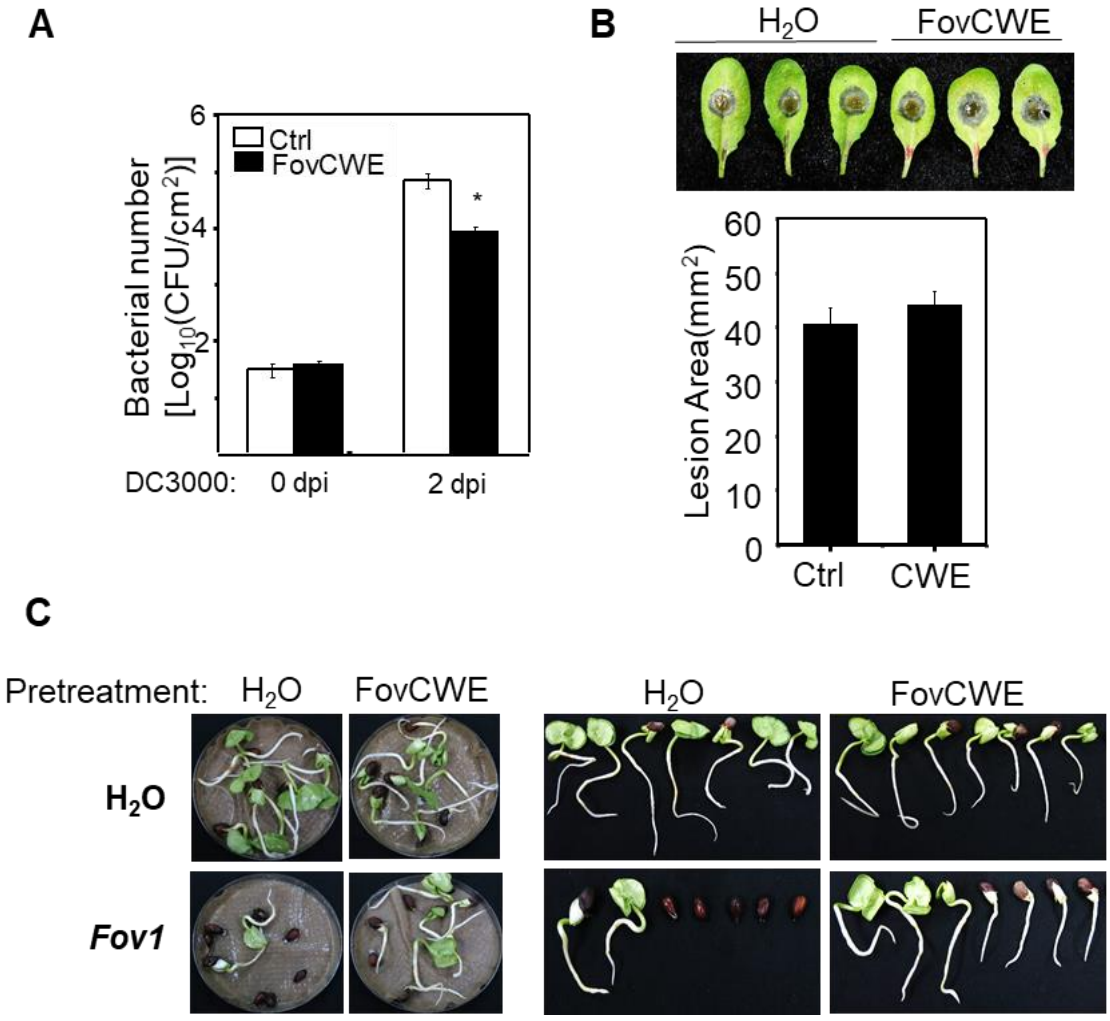

Figure 14. **FovCWE promotes plant resistance to pathogen infection**.
(A) FovCWE protection against *Pst* DC3000 infections. Leaves of four-week-old *Arabidopsis* plants were pre-inoculated with FovCWE (1 mg/ml) or sterile water one day before inoculation with *Pst* DC3000 (OD=0.00001). Bacterial colony forming units (CFU) were counted 0 and 2 days after pathogen inoculation. Data shown as mean ± SE from three independent repeats. * indicates a significant difference with a Student's t-test ($p<0.05$) when compared to Ctrl. (B) FovCWE cannot protect Arabidopsis against Botrytis infections. Four-week-old Arabidopsis leaves were pre-inoculated with FovCWE (1 mg/ml) or sterile water one day before the application of 8 µl of Botrytis spores (2.5×10^5/ml). Images were taken at 2 dpi and lesion areas were calculated by Image J. (C) FovCWE protects cotton against *Fov* CA10 race1 (*Fov*1). Cotton seeds (CA 4002) were incubated with spores (1×10^8/ml) of *Fov1* or sterile water (H_20) for 12 hours after a 12 hours pre-treatment with FovCWE (1 mg/ml) or sterile water (H_2O). Images taken at four days post infection.

3.4.5. FovCWE-induced immune responses does not require the major known PRR involved in immunity

The Arabidopsis FLS2 is a well-known PRR that recognizes the short peptide flg22 found in bacterial flagellin (Li et al., 2016a). Although flagellin is not a component of the fungal cell wall, we performed a FovCWE-induced MAPK activation assay in the Arabidopsis *fls2* mutant to rule out the possibility of flg22 contamination in our elicitor. FovCWE induced a normal MAPK activation in the *fls2* mutant at 15- and 30-min post-treatment (Figure 15A), and no flg22-induced MAPK activation was observed (Figure 15B, bottom). Chitin is an important fungal cell wall component that triggers robust defense responses in plants (Sanchez-Vallet et al., 2015). To test whether the elicitor within FovCWE is chitin, we also included the Arabidopsis *cerk1* mutant. FovCWE induced MAPK activation in the Arabidopsis *cerk1* mutant, although the activation was partially reduced (Figure 15B, top). This reduction suggests that chitin is not completely eliminated by the FovCWE extraction procedure, thus a higher MAPK activation is observed in WT plants. We did not detect any chitin-induced MAPK activation in the *cerk1* mutant (Figure 15B, bottom). Plant PRRs are divided into receptor-like kinases (RLKs) and receptor-like proteins (RLPs). Upon PAMP perception, PRRs associate with other plasma membrane receptors or co-receptors to form a complex that can trigger defense responses (Liebrand et al., 2013; Ma et al., 2016). The kinase adapter SOBIR1 has been found in complex with multiple RLPs involved in plant immunity and is therefore required for their functionality (Liebrand et al., 2013). Similarly, BAK1 and SERK4 function in plant immunity by their association with many RLKs, including FLS2 (de

Oliveira et al., 2016; Roux et al., 2011). However, we also detected normal levels of MAPK activation in the Arabidopsis *sobir1* mutant after FovCWE treatment (Figure 15C, top). Similar results were observed in the leaves of three-week-old cotton plants with silenced *GhSOBIR1* by VIGS (Figure 15C, bottom). When using the Arabidopsis *bak1-5/serk4* double mutant, normal MAPK activation levels were observed, a result which was later confirmed when the same assay was performed on cotton plants in which *GhBAK1* was silenced using VIGS (Fig 15D). Furthermore, FovCWE could inhibit root growth similar to WT in 10-week-old seedlings of *bak1-5/serk4* and *sobir1* Arabidopsis mutants at seven days post-treatment (Figure 15E). Lastly, we measured the total ethylene produced during a course of four hours after FovCWE treatment in Arabidopsis *sobir1* and *bak1-5/serk4* mutants, and observed normal induction levels when compared to WT (Figure 15F). To further confirm that the elicitor in FovCWE is not chitin, we measured the FovCWE-induced ethylene biosynthesis in Arabidopsis *cerk1* and included the *lyk4/5* double mutant because LYK4 and AtLYK5 are also required for chitin perception (Petutschnig et al., 2014). We also observed normal FovCWE-induced ethylene biosynthesis in the Arabidopsis *cerk1* and *lyk4/5* mutants (Figure 15G). No ethylene production was observed in the *cerk1* and *lyk4/5* mutants when using chitin as a control (Figure 15G). Together, these results indicate that the FovCWE-mediated immune activation is not AtFLS2, AtBAK1, AtCERK, AtLYK4/5, or AtSOBIR1 dependent.

Figure 15. **FovCWE-induced immune responses does not require the major known PRRs involved in immunity.**
(A) FovCWE-induced MAPK activation is AtFLS2 independent. Ten-day-old seedlings of WT (Col-0) and *fls2* mutant were grown on ½MS plates and treated with FovCWE (1 mg/ml) and chitin (0.1 mg/ml) for 15 and 30 min. The MAPK activation was analyzed by immunoblot with α-pERK antibodies (top panel). The protein loading is shown by Ponceau S staining for RuBisCo (RBC) (bottom panel). (B) FovCWE-induced MAPK activation is AtCERK1 independent. Ten-day-old seedlings of WT (Col-0) and *cerk1* mutant were grown on ½MS plates and treated with FovCWE (1 mg/ml) and chitin (0.1 mg/ml) for 15 and 30 min. (C) FovCWE-induced MAPK activation is SOBIR1 independent. Ten-day-old seedlings of Arabidopsis WT (Col-0) and *sobir1* mutant were grown on ½MS plates and treated with FovCWE (1 mg/ml) for 15 and 30 min. Leaf disks from four-week-old cotton plants with silenced *GhSOBIR1* by VIGS were treated with FovCWE (1 mg/ml) for 15 and 30 min. (D) FovCWE-induced MAPK activation is BAK1 independent. Ten-day-old seedlings of Arabidopsis WT (Col-0) and *bak1-5/serk4* mutant were grown on ½MS plates and treated with FovCWE (1 mg/ml) for 15 and 30 min. Leaf disks from four-week-old cotton plants with silenced *GhBAK1* by VIGS were treated with FovCWE (1 mg/ml) for 15 and 30 min. (E) FovCWE-induced root growth inhibition is AtSOBIR1 and AtBAK1 independent. Three-week-old seedlings of WT (Col-0), *sorbir1*, and *bak1-5/serk4* were grown in solid ½MS plates and transferred into liquid ½MS with or without FovCWE (1 mg/ml) for another seven days. Fresh weight data is shown as mean ± SE from three independent repeats. * indicates a significant difference with a Student's t-test ($p<0.05$) when comparing to mock treatment (Control). (F) FovCWE-induced ethylene production is AtBAK1 and AtSOBIR1 independent. Leaf disks from four-week-old WT (Col-0), *bak1-5/serk4* double mutant, and *sobir1* mutant were transferred to a 25 ml glass vial and assayed for ethylene production upon FovCWE (1 mg/ml) treatment. Total ethylene produced during a course of four hours was measured by injecting 1 ml of the headspace to a GC-FID detector. Data shown as mean ± SE from three independent repeats. * indicates a significant difference with a Student's t-test ($p<0.05$) when compared to mock treatment. (G) FovCWE-induced ethylene production is AtCERK1 and AtLYK4/5 independent. Leaf disks from four-week-old WT (Col-0), *cerk1* mutant, and *lyk4/5* double mutant were assayed for total ethylene production upon FovCWE treatment as described above. Data shown as mean ± SE from three independent repeats. * indicates a significant difference with a Student's t-test ($p<0.05$) when compared to mock treatment.

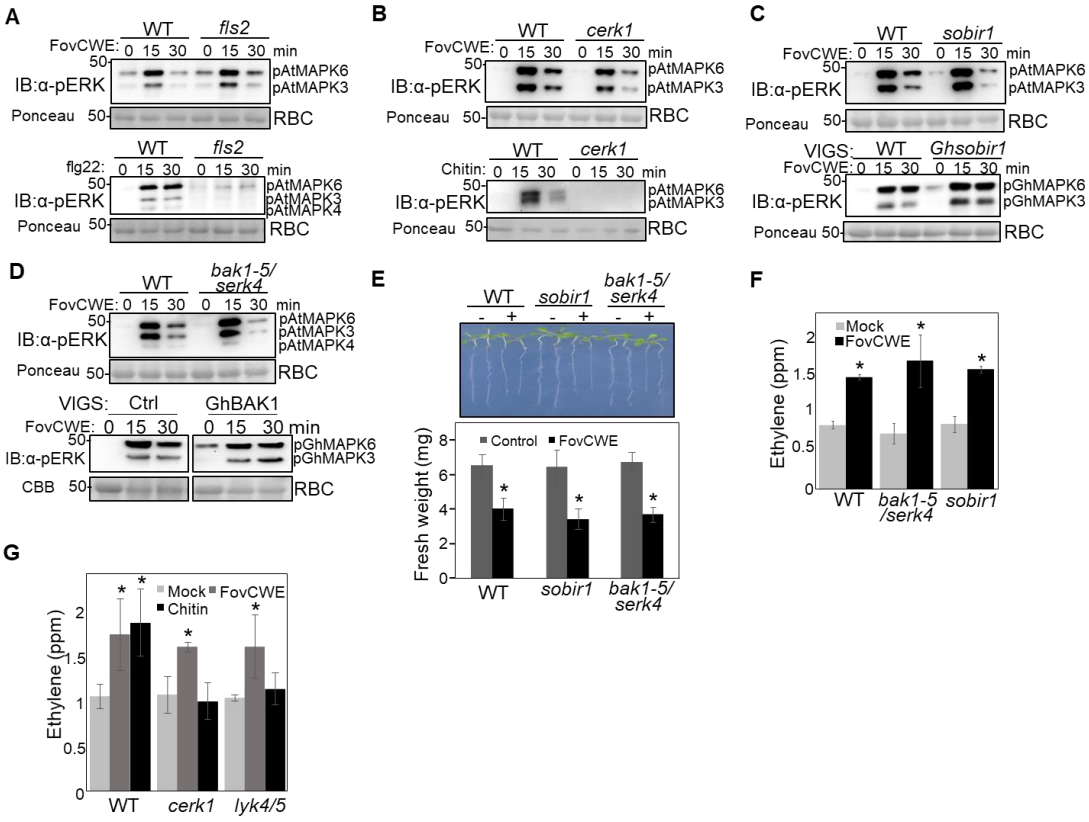
A
WT
fls2
FovCWE: 0 15 30 0 15 30 min
50
IB:α-pERK
pAtMAPK6
pAtMAPK3
Ponceau 50
RBC
flg22: 0 15 30 0 15 30 min
pAtMAPK4
B
Chitin: 0 15 30 0 15 30 min
cerk1
C
sobir1
VIGS: Ctrl GhBAK1
Ghsobir1
pGhMAPK6
pGhMAPK3
D
bak1-5/ serk4
CBB
E
- + - + - +
Control
FovCWE
Fresh weight (mg)
F
Mock
Ethylene (ppm)
WT
bak1-5 /serk4
sobir1
G
Chitin
lyk4/5

3.4.6. FovCWE is a soluble, heat-stable PAMP

To determine the nature of the elicitor, FovCWE was subjected to protease and heat treatment before MAPK elicitation in 10-week-old Arabidopsis seedlings. First, to determine if the protease itself can activate MAPK, seedlings were treated with a mock solution containing Protease K. As shown in Figure 16A, the residual Protease K was sufficient to degrade all total proteins even after elicitation as seen in the lack of a RuBisCo band in the loading control, thus resulting in no MAPK activation. On the other hand, when the Proteinase K was heat inactivated at 95°C before seedling treatment, minimal MAPK activation was observed, indicating that the inactivated Protease K cannot induce a strong MAPK activation (Figure 16A). FovCWE treated with Protease K and subjected to heat inactivation was able to induce MAPK activation at the same extent as FovCWE (Figure 16A).

Because FovCWE does not completely dissolve in water, we wanted to determine if the immune-eliciting component within FovCWE is water-soluble. The elicitor was centrifuged to remove the supernatant and the remaining pellet was resuspended in the same volume of sterile distilled water to test the capability of both the supernatant and the resuspended pellet to elicit MAPK in Arabidopsis seedlings. Interestingly, the supernatant but not the resuspended pellet could induce MAPK activation (Figure 16B). Taken together, these results suggest that the immune-eliciting component in FovCWE is a non-proteinaceous, heat-stable, and water-soluble PAMP.

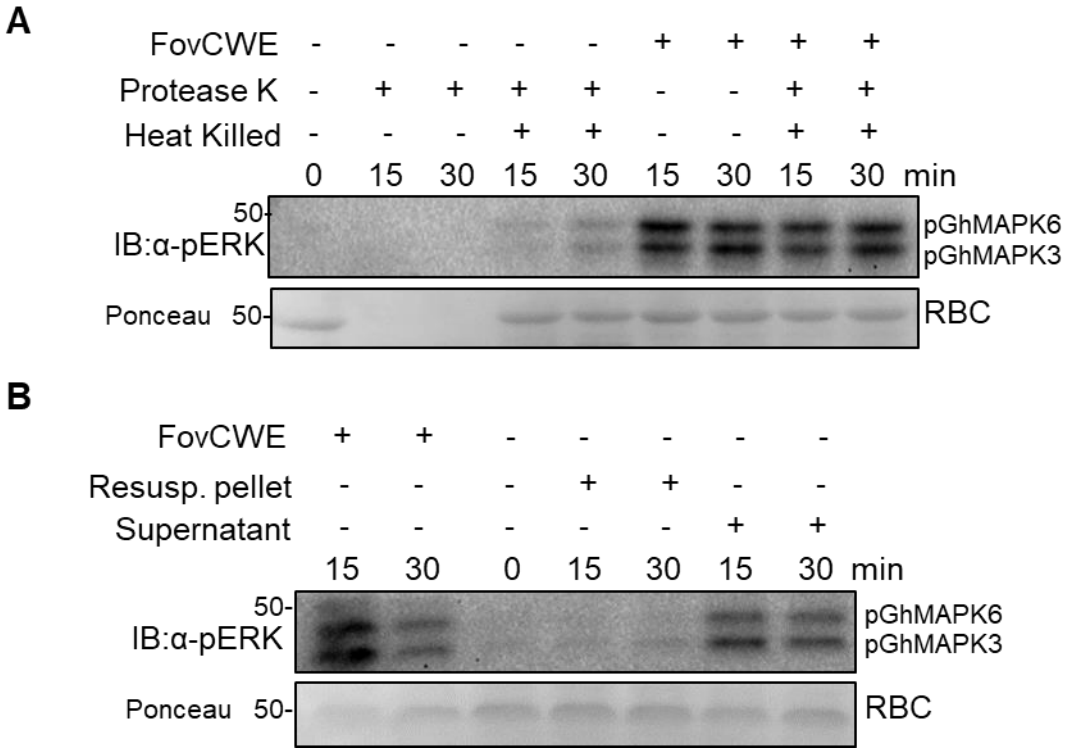

Figure 16. **FovCWE is a water-soluble, heat-stable PAMP**.
(A) Protease K or heat treatment does not affect FovCWE-induced MAPK activation. FovCWE (1 mg/ml) was used to elicit MAPK activity in 10-day-old Arabidopsis seedlings. Prior to elicitation, the elicitor was subjected to treatment with 80 U/ml Protease K (NEB) for 15 minutes at 37°C. After treatment, the enzyme was heat inactivated at 95°C for five minutes. Controls without protease treatment and without heat inactivation after protease treatment are included. (B) The immune-eliciting component(s) within FovCWE is water-soluble. The FovCWE was centrifuged at 14,800 rpm for 15 minutes in a benchtop centrifuge. The supernatant was removed and the pellet was resuspended in the same volume of sterile distilled water. Both the supernatant and the resuspended pellet were tested for their capacity to elicit MAPK in Arabidopsis seedlings.

3.4.7. Several FovCWE induced-genes are suppressed during *Fov* infections

To determine the transcriptome dynamics during FovCWE elicitation, we performed RNA sequencing (RNA-seq) analysis of cotton roots (WT) treated with or without FovCWE for 1 hr. The correlation coefficient (r) for the expression profile of each detectable transcript in cotton seedlings with or without FovCWE treatment is close to linear (Figure 17A). Among 72,762 detectable transcripts, 546 showed reduced and 980 showed enhanced expression (fold change ≥2 and false discovery rate [FDR] < 0.05) after FovCWE treatment compared to H_2O Ctrl. The gene process annotations among the genes found to be upregulated in the FovCWE-treated seedlings can be found in Figure 17B. Notably, a large portion of upregulated genes are classified to be associated with photosynthesis (Figure 17B).

Because we hypothesized that some of the FovCWE-induced genes can be suppressed upon infection of virulent isolates of *Fov*, we performed another RNA-seq experiment to determine transcriptome dynamics in the roots of cotton seedlings during *Fov* infection and to compare it to the FovCWE dataset. We observed 440 upregulated and 581 downregulated genes at three days post *Fov* infection (Figure 17C). Similarly, we observed 716 upregulated and 636 downregulated genes at five days post *Fov* infection (Figure 17C). Among the differentially expressed genes (DEGs), 36 were upregulated at both three- and five-days post infection, while 61 were downregulated at both three- and five-days post infection (Figure 17C). We then compared the two datasets to look for any genes upregulated upon FovCWE treatment but downregulated during *Fov* infection. Interestingly, 12 of the upregulated genes upon FovCWE treatment were downregulated

at three days after *Fov* infection (Figure 17D), while 44 of the upregulated genes upon FovCWE treatment were downregulated at five days after *Fov* infection (Figure 17E). The ID and annotation of the genes upregulated upon FovCWE, but downregulated at three- or five-days post *Fov* infection, can be found in Table 6.

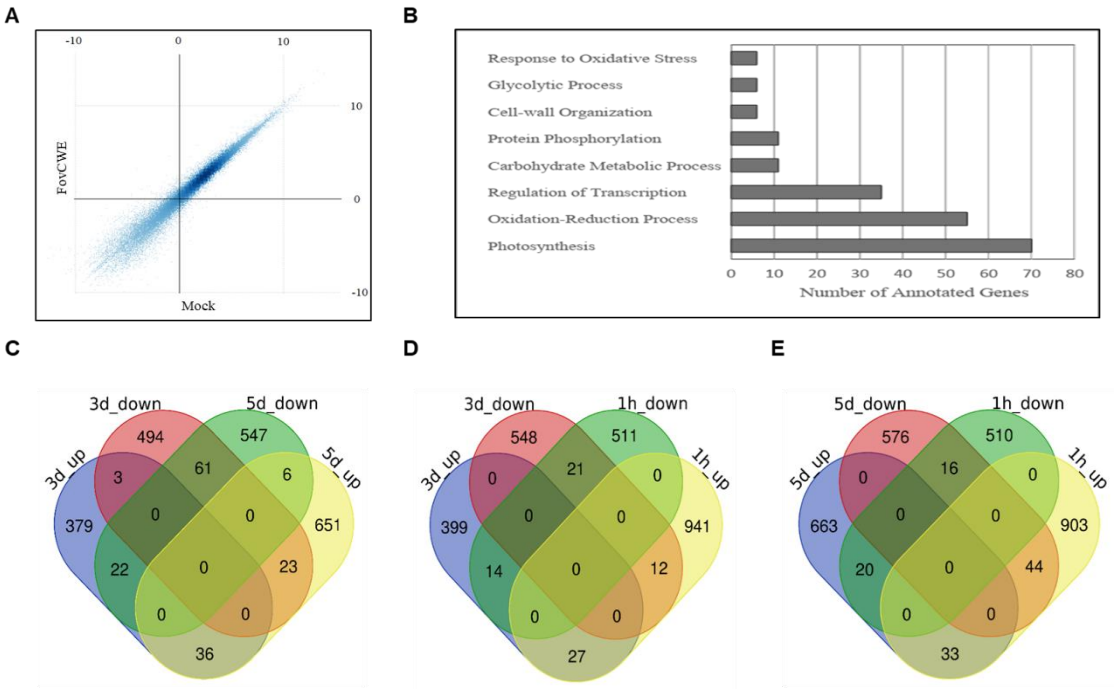

Figure 17. Transcriptome reprograming upon FovCWE inoculation and *Fov* infection.

(A) Scatter plot comparing the mean expression in transcripts per million (TPM) for each transcript between mock and treated (FovCWE) samples. Roots of ten-day-old cotton seedlings were used for analysis. The Y-axis indicates gene expression in treated samples, and the X-axis indicates gene expression in mock-treated samples. (B) Bar chart indicating the most frequent gene process annotations among the upregulated genes in the FovCWE-treated samples (FDR <0.05, Log2FC > 1). (C) Venn diagram of differentially expressed genes (DEGs) at three -and five-days after *Fov* infections (D) Venn diagram comparing DEGs between FovCWE treatment (1h_down/up) and three days after *Fov* infection (3d_down/up). (B) Venn diagram comparing DEGs between FovCWE treatment (1h_down/up) and five days after *Fov* infection (5d_down/up). Venn diagrams: Oliveros, J.C. (2007-2015) Venny. An interactive tool for comparing lists with Venn's diagrams. https://bioinfogp.cnb.csic.es/tools/venny/index.html.

Table 6. Suppressed FovCWE-inducible genes in cotton plants infected with *Fov*

Gene ID	Annotation
Gh_A01G1311	RING/U-box superfamily protein
Gh_A01G1972	light harvesting complex photosystem II
Gh_A02G0959	Aluminium activated malate transporter family protein
Gh_A03G1705	2Fe-2S ferredoxin-like superfamily protein
Gh_A03G1927	photosystem I subunit K
Gh_A04G0098	syntaxin of plants 51
Gh_A05G0654	photosystem I subunit O
Gh_A05G1261	chlorophyll A/B binding protein 1
Gh_A05G2108	light harvesting complex of photosystem II 5
Gh_A05G3469	PAP/OAS1 substrate-binding domain superfamily
Gh_A05G3490	Unkown
Gh_A07G1850	photosystem I subunit E-2
Gh_A07G2172	Ribulose bisphosphate carboxylase (small chain) family protein
Gh_A07G2184	photosystem II light harvesting complex gene 2.1
Gh_A07G2201	photosystem I subunit l
Gh_A08G1309	Unkown
Gh_A09G1680	RING/U-box superfamily protein
Gh_A09G1927	G-protein gamma subunit 2
Gh_A10G0618	glyceraldehyde 3-phosphate dehydrogenase A subunit 2
Gh_A11G1981	Unknown

Table 6. Continued

Gene ID	Annotation
Gh_A11G2563	Dynein light chain type 1 family protein
Gh_A12G0502	Unkown
Gh_A13G1057	Cation efflux family protein
Gh_A13G1345	2-oxoglutarate (2OG) and Fe(II)-dependent oxygenase superfamily protein
Gh_D01G1136	Unkown
Gh_D01G2012	Unkown
Gh_D01G2232	light harvesting complex photosystem II
Gh_D02G2126	2Fe-2S ferredoxin-like superfamily protein
Gh_D04G1495	Vacuolar iron transporter (VIT) family protein
Gh_D05G0192	Unkown
Gh_D05G0272	Unkown
Gh_D05G0860	photosystem I light harvesting complex gene 1
Gh_D05G1266	Unkown
Gh_D05G1774	ferredoxin-NADP(+)-oxidoreductase 1
Gh_D05G2361	light harvesting complex of photosystem II 5
Gh_D06G0421	natural resistance-associated macrophage protein 1
Gh_D06G1627	ATPase, F1 complex, gamma subunit protein
Gh_D07G1090	photosystem I subunit O
Gh_D07G1759	Ribulose bisphosphate carboxylase (small chain) family protein

Table 6. Continued

Gene ID	Annotation
Gh_D08G0702	photosystem I subunit D-2
Gh_D08G1007	Unkown
Gh_D09G1856	Glycosyl hydrolases family 32 protein
Gh_D10G0167	photosystem II subunit Q-2
Gh_D10G0369	chlorophyll A/B binding protein 1
Gh_D10G1152	SOS3-interacting protein 4
Gh_D10G2299	rubisco activase
Gh_D11G1124	NIM1-interacting 1
Gh_D11G1671	Ribulose bisphosphate carboxylase (small chain) family protein
Gh_D11G3081	basic helix-loop-helix (bHLH) DNA-binding superfamily protein
Gh_D12G0423	Protein kinase superfamily protein
Gh_D12G1264	Adenine nucleotide alpha hydrolases-like superfamily protein
Gh_D13G1322	Cation efflux family protein
Gh_D13G1656	UDP-glucosyl transferase 73C1

Table 6. Primers used in this study.

Cloning primers for VIGS analysis.

Gene	Forward primer	Reverse Primer
GhMPK3	GGGGTACCGGCATTTGGATCACGAGAAT	CCGCTCGAGCCAAGCAGCTCTGTCAACAA
GhMPK6	CGGAATTCGATCAAGCTGCTTCGTCACA	CCGCTCGAGAAATGCAACCCACTGACCAT
GhSOBIR1-1	CGGAATTCCGTACAACAAGTATCAGAAGGC	GGGGATTTGATCAGCTGATGATATTCAGGTGCG
GhSOBIR1-2	ACCTGAATATCATCAGCTGATCAAATCCCCGCC	GGGGTACCCCAATTGATTGTTTGCAAGGG
GhBAK1	CGGAATTCGCACTCGGAGCTGCAAGG	GGGGTACCGAGTGCACAACAGAGCC

3.5. Discussion

Fusarium wilt is a devasting disease affecting crop production across the US and other countries. *Fo* isolates infect a wide range of hosts and their virulence is plant species specific. Although most *Fo* isolates display some level of pathogenicity, some are non-pathogenic and instead protect plants from infections of virulent isolates. However, the mechanisms underlying the protection and virulence of Fusarium remain largely unknown. Here, we found a species and race-independent elicitor from *Fo* cell wall preparations that can induce defense responses in cotton and Arabidopsis, and its

perception is independent of some of the major immunity PRRs known to date. These results could explain the different pathogenicity levels in *Fo* isolates.

The activation of MAPK cascades is one of the earliest PRR signaling events triggered by PAMPs (Yu et al., 2017). MAPK cascades typically contain three sequentially activated kinases. In Arabidopsis, MPK3, MPK6, and MPK4 are among the well-studied MAPKs activated by different PAMPs (Colcombet and Hirt, 2008; Meng and Zhang, 2013). We showed that *Fo47* spores and FoCWEs can activate MPK3, MPK6 and MPK4, similarly to other PAMPs in Arabidopsis (Figure 11A,D). We also established PAMP-induced MAPK activation assays in cotton and showed that FovCWE could also activate at least MPK3 and MPK6 in true leaves and protoplasts isolated from cotyledons, similarly to the MAPK results in Arabidopsis (Figure 13A,B). In addition, Arabidopsis transgenic plants carrying the firefly luciferase gene under the control of the *FRK1* gene promoter serve as a convenient tool to readily quantify PAMP-induced gene transcription activation (Li et al., 2014). Using the *pFRK1::LUC* reporter lines, we showed that spores from *Fo47*, a non-virulent Fusarium isolate, could strongly induce *FRK1::LUC* activities (Figure 11B). It appears that the *Fo47* spore-induced *FRK1::LUC* activities peak occurs later than those induced by flg22 treatment (Figure 11B). This observation is similar to the FovCWE-induced MAPK activation often peaked at 30 min in cotton leaves (Figure 13A,B), while the highest flg22 or chitin-induced MAPK activation peak is often observed at 15 min after treatment. It remains possible that different complexes mediating FovCWE and other PAMPs perception and signaling display different temporal dynamics of MAPK activation and immune gene transcription reprograming.

Other typical PAMP-induced defense responses include ethylene biosynthesis, ROS burst, stomatal closure and root inhibition. Ethylene biosynthesis is believed to regulate multiple PTI responses, including ROS production and expression of defense genes, and it may play an important role against soil-borne fungal pathogens, including *Fo* (Berrocal-Lobo and Molina, 2004; Bouchez et al., 2007; Kavroulakis et al., 2007; Yang et al., 2017). ROS is known to regulate callose deposition for cell wall strengthening to prevent pathogen entry, and to function as a signal molecule to regulate other responses (Luna et al., 2011; Mittler and Blumwald, 2015). Interestingly, a ROS burst was reported in *Arabidopsis* leaves treated with a cell wall preparation of *F. oxysporum f.sp.* matthioli race 1 (Davies et al., 2006). Regulation of stomatal closure is also part of the first line of defense against pathogen invasion to prevent the pathogen entry via stomata (Melotto et al., 2006). Lastly, growth inhibition is thought to occur due to the growth-defense tradeoffs in which there is prioritization towards either growth or defense (Gomez-Gomez et al., 1999; Huot et al., 2014). The fact that FoCWE can activate all of the previous defense responses in cotton and Arabidopsis (Figures 12 and 13) confirms that a PAMP within FoCWE exists, and that it may be perceived in different plant species.

PAMPs can be used as a crop disease control strategy due to their ability to enhance innate immune responses (El Hadrami et al., 2010). It has been reported that *Fo47* functions as a biocontrol agent by inducing systemic resistance in tomato and flax, likely by inducing the expression of pathogenesis-related genes (Aime et al., 2013; Duijff et al., 1998; Olivain et al., 1995). In addition, *Fo47* was reported to protect tomato and pepper against Fusarium and Verticillium wilt, respectively (Fuchs et al., 1997; Veloso et al.,

2016). We observed significant FovCWE protection against the bacterial pathogen *Pst* DC3000 in Arabidopsis (Figure 14A), and against *Fov1* in cotton seeds (Figure 14C), which is consistent with the previous reports. However, we did not see a protection in Arabidopsis against *B. cinerea* (Figure 14B). These results are compelling because both *Fov* and *P. syringae* are considered hemi-biotrophs, as they have a biotrophic stage early in the infection process, while *B. cinerea* is considered a necrotroph due to the extensive tissue damage and cell death observed at very early stages (Glazebrook, 2005; Warman and Aitken, 2018). It would be interesting to study the overlap between FovCWE and biotrophic/hemi-biotrophic pathogens perception and signaling.

To gain insights into the molecular mechanisms of FovCWE perception, we measured PTI responses in Arabidopsis and cotton plants lacking some of the PRRs involved in fungal immunity. The bacterial flagellin receptor FLAGELLIN-SENSITIVE 2 (FLS2) recognizes flg22 in Arabidopsis and heterodimerize with the co-receptor AtBAK1 after ligand perception (Li et al., 2016a; Ma et al., 2016). The formation of the heteromeric complex then initiates intracellular signaling and defense responses by its interaction with receptor-like cytoplasmic kinases. Unsurprisingly, the Arabidopsis *fls2* mutant showed a normal FovCWE-induced MAPK activation, contrary to flg22, thus also ruling out the possibility of flg22 contamination in our elicitor (Figure 15A). On the other hand, the partially reduced MAPK activation observed in the Arabidopsis *cerk1* mutant can be explained by the presence of chitin in our elicitor, as we know it is a component of the fungal cell wall (Figure 15B, top). It is clear that chitin itself is not the only component triggering PTI in Arabidopsis because no MAPK activation is observed in the *cerk1*

mutant when using chitin (Figure 15B, bottom). This was later reaffirmed by the normal FovCWE-induced ethylene biosynthesis in the Arabidopsis *cerk1* and *lyk4/5* mutants, which are defective in chitin perception (Figure 15G, top). AtBAK1 also plays a key role in different plasma membrane-associated protein complexes important in immunity, including RLPs involved in fungal resistance such as the Arabidopsis RLP23 and RLP30, and the tomato Ve1, Eix1 and Eix2 (Albert et al., 2015; Bar et al., 2010; Fradin et al., 2011; Liebrand et al., 2013; Monaghan and Zipfel, 2012; Zhang et al., 2013). However, we also observed normal FovCWE-induced MAPK activation in cotton plants with silenced *GhBAK1* (Figure 15D, bottom). Because AtSERK4 also plays a role in immunity by association with immune receptors (Roux et al., 2011), we included the Arabidopsis *bak1/serk4* double mutant in the experiments. The normal FovCWE-induced MAPK activation, ethylene biosynthesis, and root growth inhibition in the double mutant indicate that AtBAK1 and SERK4 are not involved in its perception (Figure 15D, top; Figure 15E, bottom; Figure 15F). Similar to BAK1, SOBIR1 has an important role as a kinase adapter for RLPs involved in fungal defense, including the tomato Cf, Eix2 and Ve1, and the *Arabidopsis* RLP30 and RBPG1 (Liebrand et al., 2013). The normal FovCWE-induced MAPK activation, ethylene biosynthesis, and root growth inhibition in the Arabidopsis *sobir1* mutant (Figure 15C, top; Figure 15E, bottom; Figure 15F), and the normal FovCWE-induced MAPK activation in cotton plants with silenced *GhSOBIR1* (Figure 15C, bottom), indicates that SOBIR1 in not involved in FovCWE perception. We therefore hypothesize that a specific FoCWE receptor exists in plants.

The observation that FovCWE pre-treated with Proteinase K retains its capacity to elicit MAPK activation in Arabidopsis seedlings cannot be used to rule out the possibility that the immune-activating component within FovCWE is a protein (Figure 16A). However, the result still serves to narrow the range of possibilities. Unfortunately, no receptors have been found to perceive fungal ergosterol or the well-characterized immunoactive polysaccharide β-glucan (Rodrigues et al. 2011; Yu et al. 2017), thus mutants defective in ergosterol and glucan perception are not available to test in this manner. Our results also suggest that the eliciting component within FovCWE is water soluble (Figure 16B), which does not support the notion that the immune activating component is a sterol. Similarly, β-glucan has low solubility in water, although polysaccharides in general display a wide range of solubility characteristics (Han et al. 2008). Most polysaccharides are relatively heat stable, and the activity of FovCWE was also found to be stable at 95°C. Therefore, we cannot exclude the possibility that a polysaccharide is the immune-activating component in FovCWE. While mycotoxins are not well documented to activate this type of immunity, we can also not exclude the possibility that the observed MAPK activation is induced by one of the many metabolites produced by Fusarium species that may be contained within FovCWE such as apicidins, fumonisins, moniliformins, and several others (Hansen et al., 2012; Waskiewicz et al., 2010).

The taxon *Fusarium oxysporum* (*Fo*) is a highly diverse and widely dispersed plant-pathogenic fungi with a large broad host range, infecting both monocotyledonous and dicotyledonous plants (Ma et al., 2010). The pathogenic *Fo* isolates have been

classified into more than 120 *formae speciales* (f. sp.) based on their host specificity (Thatcher et al., 2012). The *Fo* infection process have been well-studied in tomato plants and we know that *F. oxysporum f. sp.* lycopersici (*Fol*), the causal agent of tomato wilt, can secrete a number of virulence effectors, known as *Secreted In Xylem* (SIX), in the xylem sap of tomato plants to facilitate disease progression (Gawehns et al., 2015; Houterman et al., 2007; Lievens et al., 2009; Ma et al., 2015; Rep et al., 2005). Virulence effectors are proteins secreted by the pathogen to suppress PTI responses and cause disease. We believe that *Fov* is also capable of secreting virulence proteins to manipulate the host defense responses. On the other hand, it is possible that the protective *Fo47* isolate do not secrete virulent effectors, in contrast to the *Fov* isolates used in this study which have different pathogenicity levels in cotton (Fuchs et al., 1997; Thatcher et al., 2012; Ulloa et al., 2013b; Ulloa et al., 2011; Veloso et al., 2016). The hypothesis that the different levels of pathogenicity in *Fo* isolates is determined by their ability to suppress PTI responses is reaffirmed in our RNA-seq data in which we see an increase in suppression of FovCWE-induced genes from three to five days post *Fov* infection. Therefore, disease progression may be accompanied by higher transcriptional changes in the host which are a result of pathogen hijacking of defense responses.

4. CONCLUSIONS

We have studied the genetic and molecular basis of *Fusarium oxysporum* f. sp. *vasinfectum* (*Fov)* interaction with cotton. On the plant side, we found several Receptor-Like Proteins (RLPs) to be important in this interaction, as demonstrated with the increased susceptibility in cotton plants when these RLPs were silenced. This is not surprising, as we know that RLPs are important in immunity against fungal pathogens. These results also validate the efficiency of our virus-induced gene silencing (VIGS) screening, which can be used to get insights for other important pathways in cotton. Future work should focus on further biochemical characterization of these RLPs to gain insights about the biochemical pathways they belong to. In addition, it would be interesting to study the interspecies transfer of RLPs to test if they can provide resistance to Fusarium wilt in other crops.

On the pathogen side, our work demonstrated that at least one component of *Fo* cell wall functions as a PAMP which can induce defense responses and transcriptional reprograming in plants. Our data supports the idea of the evolution of *Fov* isolates to cause disease by secreting virulence effectors to suppress defense responses. Future work should focus on elucidating the mechanisms of FoCWE perception in plants and the identification of virulence effectors across different *Fo* isolates. These findings will contribute towards the understanding of the conserved and isolate-nonspecific features of *Fo.*

To conclude, our work provides knowledge that can facilitate efforts by plant breeders and geneticists to produce durable resistance against Fusarium wilt.

REFERENCES

Afzal, A.J., Wood, A.J., and Lightfoot, D.A. (2008) Plant receptor-like serine threonine kinases: roles in signaling and plant defense. Mol Plant Microbe Interact *21*, 507-517.

Aime, S., Alabouvette, C., Steinberg, C., and Olivain, C. (2013) The endophytic strain Fusarium oxysporum Fo47: a good candidate for priming the defense responses in tomato roots. Mol Plant Microbe Interact *26*, 918-926.

Albert, I., Bohm, H., Albert, M., Feiler, C.E., Imkampe, J., Wallmeroth, N., Brancato, C., Raaymakers, T.M., Oome, S., Zhang, H., Krol, E., et al. (2015) An RLP23-SOBIR1-BAK1 complex mediates NLP-triggered immunity. Nat Plants *1*, 15140.

Appel, D.J., and Gordon, T.R. (1996) Relationships among pathogenic and nonpathogenic isolates of Fusarium oxysporum based on the partial sequence of the intergenic spacer region of the ribosomal DNA. Molecular Plant Microbe Interactions *9*, 125-138.

Asai, T., Tena, G., Plotnikova, J., Willmann, M.R., Chiu, W.L., Gomez-Gomez, L., Boller, T., Ausubel, F.M., and Sheen, J. (2002) MAP kinase signalling cascade in Arabidopsis innate immunity. Nature *415*, 977-983.

Atkinson, G.F. (1892) Some diseases of cotton. Alabama Agricultural Experimental Station, 41-65.

Bar, M., Sharfman, M., Ron, M., and Avni, A. (2010) BAK1 is required for the attenuation of ethylene-inducing xylanase (Eix)-induced defense responses by the decoy receptor LeEix1. Plant J *63*, 791-800.

Beattie, G.A. (2011) Water relations in the interaction of foliar bacterial pathogens with plants. Annu Rev Phytopathol *49*, 533-555.

Bej, A., Sahoo, B.R., Swain, B., Basu, M., Jayasankar, P., and Samanta, M. (2014) LRRsearch: An asynchronous server-based application for the prediction of leucine-rich repeat motifs and an integrative database of NOD-like receptors. Comput Biol Med *53*, 164-170.

Belkhadir, Y., Yang, L., Hetzel, J., Dangl, J.L., and Chory, J. (2014) The growth-defense pivot: crisis management in plants mediated by LRR-RK surface receptors. Trends Biochem Sci *39*, 447-456.

Berrocal-Lobo, M., and Molina, A. (2004) Ethylene response factor 1 mediates Arabidopsis resistance to the soilborne fungus Fusarium oxysporum. Mol Plant Microbe Interact *17*, 763-770.

Bigeard, J., Colcombet, J., and Hirt, H. (2015) Signaling mechanisms in pattern-triggered immunity (PTI). Mol Plant *8*, 521-539.

Bleckmann, A., Weidtkamp-Peters, S., Seidel, C.A., and Simon, R. (2010) Stem cell signaling in Arabidopsis requires CRN to localize CLV2 to the plasma membrane. Plant Physiol *152*, 166-176.

Bohn, G.W., and Tucker, C.M. (1939) Immunity to Fusarium Wilt in the Tomato. Science *89*, 603-604.

Boller, T., and Felix, G. (2009) A renaissance of elicitors: perception of microbe-associated molecular patterns and danger signals by pattern-recognition receptors. Annu Rev Plant Biol *60*, 379-406.

Bouchez, O., Huard, C., Lorrain, S., Roby, D., and Balague, C. (2007) Ethylene is one of the key elements for cell death and defense response control in the Arabidopsis lesion mimic mutant vad1. Plant Physiol *145*, 465-477.

Cao, Y., Liang, Y., Tanaka, K., Nguyen, C.T., Jedrzejczak, R.P., Joachimiak, A., and Stacey, G. (2014) The kinase LYK5 is a major chitin receptor in Arabidopsis and forms a chitin-induced complex with related kinase CERK1. Elife *3*,

Catanzariti, A.M., Lim, G.T., and Jones, D.A. (2015) The tomato I-3 gene: a novel gene for resistance to Fusarium wilt disease. New Phytol *207*, 106-118.

Chakrabarti, A., Rep, M., Wang, B., Ashton, A., Dodds, P., and Ellis, J. (2011) Variation in potential effector genes distinguishing Australian and non-Australian isolates of the cotton wilt pathogen *Fusarium oxysporum f. sp. vasinfectum*. Plant Pathology *60*, 232-243.

Chaves, M.M., Pereira, J.S., Maroco, J., Rodrigues, M.L., Ricardo, C.P., Osorio, M.L., Carvalho, I., Faria, T., and Pinheiro, C. (2002) How plants cope with water stress in the field. Photosynthesis and growth. Ann Bot *89 Spec No*, 907-916.

Chen, M., Zeng, H., Qiu, D., Guo, L., Yang, X., Shi, H., Zhou, T., and Zhao, J. (2012) Purification and characterization of a novel hypersensitive response-inducing elicitor from Magnaporthe oryzae that triggers defense response in rice. PLoS One *7*, e37654.

Cianchetta, A.N., and Davis, R.M. (2015) Fusarium wilt of cotton: Management strategies. Crop Prot *73*, 40-44.

Clarke, C.R., Chinchilla, D., Hind, S.R., Taguchi, F., Miki, R., Ichinose, Y., Martin, G.B., Leman, S., Felix, G., and Vinatzer, B.A. (2013) Allelic variation in two distinct Pseudomonas syringae flagellin epitopes modulates the strength of plant immune responses but not bacterial motility. New Phytol *200*, 847-860.

Colcombet, J., and Hirt, H. (2008) Arabidopsis MAPKs: a complex signalling network involved in multiple biological processes. Biochem J *413*, 217-226.

Cole, S.J., and Diener, A.C. (2013) Diversity in receptor-like kinase genes is a major determinant of quantitative resistance to Fusarium oxysporum f.sp. matthioli. New Phytol *200*, 172-184.

Couto, D., and Zipfel, C. (2016) Regulation of pattern recognition receptor signalling in plants. Nat Rev Immunol *16*, 537-552.

Cox, K.L., Jr., Babilonia, K., Wheeler, T., He, P., and Shan, L. (2019) Return of old foes - recurrence of bacterial blight and Fusarium wilt of cotton. Curr Opin Plant Biol *50*, 95-103.

Dangl, J.L., and Jones, J.D. (2001) Plant pathogens and integrated defence responses to infection. Nature *411*, 826-833.

Davies, D.R., Bindschedler, L.V., Strickland, T.S., and Bolwell, G.P. (2006) Production of reactive oxygen species in Arabidopsis thaliana cell suspension cultures in response to an elicitor from Fusarium oxysporum: implications for basal resistance. J Exp Bot *57*, 1817-1827.

Davis, R.M., Colyer, P.D., Rothrock, C.S., and Kochman, J.K. (2006) Fusarium wilt of cotton: Population diversity and implications for management. Plant Disease *90*, 692-703.

de Oliveira, M.V., Xu, G., Li, B., de Souza Vespoli, L., Meng, X., Chen, X., Yu, X., de Souza, S.A., Intorne, A.C., de, A.M.A.M., Musinsky, A.L., et al. (2016) Specific control of Arabidopsis BAK1/SERK4-regulated cell death by protein glycosylation. Nat Plants *2*, 15218.

De Wit, P.J. (2016) Apoplastic fungal effectors in historic perspective; a personal view. New Phytol *212*, 805-813.

Di, X., Gomila, J., and Takken, F.L.W. (2017) Involvement of salicylic acid, ethylene and jasmonic acid signalling pathways in the susceptibility of tomato to Fusarium oxysporum. Mol Plant Pathol *18*, 1024-1035.

Diener, A.C., and Ausubel, F.M. (2005) RESISTANCE TO FUSARIUM OXYSPORUM 1, a dominant Arabidopsis disease-resistance gene, is not race specific. Genetics *171*, 305-321.

Divon, H.H., Ziv, C., Davydov, O., Yarden, O., and Fluhr, R. (2006) The global nitrogen regulator, FNR1, regulates fungal nutrition-genes and fitness during Fusarium oxysporum pathogenesis. Molecular plant pathology *7*, 485-497.

Du, J., Verzaux, E., Chaparro-Garcia, A., Bijsterbosch, G., Keizer, L.C., Zhou, J., Liebrand, T.W., Xie, C., Govers, F., Robatzek, S., van der Vossen, E.A., et al. (2015) Elicitin recognition confers enhanced resistance to Phytophthora infestans in potato. Nat Plants *1*, 15034.

Duijff, B.J., Pouhair, D., Olivain, C., Alabouvette, C., and Lemanceau, P. (1998) Implication of systemic induced resistance in the suppression of Fusarium wilt of tomato by Pseudomonas fluorescens WCS417r and by nonpathogenic Fusarium oxysporum Fo47. European Journal of Plant Pathology *104*, 903-910.

Edel-Hermann, V., and Lecomte, C. (2019) Current Status of Fusarium oxysporum Formae Speciales and Races. Phytopathology *109*, 512-530.

El Hadrami, A., Adam, L.R., El Hadrami, I., and Daayf, F. (2010) Chitosan in plant protection. Mar Drugs *8*, 968-987.

Felix, G., Duran, J.D., Volko, S., and Boller, T. (1999) Plants have a sensitive perception system for the most conserved domain of bacterial flagellin. Plant J *18*, 265-276.

Flagel, L.E., Wendel, J.F., and Udall, J.A. (2012) Duplicate gene evolution, homoeologous recombination, and transcriptome characterization in allopolyploid cotton. BMC Genomics *13*, 302.

Flexas, J., and Medrano, H. (2002) Drought-inhibition of photosynthesis in C3 plants: stomatal and non-stomatal limitations revisited. Ann Bot *89*, 183-189.

Fradin, E.F., Abd-El-Haliem, A., Masini, L., van den Berg, G.C., Joosten, M.H., and Thomma, B.P. (2011) Interfamily transfer of tomato Ve1 mediates Verticillium resistance in Arabidopsis. Plant Physiol *156*, 2255-2265.

Fradin, E.F., and Thomma, B.P. (2006) Physiology and molecular aspects of Verticillium wilt diseases caused by V. dahliae and V. albo-atrum. Mol Plant Pathol *7*, 71-86.

Fuchs, J.G., Moenne-Loccoz, Y., and Defago, G. (1997) Nonpathogenic Fusarium oxysporum Strain Fo47 Induces Resistance to Fusarium Wilt in Tomato. Plant Dis *81*, 492-496.

Gao, X., Britt, R.C., Jr., Shan, L., and He, P. (2011) Agrobacterium-mediated virus-induced gene silencing assay in cotton. J Vis Exp,

Gao, X., Li, F., Li, M., Kianinejad, A.S., Dever, J.K., Wheeler, T.A., Li, Z., He, P., and Shan, L. (2013) Cotton GhBAK1 mediates Verticillium wilt resistance and cell death. J Integr Plant Biol *55*, 586-596.

Gawehns, F., Ma, L., Bruning, O., Houterman, P.M., Boeren, S., Cornelissen, B.J., Rep, M., and Takken, F.L. (2015) The effector repertoire of Fusarium oxysporum determines the tomato xylem proteome composition following infection. Frontiers in plant science *6*, 967.

Gijzen, M., and Nurnberger, T. (2006) Nep1-like proteins from plant pathogens: recruitment and diversification of the NPP1 domain across taxa. Phytochemistry *67*, 1800-1807.

Gish, L.A., and Clark, S.E. (2011) The RLK/Pelle family of kinases. Plant J *66*, 117-127.

Glazebrook, J. (2005) Contrasting mechanisms of defense against biotrophic and necrotrophic pathogens. Annu Rev Phytopathol *43*, 205-227.

Gomez-Gomez, L., Felix, G., and Boller, T. (1999) A single locus determines sensitivity to bacterial flagellin in Arabidopsis thaliana. Plant J *18*, 277-284.

Gonzalez-Cendales, Y., Catanzariti, A.M., Baker, B., McGrath, D.J., and Jones, D.A. (2016) Identification of I-7 expands the repertoire of genes for resistance to Fusarium wilt in tomato to three resistance gene classes. Mol Plant Pathol *17*, 448-463.

Gracia-Garza, J.A., and Fravel, D.R. (1998) Effect of Relative Humidity on Sporulation of Fusarium oxysporum in Various Formulations and Effect of Water on Spore Movement Through Soil. Phytopathology *88*, 544-549.

Gust, A.A., and Felix, G. (2014) Receptor like proteins associate with SOBIR1-type of adaptors to form bimolecular receptor kinases. Curr Opin Plant Biol *21*, 104-111.

Halpern, H.C., Bell, A.A., Wagner, T.A., Liu, J., Nichols, R.L., Olvey, J., Woodward, J.E., Sanogo, S., Jones, C.A., Chan, C.T., and Brewer, M.T. (2017) First report of Fusarium wilt of cotton caused by *Fusarium oxysporum* f. sp. *vasinfectum* Race 4 in Texas, U.S.A. Plant Disease *102*, 446.

Hansen, F.T., Sorensen, J.L., Giese, H., Sondergaard, T.E., and Frandsen, R.J. (2012) Quick guide to polyketide synthase and nonribosomal synthetase genes in Fusarium. Int J Food Microbiol *155*, 128-136.

Hao, J.J., Yang, M.E., and Davis, R.M. (2009) Effect of soil inoculum density of *Fusarium oxysporum f. sp. vasinfectum* Race 4 on disease development in cotton. Plant Disease *93*, 1324-1328.

He, P., Shan, L., Lin, N.C., Martin, G.B., Kemmerling, B., Nurnberger, T., and Sheen, J. (2006) Specific bacterial suppressors of MAMP signaling upstream of MAPKKK in Arabidopsis innate immunity. Cell *125*, 563-575.

He, Y., Zhou, J., Shan, L., and Meng, X. (2018) Plant cell surface receptor-mediated signaling - a common theme amid diversity. J Cell Sci *131*.

Hind, S.R., Strickler, S.R., Boyle, P.C., Dunham, D.M., Bao, Z., O'Doherty, I.M., Baccile, J.A., Hoki, J.S., Viox, E.G., Clarke, C.R., Vinatzer, B.A., et al. (2016) Tomato receptor FLAGELLIN-SENSING 3 binds flgII-28 and activates the plant immune system. Nat Plants *2*, 16128.

Holzwart, E., Huerta, A.I., Glockner, N., Garnelo Gomez, B., Wanke, F., Augustin, S., Askani, J.C., Schurholz, A.K., Harter, K., and Wolf, S. (2018) BRI1 controls vascular cell fate in the Arabidopsis root through RLP44 and phytosulfokine signaling. Proc Natl Acad Sci U S A *115*, 11838-11843.

Houterman, P.M., Cornelissen, B.J., and Rep, M. (2008) Suppression of plant resistance gene-based immunity by a fungal effector. PLoS Pathog *4*, e1000061.

Houterman, P.M., Speijer, D., Dekker, H.L., CG, D.E.K., Cornelissen, B.J., and Rep, M. (2007) The mixed xylem sap proteome of Fusarium oxysporum-infected tomato plants. Molecular plant pathology *8*, 215-221.

Huot, B., Yao, J., Montgomery, B.L., and He, S.Y. (2014) Growth-defense tradeoffs in plants: a balancing act to optimize fitness. Mol Plant *7*, 1267-1287.

Ichimura, K., Shinozaki, K., Tena, G., Sheen, J., Henry, Y., and al., e. (2002) Mitogen-activated protein kinase cascades in plants: a new nomenclature. Trends Plant Sci *7*, 301-308.

Jamieson, P.A., Shan, L., and He, P. (2018) Plant cell surface molecular cypher: Receptor-like proteins and their roles in immunity and development. Plant Sci *274*, 242-251.

Jehle, A.K., Lipschis, M., Albert, M., Fallahzadeh-Mamaghani, V., Furst, U., Mueller, K., and Felix, G. (2013) The receptor-like protein ReMAX of Arabidopsis detects the microbe-associated molecular pattern eMax from Xanthomonas. Plant Cell *25*, 2330-2340.

Jones, J.D., and Dangl, J.L. (2006) The plant immune system. Nature *444*, 323-329.

Kavroulakis, N., Ntougias, S., Zervakis, G.I., Ehaliotis, C., Haralampidis, K., and Papadopoulou, K.K. (2007) Role of ethylene in the protection of tomato plants against soil-borne fungal pathogens conferred by an endophytic Fusarium solani strain. J Exp Bot *58*, 3853-3864.

Kawchuk, L.M., Hachey, J., Lynch, D.R., Kulcsar, F., van Rooijen, G., Waterer, D.R., Robertson, A., Kokko, E., Byers, R., Howard, R.J., Fischer, R., et al. (2001) Tomato Ve disease resistance genes encode cell surface-like receptors. Proc Natl Acad Sci U S A *98*, 6511-6515.

Kim, Y., Hutmacher, R.B., and Davis, R.M. (2005) Characterization of California isolates of *Fusarium oxysporum* f. sp. *vasinfectum*. Plant Disease *89*, 366-372.

Kochman, J.K. (1995) Fusarium wilt in cotton - a new record in Australia. Australasian Plant Pathology *24*,

Kourelis, J., and van der Hoorn, R.A.L. (2018) Defended to the Nines: 25 Years of Resistance Gene Cloning Identifies Nine Mechanisms for R Protein Function. The Plant cell *30*, 285-299.

Larkan, N.J., Lydiate, D.J., Parkin, I.A., Nelson, M.N., Epp, D.J., Cowling, W.A., Rimmer, S.R., and Borhan, M.H. (2013) The Brassica napus blackleg resistance gene LepR3 encodes a receptor-like protein triggered by the Leptosphaeria maculans effector AVRLM1. New Phytol *197*, 595-605.

Larkan, N.J., Ma, L., and Borhan, M.H. (2015) The Brassica napus receptor-like protein RLM2 is encoded by a second allele of the LepR3/Rlm2 blackleg resistance locus. Plant Biotechnol J *13*, 983-992.

Lee, J.S., Kuroha, T., Hnilova, M., Khatayevich, D., Kanaoka, M.M., McAbee, J.M., Sarikaya, M., Tamerler, C., and Torii, K.U. (2012) Direct interaction of ligand-receptor pairs specifying stomatal patterning. Genes Dev *26*, 126-136.

Li, B., Meng, X., Shan, L., and He, P. (2016a) Transcriptional Regulation of Pattern-Triggered Immunity in Plants. Cell Host Microbe *19*, 641-650.

Li, F., Cheng, C., Cui, F., de Oliveira, M.V., Yu, X., Meng, X., Intorne, A.C., Babilonia, K., Li, M., Li, B., Chen, S., et al. (2014) Modulation of RNA polymerase II phosphorylation downstream of pathogen perception orchestrates plant immunity. Cell Host Microbe *16*, 748-758.

Li, P., Linhardt, R.J., and Cao, Z. (2016b) Structural Characterization of Oligochitosan Elicitor from Fusarium sambucinum and Its Elicitation of Defensive Responses in Zanthoxylum bungeanum. Int J Mol Sci *17*,

Li, S., Nie, H., Qiu, D., Shi, M., and Yuan, Q. (2019) A novel protein elicitor PeFOC1 from Fusarium oxysporum triggers defense response and systemic resistance in tobacco. Biochem Biophys Res Commun *514*, 1074-1080.

Liebrand, T.W., van den Berg, G.C., Zhang, Z., Smit, P., Cordewener, J.H., America, A.H., Sklenar, J., Jones, A.M., Tameling, W.I., Robatzek, S., Thomma, B.P., et al. (2013) Receptor-like kinase SOBIR1/EVR interacts with receptor-like proteins in plant immunity against fungal infection. Proc Natl Acad Sci U S A *110*, 10010-10015.

Lievens, B., Houterman, P.M., and Rep, M. (2009) Effector gene screening allows unambiguous identification of Fusarium oxysporum f. sp. lycopersici races and discrimination from other formae speciales. FEMS microbiology letters *300*, 201-215.

Lin, G., Zhang, L., Han, Z., Yang, X., Liu, W., Li, E., Chang, J., Qi, Y., Shpak, E.D., and Chai, J. (2017) A receptor-like protein acts as a specificity switch for the regulation of stomatal development. Genes Dev *31*, 927-938.

Lozano-Duran, R., Macho, A.P., Boutrot, F., Segonzac, C., Somssich, I.E., and Zipfel, C. (2013) The transcriptional regulator BZR1 mediates trade-off between plant innate immunity and growth. Elife *2*, e00983.

Luna, E., Pastor, V., Robert, J., Flors, V., Mauch-Mani, B., and Ton, J. (2011) Callose deposition: a multifaceted plant defense response. Mol Plant Microbe Interact *24*, 183-193.

Lv, Y., Yang, N., Wu, J., Liu, Z., Pan, L., Lv, S., and Wang, G. (2016) New insights into receptor-like protein functions in Arabidopsis. Plant Signal Behav *11*, e1197469.

Ma, L., Houterman, P.M., Gawehns, F., Cao, L., Sillo, F., Richter, H., Clavijo-Ortiz, M.J., Schmidt, S.M., Boeren, S., Vervoort, J., Cornelissen, B.J., et al. (2015) The AVR2-SIX5 gene pair is required to activate I-2-mediated immunity in tomato. New Phytol *208*, 507-518.

Ma, L.J., van der Does, H.C., Borkovich, K.A., Coleman, J.J., Daboussi, M.J., Di Pietro, A., Dufresne, M., Freitag, M., Grabherr, M., Henrissat, B., Houterman, P.M., et al. (2010) Comparative genomics reveals mobile pathogenicity chromosomes in Fusarium. Nature *464*, 367-373.

Ma, X., Xu, G., He, P., and Shan, L. (2016) SERKing Coreceptors for Receptors. Trends Plant Sci *21*, 1017-1033.

Macho, A.P., and Zipfel, C. (2014) Plant PRRs and the activation of innate immune signaling. Mol Cell *54*, 263-272.

Malnoy, M., Xu, M., Borejsza-Wysocka, E., Korban, S.S., and Aldwinckle, H.S. (2008) Two receptor-like genes, Vfa1 and Vfa2, confer resistance to the fungal pathogen Venturia inaequalis inciting apple scab disease. Mol Plant Microbe Interact *21*, 448-458.

Marchler-Bauer, A., Derbyshire, M.K., Gonzales, N.R., Lu, S., Chitsaz, F., Geer, L.Y., Geer, R.C., He, J., Gwadz, M., Hurwitz, D.I., Lanczycki, C.J., et al. (2015) CDD: NCBI's conserved domain database. Nucleic Acids Res *43*, D222-226.

Medzhitov, R., Preston-Hurlburt, P., and Janeway, C.A., Jr. (1997) A human homologue of the Drosophila Toll protein signals activation of adaptive immunity. Nature *388*, 394-397.

Melotto, M., Underwood, W., Koczan, J., Nomura, K., and He, S.Y. (2006) Plant stomata function in innate immunity against bacterial invasion. Cell *126*, 969-980.

Meng, X., and Zhang, S. (2013) MAPK cascades in plant disease resistance signaling. Annu Rev Phytopathol *51*, 245-266.

Mittler, R., and Blumwald, E. (2015) The roles of ROS and ABA in systemic acquired acclimation. Plant Cell *27*, 64-70.

Monaghan, J., and Zipfel, C. (2012) Plant pattern recognition receptor complexes at the plasma membrane. Curr Opin Plant Biol *15*, 349-357.

Nadeau, J.A., and Sack, F.D. (2002) Control of stomatal distribution on the Arabidopsis leaf surface. Science *296*, 1697-1700.

Newman, M.A., Sundelin, T., Nielsen, J.T., and Erbs, G. (2013) MAMP (microbe-associated molecular pattern) triggered immunity in plants. Front Plant Sci *4*, 139.

O'Donnell, K., Gueidan, C., Sink, S., Johnston, P.R., Crous, P.W., Glenn, A., Riley, R., Zitomer, N.C., Colyer, P., Waalwijk, C., Lee, T., et al. (2009) A two-locus DNA sequence database for typing plant and human pathogens within the Fusarium oxysporum species complex. Fungal Genet Biol *46*, 936-948.

Offord, V., Coffey, T.J., and Werling, D. (2010) LRRfinder: a web application for the identification of leucine-rich repeats and an integrative Toll-like receptor database. Dev Comp Immunol *34*, 1035-1041.

Ogallo, J.L., Goodell, P.B., Eckert, J., and Roberts, P.A. (1997) Evaluation of NemX, a New Cultivar of Cotton with High Resistance to Meloidogyne incognita. Journal of nematology *29*, 531-537.

Ogawa, M., Shinohara, H., Sakagami, Y., and Matsubayashi, Y. (2008) Arabidopsis CLV3 peptide directly binds CLV1 ectodomain. Science *319*, 294.

Olivain, C., Steinberg, C., and Alabouvette, C. (1995) Evidence of induced resistance in tomato inoculated by non-pathogenic strains of Fusarium oxysporum, Poznan, Poland: The Polish Phytopathological Society

Oome, S., and Van den Ackerveken, G. (2014) Comparative and functional analysis of the widely occurring family of Nep1-like proteins. Mol Plant Microbe Interact *27*, 1081-1094.

Pan, L., Lv, S., Yang, N., Lv, Y., Liu, Z., Wu, J., and Wang, G. (2016) The Multifunction of CLAVATA2 in Plant Development and Immunity. Front Plant Sci *7*, 1573.

Petersen, M., Brodersen, P., Naested, H., Andreasson, E., Lindhart, U., Johansen, B., Nielsen, H.B., Lacy, M., Austin, M.J., Parker, J.E., Sharma, S.B., et al. (2000) Arabidopsis map kinase 4 negatively regulates systemic acquired resistance. Cell *103*, 1111-1120.

Petutschnig, E.K., Stolze, M., Lipka, U., Kopischke, M., Horlacher, J., Valerius, O., Rozhon, W., Gust, A.A., Kemmerling, B., Poppenberger, B., Braus, G.H., et al. (2014) A novel Arabidopsis CHITIN ELICITOR RECEPTOR KINASE 1 (CERK1) mutant with enhanced pathogen-induced cell death and altered receptor processing. New Phytol *204*, 955-967.

Postma, J., Liebrand, T.W., Bi, G., Evrard, A., Bye, R.R., Mbengue, M., Kuhn, H., Joosten, M.H., and Robatzek, S. (2016) Avr4 promotes Cf-4 receptor-like protein association with the BAK1/SERK3 receptor-like kinase to initiate receptor endocytosis and plant immunity. New Phytol *210*, 627-642.

Pruitt, R.N., Schwessinger, B., Joe, A., Thomas, N., Liu, F., Albert, M., Robinson, M.R., Chan, L.J., Luu, D.D., Chen, H., Bahar, O., et al. (2015) The rice immune receptor XA21 recognizes a tyrosine-sulfated protein from a Gram-negative bacterium. Sci Adv *1*, e1500245.

Ramonell, K., Berrocal-Lobo, M., Koh, S., Wan, J., Edwards, H., Stacey, G., and Somerville, S. (2005) Loss-of-function mutations in chitin responsive genes show increased susceptibility to the powdery mildew pathogen Erysiphe cichoracearum. Plant Physiol *138*, 1027-1036.

Ranf, S., Gisch, N., Schaffer, M., Illig, T., Westphal, L., Knirel, Y.A., Sanchez-Carballo, P.M., Zahringer, U., Huckelhoven, R., Lee, J., and Scheel, D. (2015) A lectin S-domain receptor kinase mediates lipopolysaccharide sensing in Arabidopsis thaliana. Nat Immunol *16*, 426-433.

Rasmussen, M.W., Roux, M., Petersen, M., and Mundy, J. (2012) MAP Kinase Cascades in Arabidopsis Innate Immunity. Front Plant Sci *3*, 169.

Rep, M., Meijer, M., Houterman, P.M., van der Does, H.C., and Cornelissen, B.J. (2005) Fusarium oxysporum evades I-3-mediated resistance without altering the matching avirulence gene. Molecular plant-microbe interactions : MPMI *18*, 15-23.

Rivas, S., and Thomas, C.M. (2005) Molecular interactions between tomato and the leaf mold pathogen Cladosporium fulvum. Annu Rev Phytopathol *43*, 395-436.

Rodrigues, O., Reshetnyak, G., Grondin, A., Saijo, Y., Leonhardt, N., Maurel, C., and Verdoucq, L. (2017) Aquaporins facilitate hydrogen peroxide entry into guard cells to mediate ABA- and pathogen-triggered stomatal closure. Proc Natl Acad Sci U S A *114*, 9200-9205.

Rodriguez-Galvez, E., and Mendgen, K. (1995) The infection process of Fusarium oxysporum in cotton root tips. Protoplasma *189*, 61–72.

Ron, M., and Avni, A. (2004) The receptor for the fungal elicitor ethylene-inducing xylanase is a member of a resistance-like gene family in tomato. Plant Cell *16*, 1604-1615.

Roux, M., Schwessinger, B., Albrecht, C., Chinchilla, D., Jones, A., Holton, N., Malinovsky, F.G., Tor, M., de Vries, S., and Zipfel, C. (2011) The Arabidopsis leucine-rich repeat receptor-like kinases BAK1/SERK3 and BKK1/SERK4 are required for innate immunity to hemibiotrophic and biotrophic pathogens. Plant Cell *23*, 2440-2455.

Sanchez-Vallet, A., Mesters, J.R., and Thomma, B.P. (2015) The battle for chitin recognition in plant-microbe interactions. FEMS Microbiol Rev *39*, 171-183.

Sanogo, S., and Zhang, J. (2016) Resistance sources, resistance screening techniques and disease management for Fusarium wilt in cotton. Euphytica *207*, 255-271.

Schwessinger, B., Roux, M., Kadota, Y., Ntoukakis, V., Sklenar, J., Jones, A., and Zipfel, C. (2011) Phosphorylation-dependent differential regulation of plant growth, cell death, and innate immunity by the regulatory receptor-like kinase BAK1. PLoS Genet *7*, e1002046.

Scott, J.C., Gordon, T.R., Shaw, D.V., and Koike, S.T. (2010) Effect of Temperature on Severity of Fusarium Wilt of Lettuce Caused by Fusarium oxysporum f. sp. lactucae. Plant Dis *94*, 13-17.

Shen, Y., and Diener, A.C. (2013) Arabidopsis thaliana resistance to fusarium oxysporum 2 implicates tyrosine-sulfated peptide signaling in susceptibility and resistance to root infection. PLoS Genet *9*, e1003525.

Shimizu, T., Nakano, T., Takamizawa, D., Desaki, Y., Ishii-Minami, N., Nishizawa, Y., Minami, E., Okada, K., Yamane, H., Kaku, H., and Shibuya, N. (2010) Two LysM receptor molecules, CEBiP and OsCERK1, cooperatively regulate chitin elicitor signaling in rice. Plant J *64*, 204-214.

Shiu, S.H., and Bleecker, A.B. (2001) Receptor-like kinases from Arabidopsis form a monophyletic gene family related to animal receptor kinases. Proc Natl Acad Sci U S A *98*, 10763-10768.

Shpak, E.D., McAbee, J.M., Pillitteri, L.J., and Torii, K.U. (2005) Stomatal patterning and differentiation by synergistic interactions of receptor kinases. Science *309*, 290-293.

Stergiopoulos, I., and de Wit, P.J. (2009) Fungal effector proteins. Annu Rev Phytopathol *47*, 233-263.

Taguchi-Shiobara, F., Yuan, Z., Hake, S., and Jackson, D. (2001) The fasciated ear2 gene encodes a leucine-rich repeat receptor-like protein that regulates shoot meristem proliferation in maize. Genes Dev *15*, 2755-2766.

Tang, D., Wang, G., and Zhou, J.M. (2017) Receptor Kinases in Plant-Pathogen Interactions: More Than Pattern Recognition. Plant Cell *29*, 618-637.

Thatcher, L.F., Gardiner, D.M., Kazan, K., and Manners, J.M. (2012) A highly conserved effector in Fusarium oxysporum is required for full virulence on Arabidopsis. Mol Plant Microbe Interact *25*, 180-190.

Thatcher, L.F., Manners, J.M., and Kazan, K. (2009) Fusarium oxysporum hijacks COI1-mediated jasmonate signaling to promote disease development in Arabidopsis. Plant J *58*, 927-939.

Ulloa, M., Hutmacher, R.B., Davis, R.M., Wright, S.D., Percy, R., and Marsh, B. (2006) Breeding for Fusarium Wilt Race 4 Resistance in Cotton under Field and Greenhouse Conditions. Journal of Cotton Science *10*, 114-127.

Ulloa, M., Hutmacher, R.B., Roberts, P.A., Wright, S.D., Nichols, R.L., and Davis, R.M. (2013a) Inheritance and QTL mapping of Fusarium wilt race 4 resistance in cotton. Theoretical and Applied Genetics *126*, 1405-1418.

Ulloa, M., Hutmacher, R.B., Roberts, P.A., Wright, S.D., Nichols, R.L., and Michael Davis, R. (2013b) Inheritance and QTL mapping of Fusarium wilt race 4 resistance in cotton. Theor Appl Genet *126*, 1405-1418.

Ulloa, M., Wang, C., Hutmacher, R.B., Wright, S.D., Davis, R.M., Saski, C.A., and Roberts, P.A. (2011) Mapping Fusarium wilt race 1 resistance genes in cotton by inheritance, QTL and sequencing composition. Mol Genet Genomics *286*, 21-36.

van Dam, P., Fokkens, L., Ayukawa, Y., van der Gragt, M., Ter Horst, A., Brankovics, B., Houterman, P.M., Arie, T., and Rep, M. (2017) A mobile pathogenicity chromosome in Fusarium oxysporum for infection of multiple cucurbit species. Sci Rep *7*, 9042.

van der Does, H.C., and Rep, M. (2007) Virulence genes and the evolution of host specificity in plant-pathogenic fungi. Mol Plant Microbe Interact *20*, 1175-1182.

Veloso, J., Alabouvette, C., Olivain, C., Flors, V., Pastor, V., García, T., and Díaz, J. (2016) Modes of action of the protective strain Fo47 in controllingverticillium wilt of pepper. Plant Pathology *65*, 997-1007.

Wang, B., Yang, X., Zeng, H., Liu, H., Zhou, T., Tan, B., Yuan, J., Guo, L., and Qiu, D. (2012) The purification and characterization of a novel hypersensitive-like response-inducing elicitor from Verticillium dahliae that induces resistance responses in tobacco. Appl Microbiol Biotechnol *93*, 191-201.

Wang, C., and Roberts, P.A. (2006) A Fusarium Wilt Resistance Gene in Gossypium barbadense and Its Effect on Root-Knot Nematode-Wilt Disease Complex. Phytopathology *96*, 727-734.

Wang, C., Ulloa, M., Duong, T., and Roberts, P.A. (2018) Quantitative Trait Loci Mapping of Multiple Independent Loci for Resistance to Fusarium oxysporum f. sp. vasinfectum Races 1 and 4 in an Interspecific Cotton Population. Phytopathology *108*, 759-767.

Wang, G., Ellendorff, U., Kemp, B., Mansfield, J.W., Forsyth, A., Mitchell, K., Bastas, K., Liu, C.M., Woods-Tor, A., Zipfel, C., de Wit, P.J., et al. (2008) A genome-wide functional investigation into the roles of receptor-like proteins in Arabidopsis. Plant Physiol *147*, 503-517.

Warman, N.M., and Aitken, E.A.B. (2018) The Movement of Fusarium oxysporum f.sp. cubense (Sub-Tropical Race 4) in Susceptible Cultivars of Banana. Front Plant Sci *9*, 1748.

Waskiewicz, A., Golinski, P., Karolewski, Z., Irzykowska, L., Bocianowski, J., Kostecki, M., and Weber, Z. (2010) Formation of fumonisins and other secondary metabolites by Fusarium oxysporum and F. proliferatum: a comparative study. Food Addit Contam Part A Chem Anal Control Expo Risk Assess *27*, 608-615.

Willmann, R., Lajunen, H.M., Erbs, G., Newman, M.A., Kolb, D., Tsuda, K., Katagiri, F., Fliegmann, J., Bono, J.J., Cullimore, J.V., Jehle, A.K., et al. (2011) Arabidopsis lysin-motif proteins LYM1 LYM3 CERK1 mediate bacterial peptidoglycan sensing and immunity to bacterial infection. Proc Natl Acad Sci U S A *108*, 19824-19829.

Wolf, S., van der Does, D., Ladwig, F., Sticht, C., Kolbeck, A., Schurholz, A.K., Augustin, S., Keinath, N., Rausch, T., Greiner, S., Schumacher, K., et al. (2014) A receptor-like protein mediates the response to pectin modification by activating brassinosteroid signaling. Proc Natl Acad Sci U S A *111*, 15261-15266.

Workman, D. (2018) Cotton exports by country [Internet],

Xiang, L., Liu, J., Wu, C., Deng, Y., Cai, C., Zhang, X., and Cai, Y. (2017) Genome-wide comparative analysis of NBS-encoding genes in four Gossypium species. BMC Genomics *18*, 292.

Yadeta, K.A., and Thomma, B. (2013) The xylem as battleground for plant hosts and vascular wilt pathogens. Front Plant Sci *4*, 97.

Yamada, K., Yamashita-Yamada, M., Hirase, T., Fujiwara, T., Tsuda, K., Hiruma, K., and Saijo, Y. (2016) Danger peptide receptor signaling in plants ensures basal immunity upon pathogen-induced depletion of BAK1. EMBO J *35*, 46-61.

Yamaguchi, Y., Huffaker, A., Bryan, A.C., Tax, F.E., and Ryan, C.A. (2010) PEPR2 is a second receptor for the Pep1 and Pep2 peptides and contributes to defense responses in Arabidopsis. Plant Cell *22*, 508-522.

Yang, C., Li, W., Cao, J., Meng, F., Yu, Y., Huang, J., Jiang, L., Liu, M., Zhang, Z., Chen, X., Miyamoto, K., et al. (2017) Activation of ethylene signaling pathways enhances disease resistance by regulating ROS and phytoalexin production in rice. Plant J *89*, 338-353.

Yingfan, C., He, X., Jianchuan, M., Quan, S., Jianping, Y., and Jinggao, L. (2009) Molecular research and genetic engineering of resistance to Verticillium wilt in cotton: A review. African Journal of Biotechnology *8*, 7363-7372.

Yoo, M.J., and Wendel, J.F. (2014) Comparative evolutionary and developmental dynamics of the cotton (Gossypium hirsutum) fiber transcriptome. PLoS Genet *10*, e1004073.

Yu, X., Feng, B., He, P., and Shan, L. (2017) From Chaos to Harmony: Responses and Signaling upon Microbial Pattern Recognition. Annu Rev Phytopathol *55*, 109-137.

Yu, Y., Ouyang, Y., and Yao, W. (2018) shinyCircos: an R/Shiny application for interactive creation of Circos plot. Bioinformatics *34*, 1229-1231.

Zeidler, D., Zahringer, U., Gerber, I., Dubery, I., Hartung, T., Bors, W., Hutzler, P., and Durner, J. (2004) Innate immunity in Arabidopsis thaliana: lipopolysaccharides activate nitric oxide synthase (NOS) and induce defense genes. Proc Natl Acad Sci U S A *101*, 15811-15816.

Zhai, C., Xu, P., Zhang, X., Guo, Q., Zhang, X., Xu, Z., and Shen, X. (2015) Development of Gossypium anomalum-derived microsatellite markers and their use for genome-wide identification of recombination between the G. anomalum and G. hirsutum genomes. Theor Appl Genet *128*, 1531-1540.

Zhang, L., Kars, I., Essenstam, B., Liebrand, T.W., Wagemakers, L., Elberse, J., Tagkalaki, P., Tjoitang, D., van den Ackerveken, G., and van Kan, J.A. (2014) Fungal endopolygalacturonases are recognized as microbe-associated molecular patterns by the arabidopsis receptor-like protein RESPONSIVENESS TO BOTRYTIS POLYGALACTURONASES1. Plant Physiol *164*, 352-364.

Zhang, W., Fraiture, M., Kolb, D., Loffelhardt, B., Desaki, Y., Boutrot, F.F., Tor, M., Zipfel, C., Gust, A.A., and Brunner, F. (2013) Arabidopsis receptor-like protein30 and receptor-like kinase suppressor of BIR1-1/EVERSHED mediate innate immunity to necrotrophic fungi. Plant Cell *25*, 4227-4241.

Zhang, Y., Yang, Y., Fang, B., Gannon, P., Ding, P., Li, X., and Zhang, Y. (2010) Arabidopsis snc2-1D activates receptor-like protein-mediated immunity transduced through WRKY70. Plant Cell *22*, 3153-3163.

Zhao, L., Li, Y., Xie, Q., and Wu, Y. (2017) Loss of CDKC;2 increases both cell division and drought tolerance in Arabidopsis thaliana. Plant J *91*, 816-828.

Zhu, Y., Wang, Y., Li, R., Song, X., Wang, Q., Huang, S., Jin, J.B., Liu, C.M., and Lin, J. (2010) Analysis of interactions among the CLAVATA3 receptors reveals a direct interaction between CLAVATA2 and CORYNE in Arabidopsis. Plant J *61*, 223-233.

Zipfel, C., Robatzek, S., Navarro, L., Oakeley, E.J., Jones, J.D., Felix, G., and Boller, T. (2004) Bacterial disease resistance in Arabidopsis through flagellin perception. Nature *428*, 764-767.